Stony Brook University

Redox Regulation of Protein Tyrosine Phosphatases in Oncogene-induced Senescence

A Dissertation Presented

by

Ming Yang

to

The Graduate School

in Partial Fulfillment of the

Requirements

for the Degree of

Doctor of Philosophy

in

Biochemistry and Structural Biology

Stony Brook University

December 2014

Stony Brook University
The Graduate School

Ming Yang

We, the dissertation committee for the above candidate for the
Doctor of Philosophy degree, hereby recommend
acceptance of this dissertation.

Dr. Nicholas K. Tonks
Professor, Cold Spring Harbor Laboratory
Dissertation advisor

Dr. Elizabeth M. Boon
Associate Professor, Department of Chemistry, Stony Brook University, Chair of the Dissertation Committee

Dr. W. Todd Miller
Professor, Department of Physiology and Biophysics, Stony Brook University

Dr. Suzanne Scarlata
Professor, Department of Physiology and Biophysics, Stony Brook University

Dr. Darryl J. Pappin
Associate Professor, Proteomics, Cold Spring Harbor Laboratory

This dissertation is accepted by the Graduate School

Charles Taber
Dean of the Graduate School

Abstract of the Dissertation

Redox Regulation of Protein Tyrosine Phosphatases in Oncogene-induced Senescence

by

Ming Yang

Doctor of Philosophy

in

Biochemistry and Structural Biology

Stony Brook University

2014

Oncogene expression in normal cells can cause an irreversible growth arrest called oncogene-induced senescence (OIS), which serves as a barrier to cancer initiation. Elevated reactive oxygen species (ROS) have been detected in most senescent cells and are thought to play a causal role in OIS. ROS are believed to have a second messenger function in transducing signals, however their molecular role in senescence remains elusive. We hypothesize that PTPs, which are prone to redox regulation, act as specific target of ROS and the redox regulation of PTPs mediates the signaling transduction in oncogene-induced senescence.

In our study, we utilized a modified cysteine labeling assay to profile the PTPs undergoing reversible oxidation in senescent cells. We demonstrated that PTP1B underwent redox regulation during oncogenic RAS (H-RASV12)-induced senescence in IMR90 cells. Inhibition of PTP1B function accelerated, and overexpressing PTP1B attenuated, H-RASV12-induced senescence. Furthermore, using the PTP1B substrate trapping mutant strategy, we found that AGO2, an Argonaute protein which is required for RISC complex function in the RNAi pathway, is a substrate of PTP1B in senescent cells. Reversible oxidation of PTP1B during senescence caused hyper-phosphorylation of AGO2 on its Y393 site. Phosphorylation of AGO2 at Tyr 393 inhibited its loading with microRNAs (miRNA) and thus miRNA-mediated gene silencing, which counteracted the function of H-RASV12-induced oncogenic miRNAs. The decrease in loading of miRNA targeted against p21 facilitated the de-repression of p21 translation and hence provoked senescence onset.

In this project, we revealed a novel mechanism that ROS promotes senescence through inactivation of PTP1B thereby enhancing tyrosine phosphorylation of AGO2 and altering translation repression. We demonstrated PTP1B is important in regulating miRNA pathway and OIS. The novel ROS/PTP1B/Ago2 pathway identified in our study might provide a potential mechanism for the development of cancer therapeutics.

To My Family

Table of Contents

List of Figures

Chapter1

Chapter 2

List of Tables

Acknowledgments

I would like to thank my advisor Dr. Tonks for his guidance and support throughout my research. I am grateful for his constructive criticism, patience and his constant encouragement. My project would not have gone so far had it not been his supervision. I acknowledge the members of my thesis committee, Drs. Todd Miller, Suzanne Scarlata, Elizabeth Boon, and Darryl Pappin. I appreciate their critical comments and helpful suggestions during my study.

I am heartily thankful to the lab member of Tonks lab: Benoit Boivin, Li Li, Navasona Krishnan, Ulla Schwertassek, Gaofeng Fan, Gyula Bencze, Guang Lin, Fauzia Chaudhary, Mathangi Ramesh, Siwei Zhang, Ioana Rus, Wei Zheng, Sai Dipikaa Akshinthala, Xiaoqun (Catherine) Zhang, Xin Cheng for their continuous support, helpful discussions and overall for creating a warm working environment in the lab. I would like to express my special appreciation to Benoit Boivin for all his efforts helping my project to move smoothly.

I thank Astrid Haase, and other members of Dr. Greg Hannon's lab: Yang Yu, Xin Zhou and Maria Mosquera for generously share of their reagents, protocols and experience. I thank Dr. Darryl Pappin's lab members: Cexiong Fu and Keith Rivera for their performing the mass spectrometry analysis on my samples. I thank Dr. Chris Chang and Bryan Dickinson for sharing the PF6-AM probe and method on detecting ROS production in living cells. I thank Dr. Thomas Neubert and Fang-Ke Huang for their generous help in proteomic analysis. I thank Shipra Das for her helpful discussion on my project. xvi

Finally, I thank my husband Fang-Ke Huang for his love and support on my career and life. I appreciate my parents and grandparents for being a constant source of inspiration in each and every step of my study and research.

Publications

Ming Yang, Astrid D. Haase, Fang-Ke Huang, Gérald Coulis, Keith D. Rivera, Bryan C. Dickinson, Christopher J. Chang, Darryl Pappin, Thomas A. Neubert, Gregory J. Hannon, Benoit Boivin, and Nicholas K. Tonks**,** Protein Tyrosine Phosphatase 1B Dephosphorylates Argonaute 2 Tyrosine 393 and Regulates Gene Silencing in Oncogenic RAS Induced Cellular Senescence. ***Molecular Cell,*** 2014 Sep 4;55(5):782-90

Benoit Boivin, **Ming Yang** and Nicholas K. Tonks, Targeting the reversibly oxidized protein tyrosine phosphatase superfamily. ***Science Signaling*** 2010 Aug 31;3(137):pl2

Chapter 1

1.1 Phosphorylation-mediated signaling

Cells can register environmental stimuli and respond by changing their growth, differentiation, survival, movement or metabolism. A series of biochemical reactions are triggered in response to the stimuli which eventually lead to an appropriate cellular response. This cascade of biochemical reactions is called signal transduction. Signal transduction predominantly involves regulating the localization or function of the proteins in the pathway, frequently through transient and reversible covalent modification. This includes reversible protein phosphorylation of key regulatory or catalytic residues of the protein, resulting in its altered activity.

1.1.1 Protein Phosphorylation and Signal Transduction

Protein phosphorylation is the covalent addition of a phosphate group to a protein. It was first identified in 1906 by Phoebus Levene as a modification on the protein vitellin (phosvitin) (Levene and Alsberg, 1906). In the mid-1950's, Edwin Krebs and Edmond Fischer discovered reversible protein phosphorylation while characterizing the enzymes glycogen phosphorylase (Fischer and Krebs, 1955; Krebs and Fischer, 1956). Glycogen hosphorylases exists in two forms: phosphorylase b, the inactive form, and phosphorylase a, the active form (Cori and Green 1943). Interconversion of phosphorylase a and b is regulated by two enzymes: phosphorylase kinase, which catalyses the transfer of the gamma-phosphate from ATP to phosphorylase and leads to its activation (Fischer and Krebs, 1955; Krebs and Fischer, 1955), and the phosphorylase phosphatase, which removes the phosphate group and inactivates it

(Graves et al., 1960; Wosilait and Sutherland, 1956). The interconversion of the two forms of phosphorylase is the first known example of “reversible protein phosphorylation”, a dynamic process regulating protein function. The activity of the phosphorylase kinase was later found to be controlled by another kinase, phosphorylase kinase kinase, otherwise known as the cyclic AMP-dependent kinase (Krebs et al., 1958; Patterson and Orr, 1968). This finding introduced for the first time the idea that protein activity can be modulated by its reversible protein phosphorylation through a series of kinases acting in tandem. This cascade of reversible protein phosphorylation facilitates the transmission of upstream signal to distinct cellular compartments, eventually triggering specific downstream effects.

To date, it is known that approximately one third of proteins in eukaryotic cells are phosphorylated(Cohen, 2001). Signal transduction pathways that distribute signals to various parts of a cell involve, at least in part, reversible protein phosphorylation (Graves and Krebs, 1999). Thus, studying the mechanisms regulating protein reversible phosphorylation will help us understand signal transduction and how it modulates cellular response to the environment (Figure 1.1).

1.1.2 Tyrosine phosphorylation, Tyrosine Kinase, and Tyrosine Phosphatase

Phosphorylation occurs predominantly on serine residues (86.4%), followed by threonine residues (11.8%) and tyrosine residues (1.8%) (Olsen et al., 2006). Although low in abundance, tyrosine phosphorylation is considered to be one of the key steps in signal transduction. Tyrosine phosphorylation plays an important role in many cellular processes including growth factor and insulin signaling, cell adhesion and migration, cell differentiation

and development, cell cycle control, and cell metabolism (Di Stefano et al., 2004; Lin et al., 2006; Meijer et al., 1991; Ushiro and Cohen, 1980).

Protein tyrosine phosphorylation is controlled by two families of enzymes: protein tyrosine kinases (PTK) and protein tyrosine phosphatases (PTP). PTKs catalyse the addition of a phosphate group to specific substrates. Once tyrosine phosphorylated, these substrates can be recognized by proteins with pTyr binding domains, such as SH2 domain. The recruitment of pTyr binding proteins is essential for initiating and propagating downstream signaling. Opposing the activity of tyrosine kinases are protein tyrosine phosphatases, which remove phosphate groups. Thus, phosphatases and kinases coordinate with each other in the regulation of signaling pathways (Lim and Pawson, 2010). Disruption of the coordinated activities of PTKs and PTPs can thus alter the normal pattern of protein phosphorylation, resulting in the propagation of abnormal responses to extracellular stimuli and development of human diseases.

So far, most studies on protein tyrosine phosphorylation have been focused on PTKs. The importance of the regulatory role of protein tyrosine kinases in cellular function is already well established. Misregulation of kinase activity has been extensively implicated in various diseases, including many different cancers. For example, v-Src, the first identified tyrosine kinase (Stehelin et al., 1977) is a well known oncogene and is found to be constitutively active in various cancer types (Smart et al., 1981) Furthermore, aberrant receptor tyrosine kinase signaling is also implicated in several types of cancers such as breast, lung cancer and glioblastoma (Giamas et al., 2010). Since the activity of kinases is counterbalanced by that of phosphatases, understanding the phosphorylation-dependent signaling pathways from the

perspective of phosphatases will not only complete our knowledge about protein tyrosine phosphorylation but also have a profound impact on drug development in major diseases.

Although historically protein phosphatases have been viewed as passive housekeeping enzymes, it is increasingly becoming apparent that phosphatases and kinases have an equally important and coordinated role in the transmission and regulation of signaling responses. It has been proposed that PTKs control the amplitude of a signaling response, whereas the PTPs are thought to play a greater role in controlling the rate and duration of the response (Heinrich et al., 2002; Hornberg et al., 2005).

There are ~100 genes that encode for PTPs in the human genome. PTPs are defined by the signature motif "HCX5R" in their active sites, in which the invariant Cys residue is essential for catalysis. Based on their substrate specificity, the family is broadly divided into two categories: classical PTPs, which only dephosphorylate phospho-tyrosine; and dual specificity phosphatases (DSPs), which in addition to phospho-tyrosine, also dephosphorylate phosphoserine and phosphothreonine, and in some cases, even non-protein substrates. Classical PTPs can be further sub-divided into two categories: the transmembrane receptor-like PTPs and the cytosolic PTPs. Compared to classical PTPs, the DSPs have smaller catalytic domains and their sequences are less conserved (Tonks, 2006b) (Figure 1.2). PTPs participate in regulating a broad range of signaling pathways which underlie various physiological processes.

1.1.3 Physiological roles of PTPs

The diverse functions of PTPs make them important regulators of signaling pathways. Now it is appreciated that PTPs are not only inhibitors of pTyr signal, but also have capability of promoting pTyr signal.

CD45 is the first characterized transmembrane receptor-like PTP (Tonks et al., 1988). Studies using CD45-deficient cell lines suggest that CD45 activity is essential for antigen receptor signaling (Desai et al., 1994; Koretzky et al., 1990; Volarevic et al., 1993). These studies revealed for the first time that a PTP can function as a positive regulator of signaling pathways. Genetic studies indicate a dose-response curve between CD45 and human autoimmune diseases (Boxall et al., 2004; Majeti et al., 2000), suggesting that CD45 is a good drug target for autoimmune disease treatment.

SHP2 is another positive regulator of signaling pathway, which can activate Ras signaling. Upon stimulation, SHP2 promotes the recruitment of Grb2/SOS, which propagate RAS signaling. SHP2 also inhibits the function of Ras-GAP or Sprouty family proteins which are negative regulators of RAS activity (Dance et al., 2008). SHP2 with constitutive activation mutation is found in 50% of the Noonan Syndrome patients. Interestingly, the Noonan Syndrome patients who do not have SHP2 mutation might have activating mutation on SOS1 or RAF, both of which are mediators of RAS signaling (Tartaglia et al., 2002; Tartaglia et al., 2003). The observations indicate that SHP2 enhances RAS signaling and activation of SHP2 leads to disease progression.

Some PTPs are important negative regulators of signaling pathway. PTEN acts against PI3K/AKT pathway by dephosphorylating PI3P(Maehama and Dixon, 1998; Myers et al., 1997;

Staveley et al., 1998) . PTEN gene is frequently lost or mutated into inactive form in human cancer such as lung, prostate (Freeman et al., 2003) or breast cancer and glioblastoma (Parsons and Simpson, 2003). PTP1B is the first PTP purified to homogeneity (Tonks et al., 1988a, b). It is a well characterized inhibitor of insulin and leptin signaling, targeting at insulin receptor, IRS1 and JAK2 (Elchebly et al., 1999a; Zabolotny et al., 2002). The PTP1B KO mice model shows resistance to high-fat diet induced obesity, but otherwise normal in phenotype (Elchebly et al., 1999a; Klaman et al., 2000). This model indicates that PTP1B is a potential therapeutic target for obesity.

The regulations that affect the activity and localization of PTPs will have direct impact on the signaling pathways. It is critical for us to understand the mechanisms involved in regulating the function of PTPs for the development of PTP-based therapeutics.

1.1.4 Catalytic mechanism of PTPs

PTPs catalyze the dephosphorylation of substrates through a conserved 2-step reaction. The first step starts with a nucleophilic attack of the phosphate group on the substrate, initiated by the catalytic cysteine residue in the signature motif (Cys215 in PTP1B) (Lohse et al., 1997). It is followed by protonation of the tyrosyl leaving group by the conserved aspartic acid residue (Asp181 in PTP1B), acting as a general acid. The conserved Arg stabilizes the Cys-thiolate, assists substrate binding and maintains the transition-state of the phosphate. The second step involves hydrolysis of the phospho-enzyme intermediate, which is mediated by a water molecule coordinated by a glutamine residue (Gln262 in PTP1B). The negatively charged

Asp181 now serves as a general base to promote the nucleophilic attack of the water molecule coordinated by Gln262, releasing the phosphoric acid. (Figure 1.3) (Tonks, 2003).

1.1.5 Substrate specificity of PTPs

The architecture of the active site defines the substrate preference of classical PTPs and DSPs. The catalytic cysteine resides at the bottom of the active site pocket (Figure 1.4). The capacity of the active site pocket to accommodate the phosphorylated residue, determined by the depth and width of the catalytic cleft, directly affects the substrate specificity of PTPs.

In classical PTPs, there is an invariant tyrosine (Tyr46 in PTP1B) (Figure 1.4), which contributes to the structure of the wall of catalytic cleft and defines the depth of the active site with its side chain. This architecture ensures that only phospho-tyrosine, which has a longer side chain than phosphoserine and phosphothreonine, can reach into the pocket. In contrast, the catalytic cleft of the DSPs is shallower and wider because the residues that contribute to the depth of the catalytic cleft have shorter side chains. This grants both phosphoserine and phosphothreonine access to the active site cysteine (Barford et al., 1994; Yuvaniyama et al., 1996).

In addition, non-catalytic regulatory sequences can also modulate the specificity of PTPs through controlling the subcellular localization and protein binding of the PTPs. For example, the SH2 domain at N-terminal of SHP2 can help localize the enzyme to its substrates by binding to the phosphor-tyrosine residues on the substrates(Neel et al., 2003). Additionally, HePTP, and two other receptor-like PTPs, PTPRR and STEP, contain a kinase-interaction motif (KIM), which

target the enzymes to their substrates, the mitogen-activated protein kinases (MAPKs) (Eswaran et al., 2006).

1.1.6 Regulation of PTP function

The activity of PTPs is regulated *in vivo* through several different mechanisms at multiple levels, including that redox regulation that affects the activity of many PTPs(Tonks, 2006b). Here, I will briefly discuss all levels of regulation and focus in particular on the redox regulation of PTPs.

PTP activity can be regulated by the level of their expression, which can be altered in response to specific stimuli. A number of PTPs are upregulated when cells reaching high densities, including DEP-1, RPTPμ, RPTPk, and PTPβ/VE-PTP(Campan et al., 1996; Fuchs et al., 1996; Gaits et al., 1995; Ostman et al., 1994).

Post-transcriptionally, alternative splicing generates structurally and functionally different PTP splice variants. The 48 kDa TC-PTP splice variant is an ER anchor protein, whereas the 45 kDa variant lacks ER anchoring sequence and is capable of shuttling in and out of the nucleus in response to mitogenic stimulation (Lorenzen et al., 1995; Tiganis et al., 1997). Alternative splicing of PTP sigma generates structural variants of its extracellular domain, which can interact with different extracellular ligands (Sajnani-Perez et al., 2003). Furthermore, microRNA mediated translational repression also plays an active role in regulating the expression of PTPs such as PTPRJ, PTEN and PTP1B (Paduano et al., 2013; Song et al., 2008; Wu et al., 2013).

Post-translational modifications have also been shown to regulate PTP activity. SHP2 has an N-terminal SH2 domain (N-SH2) which associates with the catalytic cleft of the PTP domain and blocks its phosphatase activity. SH2 domains can bind to the phosphorylated tyrosine residues on the C-tail and release the catalytic cleft of SHP2 (Bennett et al., 1994; Li et al., 1995). Sumoylation of PTP1B impairs its function and inhibits the negative effect of PTP1B on insulin receptor signalling(Dadke et al., 2007).Limited proteolysis is also observed in regulating the activity of PTPs such as PTP1B, PTP-MEG, and SHP1 by generating truncated form of PTPs and altering their localization and interaction partners (Aicher et al., 1997; Frangioni et al., 1993; Halle et al., 2007).

The receptor-like PTPs (RPTPs) are transmembrane proteins that possess extracellular segments with varying domains. RPTPs have two intracellular PTP domains. The membrane proximal D1 domains of RPTPs are catalytically active. The D2 domains, which are distal to the membrane, are catalytically inactive or have minimal activity(Lim et al., 1997). RPTPs can be regulated by ligand binding to their extracellular domain (Johnson et al., 2006; Meng et al., 2000). The dimerization of RPTPs has been proposed to influence their phosphatase activity. A proposed model suggests that a juxtamembrane wedge motif N-terminal to the D1 domain, which is conserved in RPTPs, plays a central role in inhibiting RPTP activity in dimers by occluding the active site of the opposing D1 domain in the dimer and preventing access of the substrates to the active site. (Desai et al., 1993; Jiang et al., 1999; Xie et al., 2006).

1.1.7 Redox regulation of PTPs

It is now well established that PTPs can be negatively regulated through reversible oxidation of the catalytic-site cysteine(Rhee, 2006; Salmeen and Barford, 2005). The microenvironment around the catalytic site makes the catalytic cysteine of most PTPs have a lower pKa at around 5, compared to the pKa of free cysteines, which is around 8(Salmeen and Barford, 2005; Weber et al., 1999). Thus, at physiological pH, the catalytic cysteine of PTP is deprotonated, making it a good nucleophile and at the same time rendering it susceptible to oxidation(Salmeen and Barford, 2005). This unique property of the PTP active site cysteine has been shown to underlie the oxidative regulation of PTPs.

Oxidative regulation can potentially affect PTP function in response to various physiological stimuli. It has been reported that several PTPs can be transiently oxidized because of H_2O_2 production in various signaling pathways. For example, PDGF stimulation causes SHP2, DEP1 oxidation in Rat1 fibroblast(Frijhoff et al., 2014; Meng et al., 2002). EGF treatment of A431 human epidermoid carcinoma cells triggers H_2O_2 production and PTP1B oxidation(Bae et al., 1997; Lee et al., 1998). Additionally, the hydrogen peroxide generated as a consequence of insulin stimulation reversibly oxidizes PTP1B(Mahadev et al., 2001b) and Erb2 signaling is known to induce PTPalpha oxidation (Boivin et al., 2013; Lee et al., 1998; Meng et al., 2002)

Depending upon the extent of oxidation, the catalytic cysteine residue in PTPs can either be oxidized into sulphenic (SOH) form which is reversible or the higher order of oxidation forms of sulphinic(SO_2H) or sulphonic(SO_3H) acid. (Figure 1.6) (Salmeen et al., 2003; van Montfort et al., 2003). PTPs have evolved to have a variety of mechanisms to stabilize their catalytic

cysteine in the reversiblly oxidized form, which prevents the cysteine to undergo higher order of oxidation and permits its reactivation (Figure 1.6).

In the case of PTP1B oxidation, mild oxidation of the active site cysteine generates a 5-atom cyclic sulphenyl-amide structure in which the sulfur atom of cysteine is covalently linked to the main-chain nitrogen of the serine residue adjacent to the cysteine(Salmeen et al., 2003; van Montfort et al., 2003). The cyclic sulphenyl-amide intermediate assists the regulation of PTP1B by protecting the enzyme from being irreversibly oxidized and helps in reverting the cysteine back to its active form by reducing agents (Tonks, 2006b).

Several DSPs such as PTEN, cdc25 and LMW-PTPs adapt a different mechanism to prevent higher order oxidation. They contain a second cysteine residue within the active site which is close enough to the catalytic cysteine. Following oxidation of the catalytic cysteine, a disulfide bond is formed between the invariant cysteine and the second cysteine in the active site. The formation of disulfide bond inactivates the phosphatase and protects the cysteine from terminal oxidation to sulfinic and sulfonic acids. It also facilities the reduction and reactivation of the phosphatases(Salmeen and Barford, 2005).

Recent studies on PTPalpha suggest an interesting novel mechanism of oxidative inhibition of RPTP activity. As mentioned before, RPTPs consist of extracellular domains and two intracellular PTP domains. The membrane proximal D1 domains of RPTPs are catalytically active. The D2 domains distal to the membrane are catalytically inactive or have minimal activity(Tonks, 2006b). The D2 domain of PTPalpha has minimal phosphatase activity and it contains a reactive cysteine(Lim et al., 1997). The oxidation of D2 cysteine causes the

formation of a disulfide bond between the 2 monomers. The dimerization blocks the active site of D1 domain and stabilizes the PTPalpha dimer in an inactive state (Persson et al., 2004; van der Wijk et al., 2004).

These findings suggest that reversible oxidation of PTPs is an important regulatory mechanism of PTP activity. ROS might indirectly affect pTyr mediated signaling via regulation of PTPs. Physiological stimuli such as growth factors, insulin, cytokines trigger the production of ROS, leading to oxidation and inactivation of PTPs and as a consequence, promoting tyrosine phosphorylation. Since the oxidation is transient, the PTPs can be reduced and reactivated and hence terminate the signal (Figure 1.5).

1.2 Redox signaling

1.2.1 Reactive oxygen species

Reactive oxygen species were initially thought to be the unwanted and toxic metabolism by-products. However, growing evidence suggest that the production of these molecules is tightly regulated and play important roles in signal transduction.

Most intracellular ROS are formed from superoxide, which can be converted into hydrogen peroxide by superoxide dismutase(Murphy, 2009). Superoxide O_2^- and H_2O_2 are produced in large amounts in immune cells during an event called respiratory burst, during which the immune cells use ROS as a defense weapon to kill the invading microorganisms.

In contrast, other cell types appear to produce significantly lower amounts of ROS as a mediator of signal transduction(Finkel, 1998). It has been demonstrated that ligand stimulation

in the non-phagocytic cells results in an increase in intracellular ROS. Such ligands include growth factors such as EGF, PDGF and VEGF(Chen et al., 2008; Colavitti et al., 2002; Sundaresan et al., 1995), insulin(Mahadev et al., 2001a) and cytokine such as TNFα(Kamata et al., 2005). Inhibition of ROS level was enough to block the normal tyrosine kinase signaling induced by these stimuli (Bae et al., 1997; Sundaresan et al., 1995), suggesting that ROS might function as a second messenger transducing signals.

1.2.2 Controlled production and elimination of ROS

1.2.2.1 Controlled production of ROS

There are two major sources of ROS production in the cells: NADPH oxidase and mitochondria. The NADPH oxidase (NOX) is a membrane-bound enzyme. NADPH oxidase generates superoxide by transferring electrons from NADPH inside the cell across the membrane and coupling these to molecular oxygen to produce superoxide anion. The superoxide dismutes to H_2O_2 which can diffuse through aquaporin channels in the plasma membrane to elicit an intracellular signaling response(Bienert et al., 2007).

The first NOX enzyme was initially found in phagocytic cells as gp91-PHOX: NOX2(Royer-Pokora et al., 1986; Teahan et al., 1987). It was soon understood that several more enzymes were required to cooperate with NOX2 for the production of ROS. A Rho guanosine triphosphatase, usually Rac1 or Rac2, p22, p40, p47, and p67 all participate in production of ROS, forming a complex with NOX2(Abo et al., 1991; Dinauer et al., 1987; Nunoi et al., 1988; Volpp et al., 1988; Wientjes et al., 1993). $p47^{phox}$ is important for organization of the complex, and $p67^{phox}$ activates the electron-transfer process. Membrane translation of Rac is essential for

the activation of NOX protein complex(Bedard and Krause, 2007). The phagocytic NOX is activated in response to bacterial products or by cytokines such as interferon gamma or IL8 stimulation (Shalaby et al., 1985).

A series of observations suggested that enzyme systems similar to the phagocyte NADPH oxidase exist in many other cell types(Brown and Griendling, 2009a). It now appears that there are seven members in the NOX enzyme family: NOX1-5 and DUOX1-2(Brown and Griendling, 2009a). Similar to NOX2, multiple regulatory subunits have to be recruited to the NOX proteins to form an active NOX complex (Bedard and Krause, 2007).

Physiological stimuli including insulin, PDGF and EGF signaling are shown to activate the NOX proteins (Chen et al., 2008; Fan et al., 2005; Krieger-Brauer and Kather, 1995; Sharma et al., 2008). For example, NOX4 has been shown to mediate insulin and EGF-stimulated H_2O_2 generation and regulate the signaling cascades (Mahadev et al., 2004; Goldstein et al., 2005). In addition, the hypertrophic agent agiontensin II can activate NOX1, which leads to the activation of several signaling pathways (Tabet et al., 2008; Ushio-Fukai et al., 1999; Ushio-Fukai et al., 1996). These studies provide evidence that regulation of NOX proteins mediates ROS production in response to signal transductions (Figure 1.7).

The mitochondria represents another source for intracellular oxidant production. ROS is generated predominantly at either Complex I or III, when electrons leak out from the electron transport chain and react with oxygen to produce superoxide anions(Brand, 2010; Lin and Beal, 2006). The superoxide released into mitochondria intermembrane space can either directly defuse out of the outer membrane into cytosol via VDAC (Voltage-dependent anion channel) or

can be converted into H_2O_2 by SOD1 which resides at the mitochondrial interspace (Finkel, 2011). The role of mitochondrial ROS in response to signal transduction is less well characterized. It is suggested that TNFalpha, PDGF stimulate the production of mitochondrial ROS (Chandel et al., 2000; Frijhoff et al., 2014; Kamata et al., 2005).

1.2.2.2 Elimination of ROS

The level of ROS *in vivo* is tightly controlled. A variety of molecules function as scavengers of superoxide and hydrogen peroxide. These antioxidants include low molecular weight molecules such as glutathione, as well as a variety of protein antioxidants including SOD, catalase, glutathione peroxidase, thioredoxin, and the peroxiredoxin family of proteins. These molecules each have specific subcellular localization and chemical reactivity towards the ROS(Finkel, 2011). They work cooperatively to maintain the intracellular redox homeostasis (Figure 1.7).

1.2.2.3 Local concentration of ROS

The balance between ROS production and reducing agents determines the local concentration of ROS. Increased local ROS concentration facilitates the ROS to target the proteins in close proximity(Finkel, 2011). A recent report shows that the transient phosphorylation and inactivation of certain membrane fraction of Prx1 allows the accumulation of ROS at the membrane and is proposed cause the oxidation of target proteins confined to this particular area(Woo et al., 2010) and thus contributes to the specificity of ROS signaling. Furthermore, the ROS produced by NOX4 protein under EGF treatment targets at PTP1B because of the colocalization of NOX4 and PTP1B on ER membrane (Chen et al., 2008), which

further supports that localized production of ROS is important for the specificity of ROS signaling.

1.2.2.4 Targets of ROS

In addition to the controlled local concentration of ROS, ROS also reactive with selectively with target proteins, which further contributes to the specificity of ROS signaling. In some proteins, the microenvironment lowers the pKa of their catalytic cysteins, making these proteins more reactive towards H_2O_2. These proteins with low pKa cysteines are susceptible to redox regulation. In mammalian cells, PTPs are major targets in ROS mediated signals(Salmeen and Barford, 2005).

1.2.3 ROS and disease

The function of ROS has been implicated in different physiological processes and linked to human health and disease.

As mentioned before, ROS production is needed for growth factor and insulin signaling, which is important for cell survival and growth (Chen et al., 2008; Colavitti et al., 2002; Sundaresan et al., 1995)Mahadev et al., 2004; Goldstein et al., 2005). However, alteration of ROS level is also implicated to cause growth arrest and apoptosis. Elevated ROS production is related to replicative senescence(Yuan et al., 1995) and oncogene-induced senescence (Colavitti and Finkel, 2005). Increasing the level of antioxidants or deleting the enzyme regulating ROS generation are shown to reduce senescence phenotype (Nemoto and Finkel,

2002; Schriner et al., 2005). Cancer treatment with chemotherapy reagents induces high level of ROS and eventually leads to cellular apoptosis (Schumacker, 2006).

The observations above suggest ROS play dual role in triggering growth or growth arrest. It implies the specificity of ROS signaling in its biological activity. The intensity and sources of oxidant, and the specific targets of ROS might contribute to the specific effects of ROS (Finkel, 2011).

We are particularly interested in studying the role of ROS in senescence, especially oncogene-induced senescence. Oncogene-induced senescence is a barrier to tumorogenesis. It is known that ROS is an important mediator of OIS(Colavitti and Finkel, 2005). However, the signaling pathways regulated by ROS in senescence remain to be elucidated.

1.3 ROS signaling in Oncogene-induced senescence

1.3.1 Senescence and oncogenesis

1.3.1.1 Cellular senescence

Senescence phenotype was first observed in 1965 by Hayflick and Moorhead in cultured human diploid fibroblast (Hayflick, 1965). The cell initially exhibited robust proliferation. However after many passages, the proliferation rate declined gradually and eventually the cells stopped growing. This growth arrest occurs despite the abundance of growth factors, nutrients and ample space. This irreversible growth arrest distinguishes senescent cells from quiescent cells which reacquire proliferation activity when given proper cellular signals.

Further studies reveal that normal human cells have limited life span. The cells cease proliferation due to gradual telomere shortening(d'Adda di Fagagna et al., 2004). Telomeres are stretches of repetitive DNA sequence at the end of chromosomes. Because of the nature of DNA synthesis in eukaryotic cells, the end of DNA cannot be fully replicated. The DNA becomes shorter after every round of DNA replication(d'Adda di Fagagna et al., 2003; Watson, 1972). The telomere provides a protection against the loss of vital genetic information. Loss of telomere eventually leads to chromosome damage and provokes the senescence program. Senescence functions as a fail-safe mechanism to prevent proliferation of cells with potential pathogenic mutations (d'Adda di Fagagna et al., 2003). The concept of this irreversible growth arrest was later applied to more forms of senescence triggered by a number of different cellular stresses, including DNA damage, radiation, expression of oncogenes and inactivation of tumor suppressors. Cellular senescence caused by high population doubling is termed replicative senescence to distinguish it from premature senescence, which is independent of telomere shortening.

In contrast to proliferating cells, senescence cells become large and flat. The markers of senescent cells include increase in beta-galatosidase activity and senescence associated heterochromatin foci.

Increased β-galactosidase activity, termed senescence associated β-galactosidase activity (SA-β-Gal), is a well defined marker for cellular senescence(Dimri et al., 1995). The increase lysosomal content, including beta-galactosidase in senescent cells allows the detection of beta-galactosidase activity at suboptimal pH-pH6.0 (Dimri et al., 1995). However, the

biochemistry underlying the phenomena is still unknown(Severino et al., 2000). There is evidence suggesting that a positive beta-gal reaction is related to cellular stress. SA-β-Gal and senescence are correlated in several cell types including fibroblasts, mammary epithelial cells and neonatal human melanocytes. SA-β-Gal is not detected in quiescent, terminal differentiated cells or immortal cells. SA-β-gal is generally assayed in cell cultures using x-gal or FDG (fluorescent analogue fluorescein-di-β-dgalactopyranoside)(Yang and Hu, 2004) . Histochemistry staining with x-gal is also used of rodent senescence model and human premalignant lesions (Braig et al., 2005; Michaloglou et al., 2005).

The senescent cells have enriched heterochromatin region, term senescence-associated heterochromatin foci (SAHF). The SAHFs have the typical marker of heterochromatin such as He3K9me3 (Narita et al., 2003). It is proposed that a global alteration of chromatin, mediated by the formation of senescence-associated heterochromatin foci, controls the irreversible growth arrest in senescence. The change in the genomic organization results in the permanent suppression of genes essential for proliferation. This genomic change gives rise to a visible morphology change of the chromosomes, forming heterochromatin foci, which can be detected under fluorescent microscope using DAPI staining.

1.3.1.2 Oncogene-induced senescence

Oncogene expression in normal cells can trigger senescence phenotype. Oncogenic RAS-induced senescence is one of well studied model of oncogene-induced senescence. Here I am using RAS-induced senescence as a system to introduce OIS.

RAS mutations have been found in 30% of human tumors, making it the most common oncogenic mutation ever found in human tumor samples(Bos, 1989). Activated RAS promotes cancer cell growth through interacting with a number of downstream effectors, including RAF family protein and PI3K(Downward, 2003).Interestingly, despite its expected role in promoting tumorigenesis, ectopic expression of oncogenic RAS in primary cells causes senescence phenotype. It was found that after the initial hyperproliferation triggered by RAS, the primary cells eventually enter an irreversible growth arrest state now known as oncogene-induced senescence. p53 and p16 activity are required for the establishment of the phenotype. Removing p16 or p53 will lead to a bypass of senescence phenotype in RAS expressing MEF cells (Serrano et al., 1997). To achieve a full-blown neoplastic transformation, multiple genetic mutations in addition to oncogenic RAS are required to cooperate to evade the senescence barrier. Oncogene-induced senescence provides a barrier to uncontrolled proliferation, serving as a bona fide tumor preventive mechanism (Figure 1.8).

The physiological relevance of oncogene-induced senescence was under debate for a long time. Tuveson, et al established an oncogenic K-RAS knock-in mouse model and showed that the oncogenic K-RAS gene promotes tumor development instead of causing senescence. The mouse embryonic fibroblast (MEF) isolated from the knock-in mouse model did not develop a senescent phenotype, but rather become immortalized (Tuveson et al., 2004). They argued that oncogene induced senescence might be an artifact of oncogene overexpression.

However, it has been shown that a subset of adenomas from these same mice do undergo senescence *in vivo* (Collado et al., 2005), raising the possibility that different cell types

may be differentially sensitive to the same signal. In addition, mutations in K-ras,*B-raf, PTEN* and *NF1* are shown to trigger cellular senescence *in vivo* in human tumors and mouse tumor models (Braig et al., 2005; Chen et al., 2005; Collado et al., 2005; Michaloglou et al., 2005; Courtois-Cox et al., 2006; Dankort et al., 2007; Sarkisian et al., 2007). In the skin, normal melanocytes exhibit a low proliferation index and negligible senescence; dysplastic nevi, the precancerous lesions, exhibit senescence marker and a low proliferation index (because senescent cells do not proliferate); and in melanoma there is loss of the senescent phenotype and a high proliferation index (Michaloglou et al., 2005). In colon, the normal tissue has a very high proliferation index; progression to adenoma, which is precancerous lesion, leads to senescence and a significant decrease in the proliferation index; whereas further progression to carcinoma is associated with escape from senescence and a high proliferation index similar to that of the normal tissue(Campisi, 2005). These findings suggest that oncogene-induced senescence exists in physiological conditions and potentially prevent the precancerous lesion from transforming into cancer.

1.3.2 Mechanism of oncogene-induced senescence

Several mechanisms are proposed to regulate oncogene-induced senescence. It is very likely that these mechanisms may work in concert for the initiation and development of OIS (Figure 1.9).

1.3.2.1 Role of p53/p21 pathway in senescence

As mentioned above, p53 is essential for OIS. The MEF cells with p53 deletion fail to enter oncogene-induced senescence. Both p53 protein stability and phosphorylation are reported to affect OIS.

The protein stability of p53 is regulated by ubiquitin pathway. There are two proteins participating the regulation of p53 stability: the E3 ubiquitin ligase MDM2 which causes p53 ubiquitination and targets it for degradation(Haupt et al., 1997); ARF, an inhibitor of MDM2. Under resting condition, p53 is easily degraded through proteosome degradation pathway(Honda and Yasuda, 1999). In response to cellular stress, ARF is upregulated and sequesters MDM2, hence prevents interaction between MDM2 and p53. Dissociation between MDM2 and p53 impairs p53 ubiquitination and increases p53 stability(Weber et al., 1999).

Phosphorylation of p53 is mediated by p38MAPK pathway in OIS. Expressing RAS leads to the activation of p38 via MKK3/6. The activated p38 can phosphorylates p53 directly or indirectly through activated PRAK (Bulavin et al., 1999; Sun et al., 2007). Ablation of p53 phosphorylation by mutation of the targeted serine residues into alanines causes attenuation of senescence phenotype, suggesting that p53-mediated senescence may rely on p38 mediated phosphorylation (Sun et al., 2007).

Activated p53 transactivates the CDK inhibitor p21 and induces senescence. p21 protein binds and inhibits the activity of cyclin-dependent kinase: CDK1, CDK2 and CDK4/6 complex and thus functions as an inhibitor against G1to S cell cycle progression(Gartel and Radhakrishnan, 2005).

1.3.2.2 Role of p16/RB pathway in senescence

p16/Rb pathway has also been shown to play an important role in senescence. p16 INK4 is an inhibitor of CDK4/6(Serrano et al., 1997). The CDK4/6 are responsible for phosphorylation of Rb protein, which upon phosphorylation will activate E2F family transcription factors and promote S-phase progression (Narita et al., 2003). Expression of oncogenic RAS results in an increase of p16 level. Increase in p16 inhibits CDK4/6 and as a consequence, Rb phosphorylation decreases and subsequently represses E2F function. The cell cycle is paused due to the repression of E2F target genes, which are essential for entry into S-phase. At the same time, p16/Rb pathway leads to the formation of senescence-associated heterochromatin foci, which prevent the access of E2F transcription factor to its target genes, hence repressing the expression of genes crucial for proliferation and further contributeing to cell-cycle arrests(Narita et al., 2003).

1.3.3 Role of ROS signaling in OIS

Reactive oxygen species production is proposed as a major cause of OIS. It has been shown that culturing oncogene expressing cells under low oxygen condition or in presence of ROS scavenger can significantly attenuate senescence phenotype(Lee et al., 1999; Parrinello et al., 2003). Conversely, treating the cells with H_2O_2 alone is able to induce senescence phenotype (Chen and Ames, 1994; Parrinello et al., 2003).

Interestingly, the ROS concentration that cause senescence is lower than that triggers apoptosis (Giorgio et al., 2007), leading to the hypothesis that ROS participate in signal transduction rather than causing damage in oncogene-induced senescence. In oncogenic RAS-induced senescence, RAS signaling regulates ROS production. It is suggested that the RAS

signaling promotes the assembly of NOX protein complex, through the activation of RAS target Rac1: one of the NOX protein activator(Sundaresan et al., 1996), thus heightens ROS production. ROS are shown to activate the p38 pathway, which in turn phosphorylates and activates p53 in OIS (Jung et al., 2004). However, the direct targets of ROS in senescence remain to be explored.

1.3.4 PTP and senescence

While several PTPS have been implicated in regulation of OIS, the redox regulation of PTPs in the context of oncogene-induced senescence has not yet been investigated. Induction of MKP1 and DUSP5 inactivate ERK pathways and rescue cells from RAS-induced senescence (Callejas-Valera et al., 2008). Furthermore, knock down of DSP, VHR or MKP3 in cancer cell lines is enough to induce senescence. It was proposed that knock down of these enzymes might activate ERK to induce senescence (Park et al., 2007). These reports indicate that inactivation of PTPs are important for OIS. We are interested to test whether the ROS mediated PTP oxidation and inactivation occurs in oncogene-induced senescence and to understand the role of PTP oxidation in OIS.

1.4 Rationale and Significance of the Study

RAS signaling induces ROS production possibly through the acute activation of NADPH oxidases (NOX) (Brown and Griendling, 2009b). Superoxide is then rapidly converted to the more stable, and membrane-permeant, oxygen derivative hydrogen peroxide by spontaneous or enzymatic dismutation (Brown and Griendling, 2009b). It is shown that ROS production is an essential element of cell-cycle arrest induced by oncogenic RAS (Chen and Ames, 1994;

DeNicola and Tuveson, 2009a; Lee et al., 1999). Although the molecular mechanism of ROS-induced senescence is unknown, it has the potential to involve the reversible redox inactivation of members of the PTP family. Oxidative inactivation of PTPs might be important in regulating signal pathways that leads to senescence.

In this project, we demonstrated that PTP1B was reversibly oxidized and inactivated in human diploid fibroblasts expressing high levels of the H-RAS^{V12} oncogene. We observed that the inactivation of PTP1B led to hyperphosphorylation of argonaute (Ago) 2 on Tyr 393. Recently, it was shown that phosphorylation of Ago2 on Tyr 393 decreases its interaction with Dicer and inhibits the maturation of miRNA (Shen et al., 2013a). Here, we have shown that this modification prevented miRNA loading on Ago2, compromised the regulation of p21 mRNA and induced senescence. These findings shed new light on the role of PTP1B in senescence and on how ROS signalling is tightly linked to miRNA-mediated post-transcriptional regulation.

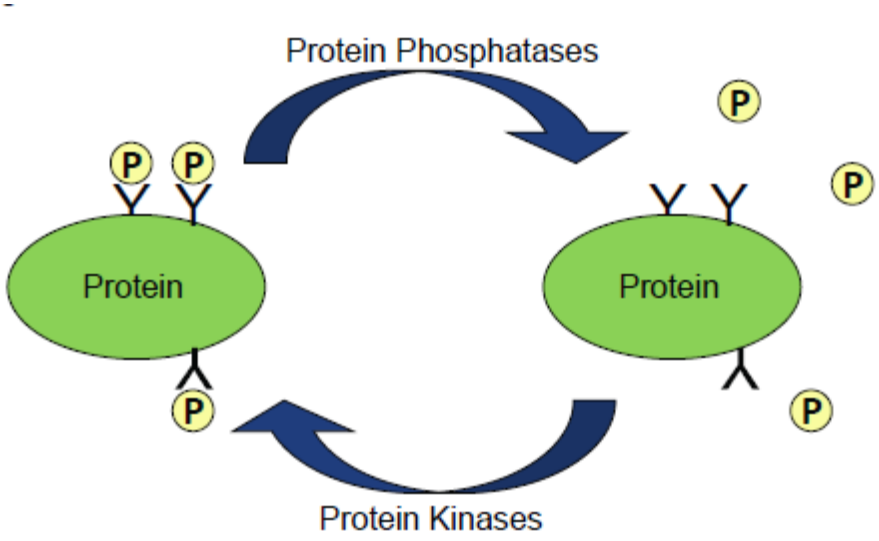

Figure1.1. Reversible phosphorylation of proteins.

Protein phosphorylation is one of the major signal transducing mechanisms in cells. Two groups of enzymes control the protein phosphorylation states: the protein kinases and the protein phosphatases. The kinases transfer phosphate groups from ATP to protein, whereas the protein phosphatases catalyze the removal of phosphate groups.

A

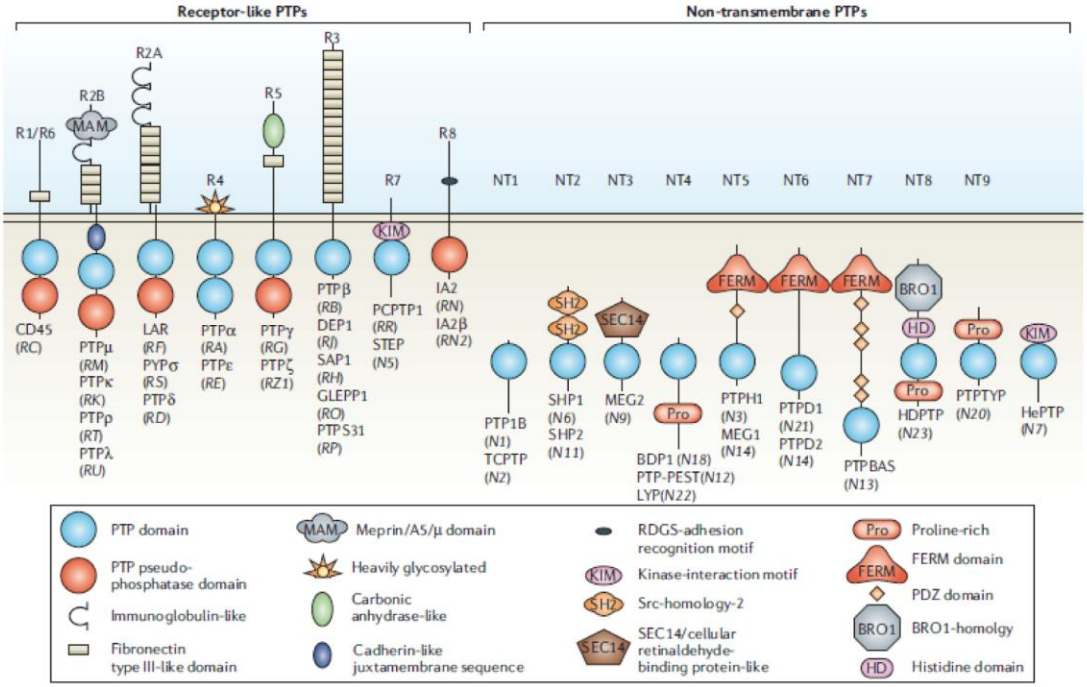
Receptor-like PTPs
Non-transmembrane PTPs
R1/R6
R2A
R2B
MAM
R3
R4
R5
R7
R8
KIM
NT1
NT2
NT3
NT4
NT5
NT6
NT7
NT8
NT9
CD45 (RC)
PTPμ (RM) PTPκ (RK) PTPρ (RT) PTPλ (RL)
LAR (RF) PYPσ (RS) PTPδ (RD)
PTPα (RA) PTPε (RE)
PTPγ (RG) PTPζ (RZ1)
PTPβ (RB) DEP1 (RJ) SAP1 (RH) GLEPP1 (RO) PTPS31 (RP)
PCPTP1 (RR) STEP (N5)
IA2 (RN) IA2β (RN2)
PTP1B (N1) TCPTP (N2)
SH2
SHP1 (N6) SHP2 (N11)
SEC14
MEG2 (N9)
Pro
BDP1 (N18) PTP-PEST(N12) LYP(N22)
FERM
PTPH1 (N3) MEG1 (N14)
PTPD1 (N21) PTPD2 (N14)
PTPBAS (N13)
BRO1
HD
HDPTP (N23)
PTPTYP (N20)
HePTP (N7)
PTP domain
PTP pseudo-phosphatase domain
Immunoglobulin-like
Fibronectin type III-like domain
MAM Meprin/A5/μ domain
Heavily glycosylated
Carbonic anhydrase-like
Cadherin-like juxtamembrane sequence
RDGS-adhesion recognition motif
Kinase-interaction motif
Src-homology-2
SEC14/cellular retinaldehyde-binding protein-like
Proline-rich
FERM domain
PDZ domain
BRO1-homolgy
Histidine domain

B

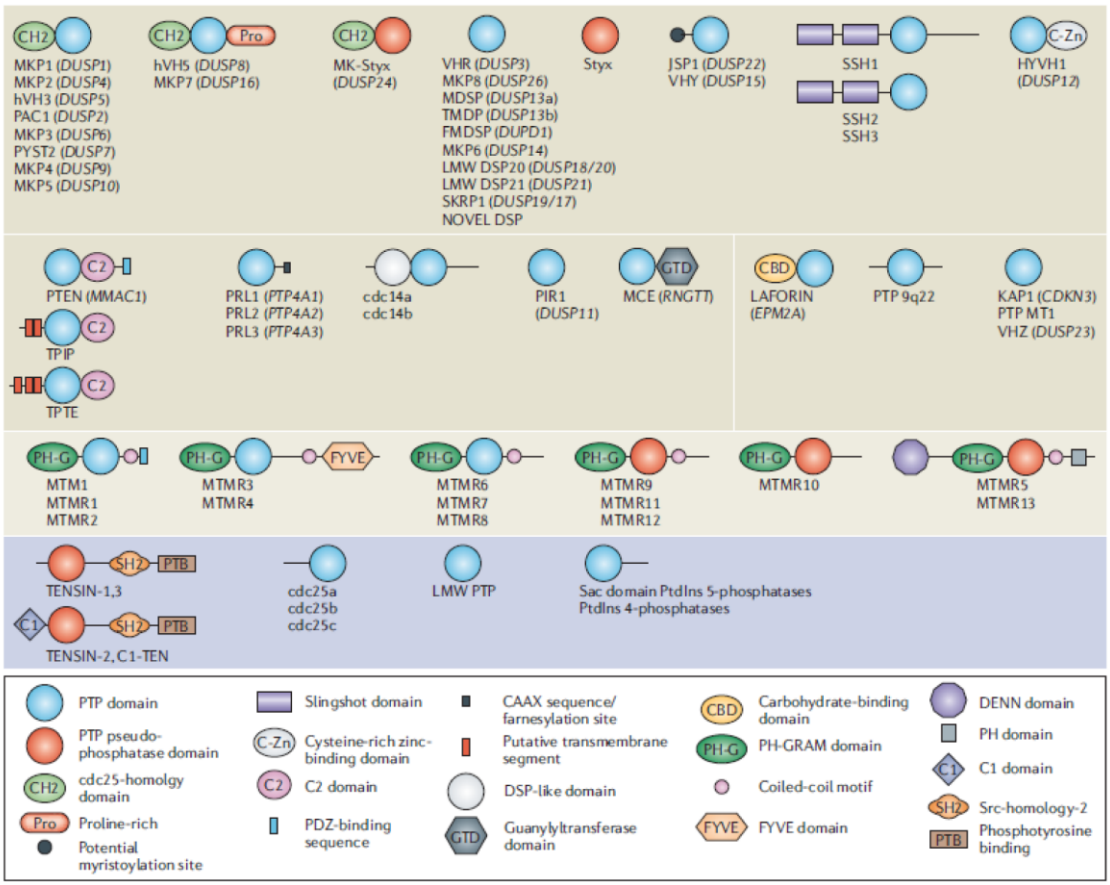
CH2
Pro
C-Zn
MKP1 (DUSP1)
MKP2 (DUSP4)
hVH3 (DUSP5)
PAC1 (DUSP2)
MKP3 (DUSP6)
PYST2 (DUSP7)
MKP4 (DUSP9)
MKP5 (DUSP10)
hVH5 (DUSP8)
MKP7 (DUSP16)
MK-Styx (DUSP24)
VHR (DUSP3)
MKP8 (DUSP26)
MDSP (DUSP13a)
TMDP (DUSP13b)
FMDSP (DUPD1)
MKP6 (DUSP14)
LMW DSP20 (DUSP18/20)
LMW DSP21 (DUSP21)
SKRP1 (DUSP19/17)
NOVEL DSP
Styx
JSP1 (DUSP22)
VHY (DUSP15)
SSH1
SSH2
SSH3
HYVH1 (DUSP12)
C2
PTEN (MMAC1)
TPIP
TPTE
PRL1 (PTP4A1)
PRL2 (PTP4A2)
PRL3 (PTP4A3)
cdc14a
cdc14b
PIR1 (DUSP11)
GTD
MCE (RNGTT)
CBD
LAFORIN (EPM2A)
PTP 9q22
KAP1 (CDKN3)
PTP MT1
VHZ (DUSP23)
PH-G
FYVE
MTM1
MTMR1
MTMR2
MTMR3
MTMR4
MTMR6
MTMR7
MTMR8
MTMR9
MTMR11
MTMR12
MTMR10
MTMR5
MTMR13
SH2
PTB
TENSIN-1,3
C1
TENSIN-2, C1-TEN
cdc25a
cdc25b
cdc25c
LMW PTP
Sac domain PtdIns 5-phosphatases
PtdIns 4-phosphatases
PTP domain
PTP pseudo-phosphatase domain
cdc25-homolgy domain
Proline-rich
Potential myristoylation site
Slingshot domain
Cysteine-rich zinc-binding domain
C2 domain
PDZ-binding sequence
CAAX sequence/ farnesylation site
Putative transmembrane segment
DSP-like domain
Guanylyltransferase domain
Carbohydrate-binding domain
PH-GRAM domain
Coiled-coil motif
FYVE domain
DENN domain
PH domain
C1 domain
Src-homology-2
Phosphotyrosine binding

Figure 1.2 The Protein Tyrosine Phosphatase Family

(A) The classical PTPs are divided in two broad groups – the transmembrane receptor-like proteins (RPTPs) and non-transmembrane (NT) cytoplasmic proteins. The PTPs are structurally and functionally different from the Ser/Thr phosphatases. They are defined by the presence of a signature motif in the catalytic core, in which Cys and Arg are essential for catalysis. Receptor-like PTPs can regulate cellular signaling by ligand controlled dephosphorylation of the tyrosine residues of the substrate proteins whereas the non-transmembrane PTPs dephosphorylate their substrates at various locations in the cytoplasm. (B)The dual specific PTPs (DSPs) also have the HC(X)5R activesite signature motif. The DSPs are more structurally diverse than the classical PTPs and possess a smaller conserved catalytic domain. [adopted from (Tonks, 2006)]

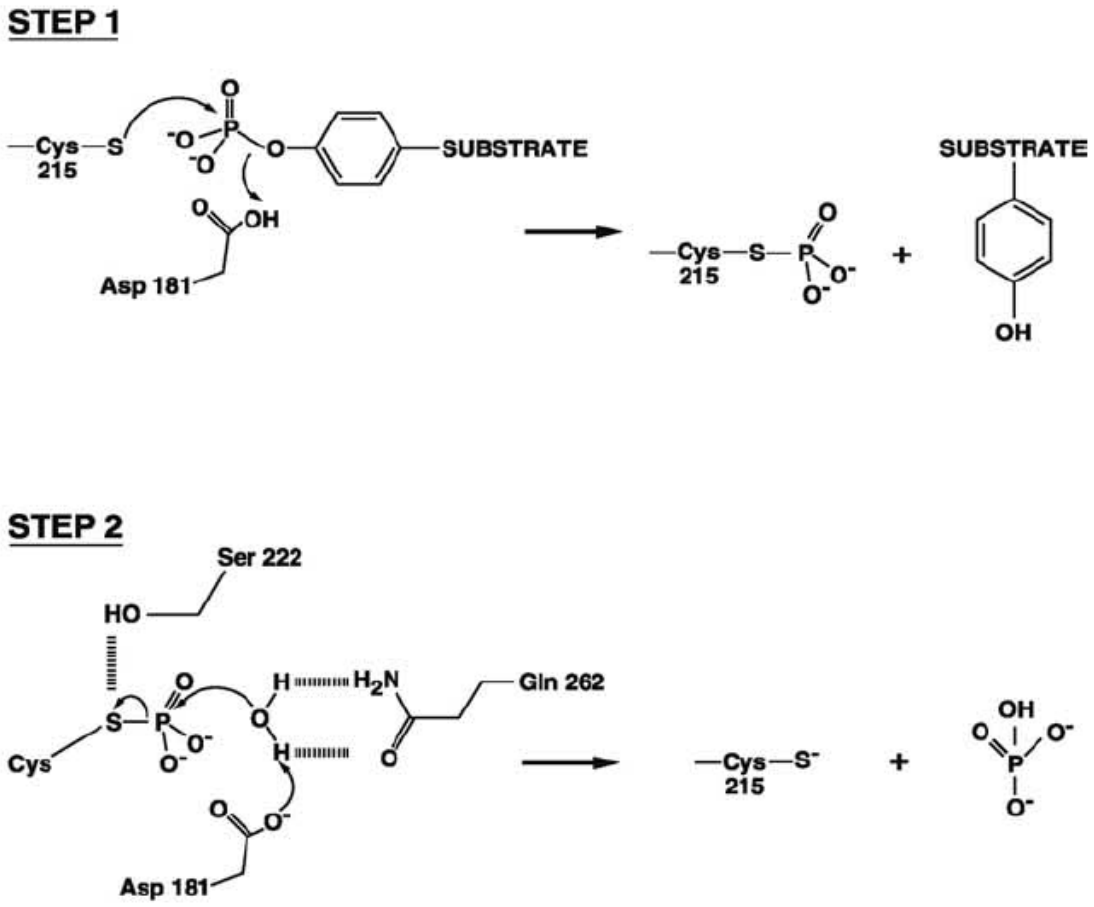

Figure 1.3 General catalytic mechanism of PTPs.

In the first step the cysteine in the active site acts as a nucleophile that attacks the incoming phosphate; the aspartate in the WPD loop functions as a general acid to form the cysteinyl phosphate as an intermediate with release of the dephosphorylated substrate. In the second step, the cysteinyl phosphate intermediate is hydrolyzed to release free phosphate and to restore the active form of the enzyme [adopted from (Tonks, 2003)].

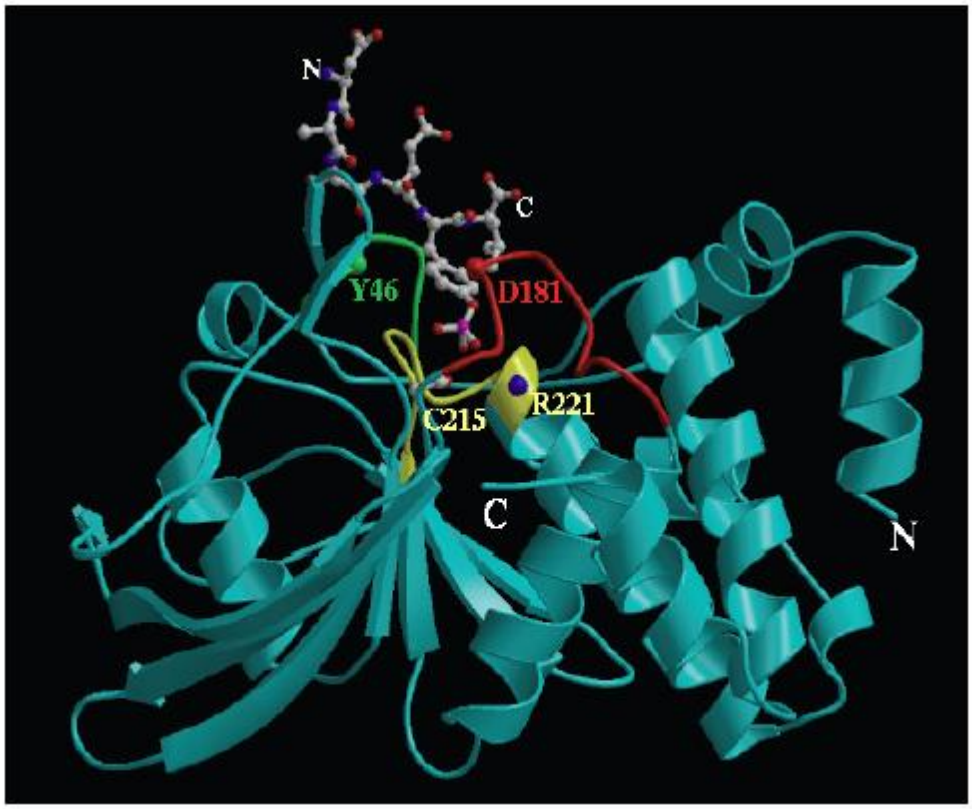

Figure 1.4 Structure of PTP1B active site

Crystal Structure of the active site of PTP1B. Ribbon representation of the crystal structure of the 37 kDa catalytic domain of PTP1B in conjunction with a hexapeptide substrate, modeled on the basis of the autophosphorylated epidermal growth factor receptor (EGFR), which is a physiological substrate of PTP1B (Jia et al., 1995). Critical elements of the catalytic core – the signature motif (yellow), the WPD loop (red) and the pTyr loop (green) are shown.

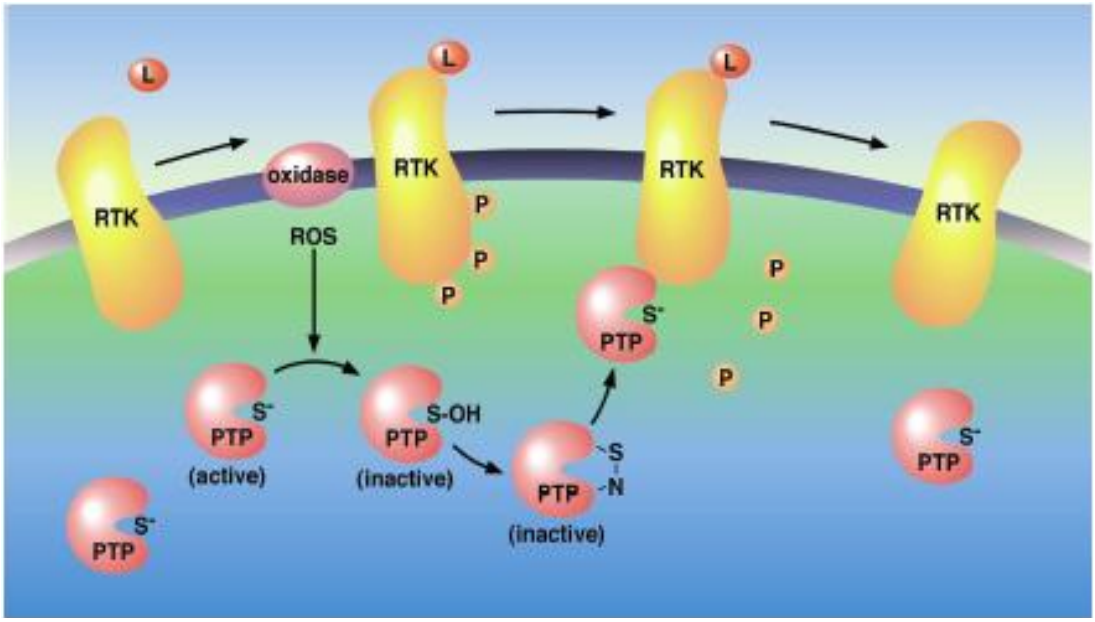

Figure 1.5. A model for regulation of signal transduction by ROS

Ligand (L) dependent activation of a receptor tyrosine kinase (RTK) triggers the production of ROS through Rac-dependent NADPH oxidase assembly at the membrane. ROS oxidize the active site Cys residue of PTPs, converting it from a thiolate ion (the active form) to sulphenic acid (inactive form). Oxidation mediated inhibition of PTP activity promotes tyrosine phosphorylation. The sulphenic acid form of the active site Cys residue is rapidly converted to a sulphenyl-amide moiety, protecting it from irreversible oxidation. This oxidation of the PTPs is reversible and the enzymes are restored to their active conformation by cellular thioredoxin or glutathione [adopted from (Tonks, 2003).

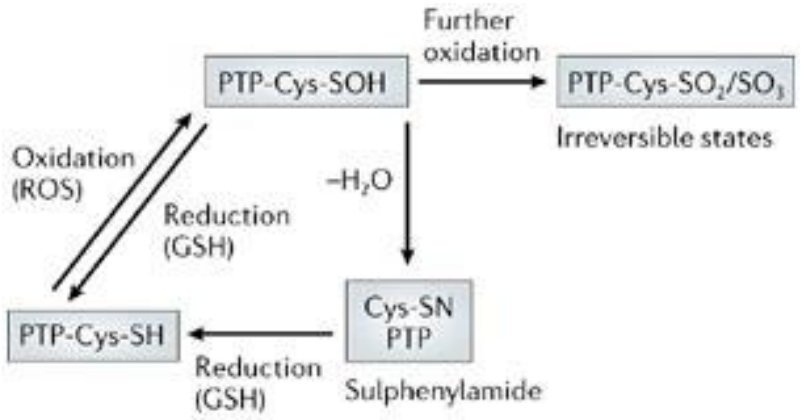

Figure 1.6 PTP Function is Regulated by Oxidation

The overall regulation of PTP1B function by oxidation is shown here. Reactive oxygen can modify the active site cysteine to a sulphenic form which no longer acts as a nucleophile and the enzyme is inactivated. This change, however, is reversible through the formation of a sulphenyl-amide intermediate. This regulatory mechanism not only protects the phosphatase from irreversible modification due to further oxidation to the sulphinic and sulphonic forms, which are permanently inactivated but it also keeps the option open for the transiently inactivated form of the enzyme to regain its active status.[adopted from (Östman, et al 2006)]

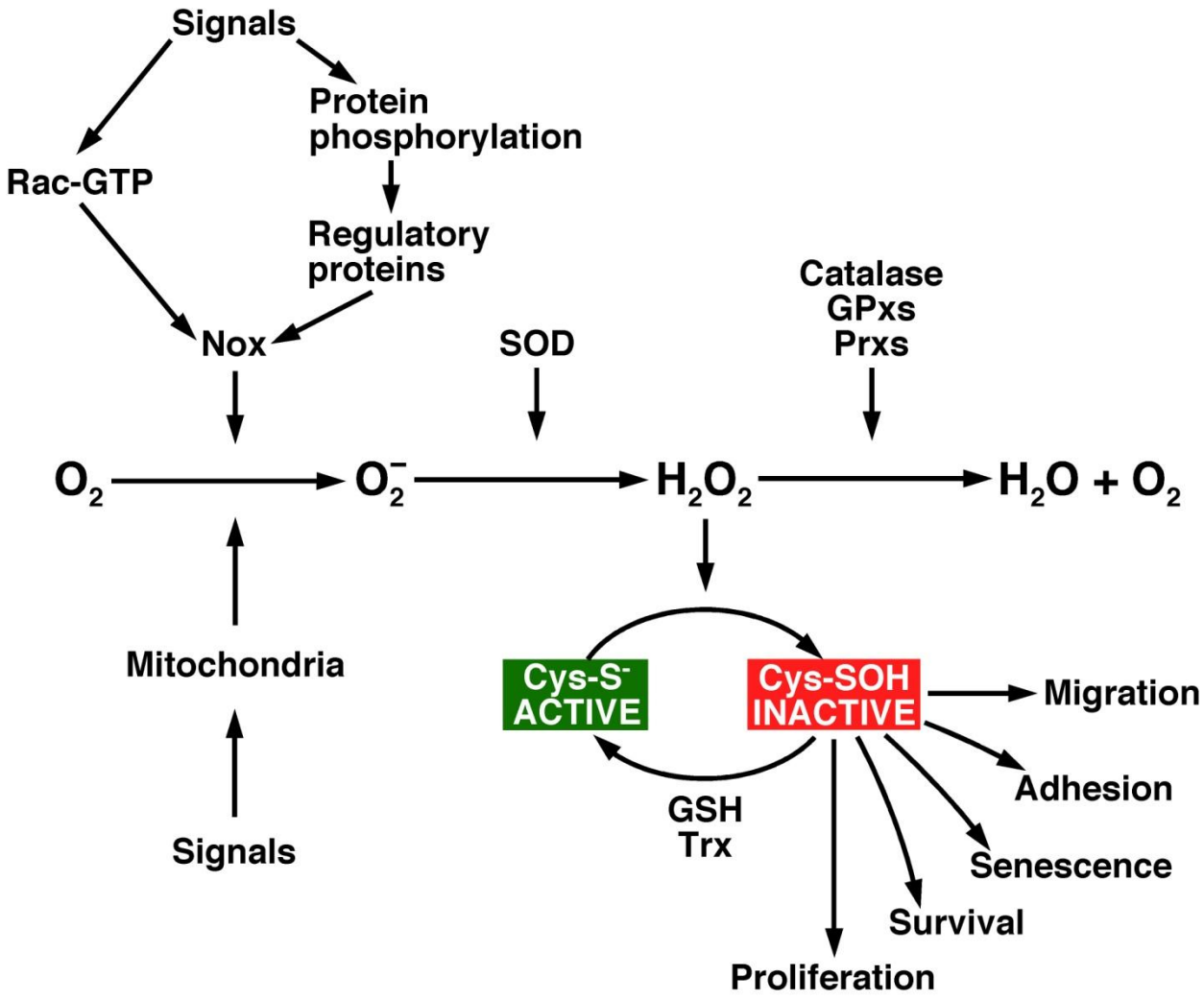

Figure 1.7 Controlled production of ROS

Two major sources of ROS production *in vivo* are NADPH oxidase and mitochondria. They produce superoxide in response to signal stimulation. The superoxide can be dismutated into H_2O_2, which can be further reduced into water and oxygen by reducing agents in the cells. H_2O_2 selectively reacts with the catalytic cysteines and regulates different cellular processes.

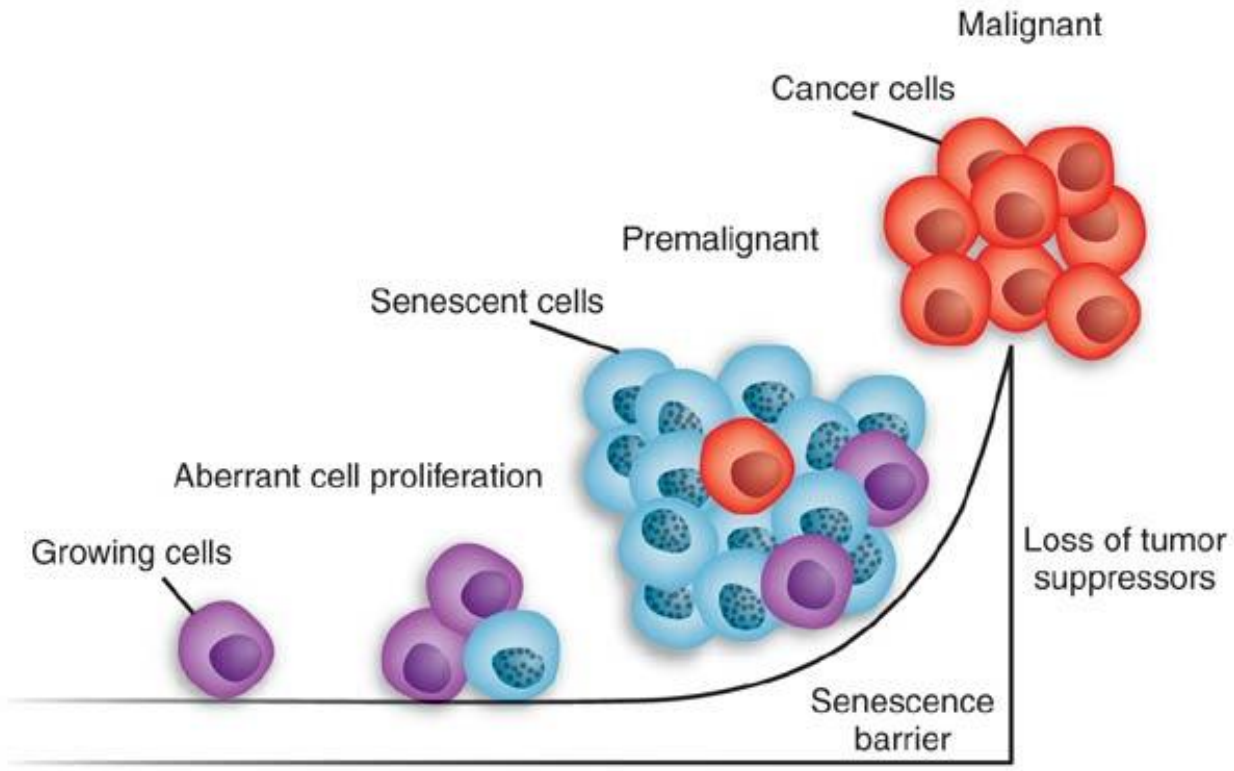

Figure 1.8 Oncogene-induced senescence

Oncogene expression in normal cells initially will cause aberrant cell proliferation (purple cells). Most of the cells eventually stop growing and become senescent (blue cells). The neoplastic growth can remain benign for years until a second mutation occurs and cooperates with the original oncogene and leads to transformation the cells into malignant cancer (red cells).[adopted from (Narita and Lowe, 2005)]

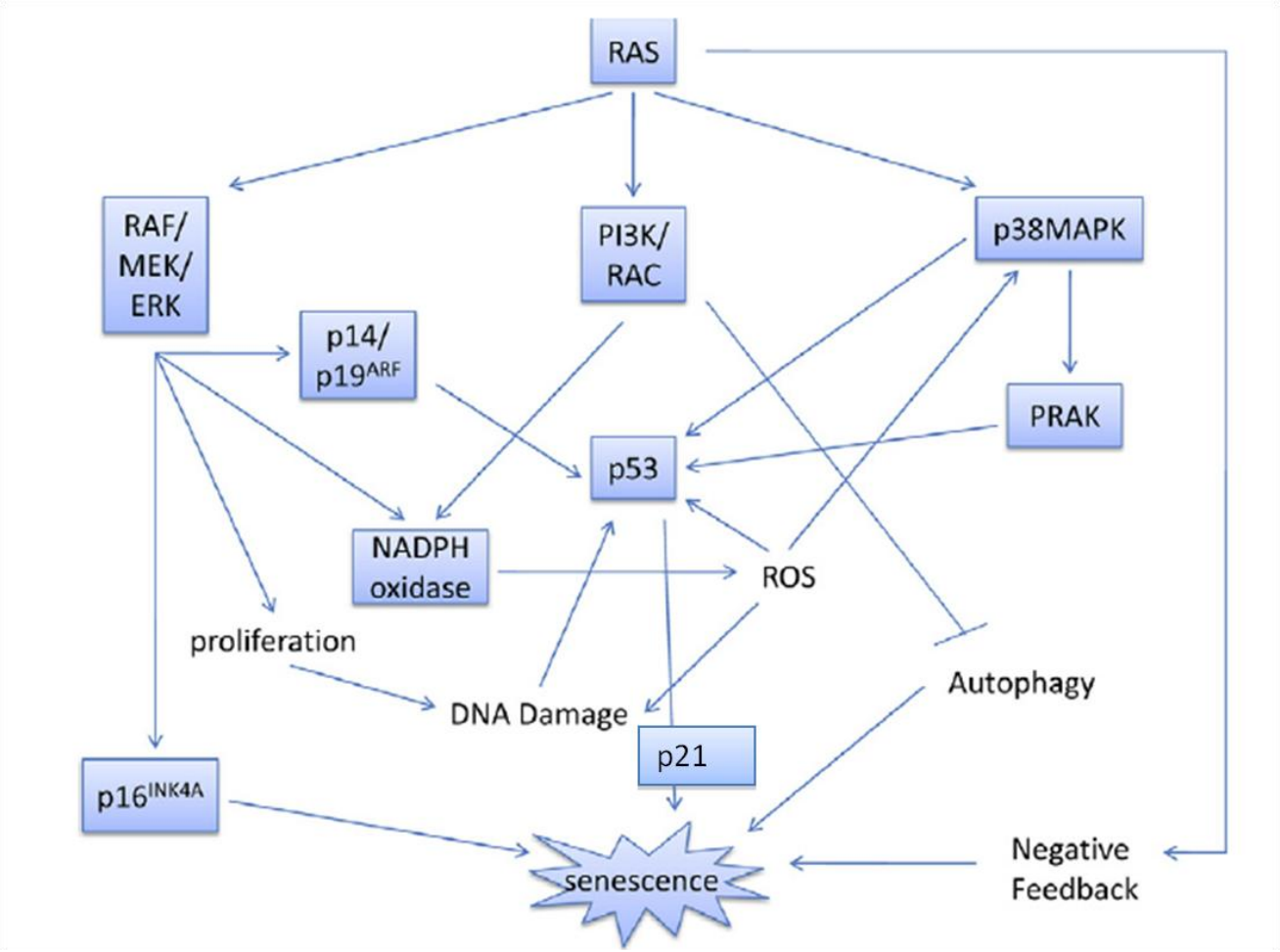

Figure 1.10 Mechanism of oncogene induced senescence. [Adopted from (DeNicola and Tuveson, 2009b)]

Chapter2

2.1 Introduction

In Chapter 1, I introduced the redox regulation of PTP activity having a profound effect on signal transduction and the significance of oncogene-induced senescence as an anti-cancer mechanism. It is thought that ROS production and the sequential induction of tumor suppressor pathways drives oncogenic-RAS induced senescence. However, the molecular mechanism of RAS-induced senescence is unknown and potentially involves the reversible oxidation and inactivation of members of the PTP family by hydrogen peroxide. To test this hypothesis, we utilized human diploid fibroblasts expressing H-RAS^{V12} oncogene as a model OIS system and applied a cysteinyl-labeling assay developed by our lab to identify PTPs that are reversibly oxidized.

2.1.1 The system to study OIS

A system to study OIS was previously established by overexpressing a constitutively active form of RAS, HRAS^{V12} protein in human diploid fibroblasts (Serrano et al., 1997). The glycine to valine mutation at G12 renders the GTPase domain of RAS insensitive to Ras-GAP, the protein that inactivates RAS. Thus, the G12V mutation locks RAS in a constitutively active state. (Downward, 2003)

The model system that I used in this project to study OIS is the human diploid fibroblast IMR90 cell lines stably overexpressing oncogenic RAS gene (H-RAS^{V12}), which is a well established and characterized model system for OIS(Courtois-Cox et al., 2008). To induce

senescence in IMR90 cells, the cells were infected with retroviruses expressing oncogenic RAS. After being selected for positive RAS expression, the cells are kept in fresh medium for up to 6 days. It was shown that the cells expressing oncogenic RAS developed senescent phenotype by day 6 post-selection.

2.1.2 Detection cellular ROS

It is suggested that H_2O_2 but not superoxide is responsible for PTP oxidation (Denu and Tanner, 1998; Meng et al., 2002; Rhee et al., 2003). In our study, we focused on measuring the production of H_2O_2 in senescent cells and studying its effect on PTP oxidation.

Chang's group synthesized a PF1 probe that displays a >500-fold response to H_2O_2 over such ROS as superoxide, tert-butylhydroperoxide (TBHP), NO, and hypochlorite. This is in contrast to traditional ROS indicators like dihydrodichlorofluorescein and dihydrorhodamine which report global oxidant indices by non-specific dye oxidation. In addition, PF1 is membrane permeable and can image changes in intracellular H_2O_2 pools within living cells(Miller et al., 2005). Upon reacting with H_2O_2, the PF1 probe generates a >1000-fold increase in green fluorescence. PF6-AM probe is the third generation of PF1 probe, which is designed based on similar chemistry. It has higher sensitivity to H_2O_2 and enhanced cellular retention (Dickinson et al., 2011a) (Figure 2.14). In our study, we used the PF6-AM probe to detect intracellular H_2O_2 .

2.1.3 Methods of detecting PTP oxidation

Several different methods have been developed in the endeavor of monitoring PTP oxidation (Table 2.1). The first methods developed to detect and quantify PTP oxidation is a

negative approach that detects the decrease of signal, compared to the control samples. Lee. et al used the radioactive labeled IAA to alkylate reduced form of PTPs when lysing the cells. The oxidized form of PTPs is left unaffected by IAA during the lysis. Specific PTPs can then be immunoprecipated and be visualized by autoradiography. The decrease of radioactivity (compared to the control) of a specific PTP reflects the increase of its oxidation level(Lee et al., 1998). However this method has certain limitations. For instance, in this method, the decrease in radioactive signal represents the level of PTPs oxidation. When a small percentage of a particular PTP undergoes oxidation and the major portion of the PTP remains in the reduced form, the change in radioactive signal might not be significant enough to detect.

The modified in-gel PTPase assay was the first technique used to detect an increase in PTP oxidation (Meng et al., 2002). The lysate is first alkylated with IAA to block the reduced form of PTPs. Then the lysate is resolved on SDS-PAGE gel, followed by reduction of the reversibly oxidized cysteine. The resolved and reduced proteins are renatured in-gel and react with a radioactively labelled PTP substrate (i.e., ^{32}P-labelled poly(GluTyr)) that is incorporated into the gel prior to polymerization. The activity of the now reactivated PTPs, which are formerly oxidized, can be detected by autoradiography as regions where ^{32}P has been selectively removed, showing as a negative band(Meng et al., 2005). The advantage of modified in-gel PTPase assay is that it enables the global, positive and more sensitive identification of PTP oxidation. The limitation of the assay is that some PTPs such as RPTPs do not renature well in-gel and their activity cannot be detected by this assay.

An antibody based approach to enrich oxidized PTPs has been developed recently. This approach uses an antibody (PTPox antibody) raised against the terminally and irreversibly oxidized (Cys-SO_3H) Val-His-Cys-Ser-Ala-Gly peptide from the PTP signature motif. To analyze PTP oxidation, the PTPs in reduced form are blocked by NEM (N-ethylmaleimide), which prevents them from the getting oxidized, while the PTPs with the sulfenic and sulfinic form of cysteine are terminally oxidized by pervanadate and enriched by PTPox antibody. The precipitates can be analyzed using antibodies blotting for particular PTPs. This method can also be coupled with MS analysis to identify the PTPs enriched by the PTPox antibody from cell lysate (Persson et al., 2004). However, the method could not distinguish between reversibly oxidized PTPs and the terminally oxidized PTPs.

Our lab has developed a modified cysteine-labeling assay that captures PTPs that have been reversibly oxidized *in vivo* (Figure 2.4). It takes advantage of the unique, low pKa of the active-site cysteine residue which is characteristic of members of the PTP family. The cells were lysed in an anaerobic condition at pH 5.5 buffer containing Iodoacetic acid (IAA). The reduced form of catalytic Cys residues of PTPs are alkylated, which excludes them from the following reduction and labeling treatment. Conversely, the Cys residues that are reversibly oxidized are protected from irreversible alkylation. Extra IAA is then removed from the lysate by buffer exchange using size-exclusion spin columns, and the reversibly oxidized Cys residues are reduced with TCEP. In the pH 5.5 buffer, the catalytic cysteine of most PTPs (including classical PTPs and DUSPs) remains in the active thiolate (S^-) state and are reactive with the alkylating IAP probe. The majority of cysteine-containing proteins are in the thiol (SH) state and cannot react with the probe. Using this low pH buffer for the labeling, we increase the specificity of the

probe, which will selectively target low pKa cysteines including the catalytic cysteines of PTPs. The biotin tag on the IAP probe enables us to enrich the protein labeled by the probe using streptavidin beads. After strepavidin pull-down, we can use anti-Biotin antibody to detect the overall proteins labeled and enriched in the cysteine-labeling assay or use antibodies against specific PTPs to detect whether the PTPs underwent reversible oxidation (Boivin et al., 2010a).

Our lab generated a conformation-sensor single chain antibody: scFv that recognized the reversibly oxidized form of PTP1B. We used a ScFv developed to measure the level of PTP1B oxidation. As mentioned in Chapter 1, PTP1B reversible oxidation on the catalytic cysteine produces a sulfenic acid (S-OH) intermediate that undergoes a rapid condensation reaction to produce a 5-atom cyclic sulfenylamide species, in which the sulfur atom of the catalytic cysteine is covalently linked to the main-chain nitrogen of the adjacent serine residue (Salmeen et al., 2003; van Montfort et al., 2003). Formation of this sulfenyl-amide intermediate causes significant conformational changes in the active site. The PTP loop containing the signature motif and Tyr46 of the phosphotyrosine loop, which are both normally buried in the structure, now are exposed to the surface of the protein and become solvent accessible. The scFv selectively binds to reversibly oxidized PTP1B. Using this antibody, we can determine PTP1B oxidation both *in vivo* and *in vitro* (Haque et al., 2011b).

2.2 Material and Method

2.2.1 DNA constructs

The retroviral vector pBabe–*H-RAS*^{V12}-Puro were generous gifts from Dr. Linda Van Aelst (Lin et al., 1998). pWZL–*PTP1B*-Hygro WT, DA and CS mutants were generated as described previously (LaMontagne et al., 1998).

2.2.2 Cell line and infection:

Human primary lung fibroblast IMR90 cells were obtained from ATCC and cultured in DMEM plus 10% FBS, pen/strep and 10% non-essential amino acid (NEAA). The virus packaging cell line Phoenix cells were obtained from Cold Spring Harbor Laboratory. The Phoenix cells were cultured in DMEM plus 10% FBS and pen/strep. Virus were generated using Phoenix cells and virus containing media was collected every 12hrs, from 24hrs after transfection. For infection, the target fibroblasts were incubated with virus containing media for 12hrs and supplied with fresh virus for another 12hrs. 36hrs later after first infection, the infected cells population were purified by adding 2microg/ml puromycin for 48hrs. For infecting cells with two virus, virus were made and collected separately from Phoenix cells, and two different virus were mixed at 1:1 ration and infected the IMR90 cells at the same time, for 3 times at 12 hr interval. The infected cells were first selected with 2 microg/ml puromycin for 48 hrs and then 40 microg/ml of hygromycin for 6 days.

2.2.3 Senescence-Associated-β-galactosidase activity staining

Senescence-Associated-β-galactosidase activity (SA-β-gal) activity was detected using Senescence b-galactosidase staining Kit following the manufacturer's instructions. Cells were washed once in PBS (pH7.2), fixed for 3-5 min (room temperature) with 0.5% glutaraldehyde (PBS [pH7.2]), washed, and supplemented with 1mM MgCl2, incubated at 37°C (no CO2) with fresh senescenceassociated (3-Gal (SA-,3-Gal) stain solution: X-gal solution (1 mg/ml X-gal [Boehringer], 5 mM K3Fe[CN], 5mM K4Fe[CN]6, 1 mM MgCl2 in PBS at pH 6.0) overnight at 37C.Numbers of senescent cells were counted using in 10 fields for each sample, using a 10X magnifying lens microscope. The percentage of senescent cells was calculated as the number senescent cells in each sample over the number of total cells.

2.2.4 Cysteine-labeling assay

Assay was preformed as previously described (Boivin, Yang et al. 2010). In brief, cells were serum starved overnight in phenol-red free DMEM before lysis under anaerobic condition in de-gas buffer (50 mM NaAc, 150 mM NaCl, 10% Glycerol, 1% Triton X100, with 5ug/ml Apotinin and Leupeptin, 60 U/ml SOD, 100U/ml Catalase, 10mM IAA,) to prevent post-lysis oxidation. After buffer exchange to remove the excessive IAA in the lysis buffer, using Zeba spin column 7KDa cut-off (Thermo scientific) and TCEP reduction, the IAP-biotin probe (Thermo scientific) was added into the lysate, at 5mM final concentration to label the reversibly oxidized proteins. The labeled proteins were then pull-down by streptavidin sepharose beads (GE healthcare), washed 3X with lysis buffer (pH 5.5) and resuspended in 20 μl 4X Laemmli sample buffer and heated at 90°C for 90 sec and resolved by SDS-PAGE.

2.2.5 Hydrogen peroxide molecular imaging

Molecular imaging of RAS-induced hydrogen peroxide production in IMR90 cells was studied using a Perkin-Elmer Ultraview Spinning Disk confocal operating on a Nikon Ti microscope with the In Vivo Scientific Chamber, heater and gas regulator as previously described (Dickinson et al., 2011b)

2.2.6 Amplex Red Assay

For measurement of ROS levels, cells were seeded in 96-well plates at $1.5 \bullet 10^4$ cells per well and incubated overnight prior to analysis. Prior to measurement, cells were washed once with serumfree Krebs-Ringer phosphate glucose buffer (KRPG:145 mm NaCl, 5.7 mm sodium phosphate pH 7.35, 4.86 mm KCl, 0.54 mm CaCl2, 1.22 mm MgSO4, 5.5 mm glucose). Cells were incubated with reaction mixture containing 50 μm Amplex Red reagent (Invitrogen) and 0.1 U/mL horseradish peroxidase in serum-free KRPG buffer at 37C for different time periods, as indicated in the figures. The intensity of H2O2-induced fluorescence was quantitated by a fluorescence microplate reader (Beckman Coulter, Fullerton, CA, USA) with excitation at 530 nm and emission at 620 nm.

2.2.7 DifMUP assay

PTP1B activity was measured as previously with some minor modifications (Haque et al., 2011). Briefly, cells were lysed in 50 mM Tris (pH 7.4), 5 mM EDTA, 150mM NaCl and 1% triton X-100. 500 □g of lysate from each sample was incubated with PTP1B antibody (DH8, pre-coupled to protein A/G agarose beads) for 2 hours at 4ºC, and the immunoprecipitated proteins were washed 3X with trapping LB and kept on ice. PTP1B activity was measured using 6,8-Difluoro-4-Methylumbelliferyl Phosphate (DiFMUP) as a substrate for 15 min at room temperature (LB

supplemented with 20 μM DiFMUP). The fluorescent reaction product DiFMU was measured at 450 nm (ex. 358 nm) to determine the enzymatic activity. The values in the absence of enzyme were taken as background and were always subtracted for correction.

2.2.8 Detection of PTP1B oxidation with PTPox antibody

Cells were serum starved overnight before being lysed under anaerobic conditions with a degassed buffer (50 mM HEPES pH 7.5 , 150 mM NaCl, 5 mM EDTA, 10% glycerol, 1% triton X-100, 10 mM IAA, protease inhibitor cocktail). The lyaste was incubated for 1 hr in 4C with the protein A/G beads precoupled with PTP1B antibody (DH8) to immunoprecipiate PTP1B. The precipitates were washed 3 times by lysis buffer without IAA. The precipitates were incubated with 10 mM DTT for 10 min on ice, and washed three times in 20 mM Hepes (pH 7.5) before incubation with 100 μM pervanadate for 15 mins room temperature. The proteins were then eluted in Laemmli sample buffer and resolved with SDS-PAGE and immunoblotted using the PTPox antibody that detects PTP-SO_3H.

2.2.9 Quantification of PTP1B reversible oxidation using scFv45:

ScFv45 bacterial expression vector was generated by subcloning from pcDNA3.2 into pET21 construct. Briefly, pPurified HA-tagged scFv45 was pre-coupled with anti-HA conjugated agarose beads (Roche) for 2 hours prior to incubation with the samples. Cells were serum starved overnight before being lysed under anaerobic conditions with a degassed buffer (50 mM HEPES pH 7.5 , 150 mM NaCl, 5 mM EDTA, 10% glycerol, 1% triton X-100, protease inhibitor cocktail). Lysates were evenly divided into two: 500 μg of lysate was incubated with scFv45-bound beads to measure the fraction of reversibly oxidized PTP1B and the second half of the

lysate (500 μg) was incubated with anti-PTP1B antibodies (FG6) bound to protein A/G agarose beads to measure the total fraction of PTP1B in the lysate. Following a 16 hour incubation at 4°C, beads were centrifuged at 5,000 x g for 1 min. The supernatant from scFv45 pull-down was subjected to an additional immunoprecipitation using FG6 to quantify the remaining PTP1B representing the reduced fraction. Beads were washed 3X with lysis buffer, resuspended in 20 μl 4X Laemmli sample buffer and heated at 90°C for 90 sec. The purified samples were resolved on SDS-PAGE and blotted for PTP1B. The intensity of the bands were quantified using ImageJ.

2.3 Result

2.3.1 Established model system to study redox regulation in OIS cells

We introduced oncogenic RAS, *HRAS*^{V12} gene into human diploid fibroblast IMR90 cells by retroviral infection. The cells were then select by puromycin for positive infection as the retroviral vector contains a puromycin selection marker. The day post the puromycin selection was counted as Day0 post-selection and the different assays were carried out at different days as late as Day6 post-selection (figure 2.1A). Cells expressing RAS developed a flat and enlarged morphology and demonstrated senescence-associated beta-galactosidase (SA beta-gal) activity at day 6 post-puromycin selection (Figure 2.1B). The result was consistent with previous reports (Serrano et al., 1997).

2.3.2 Elevated ROS production in senescent cells

It is shown that senescent cells produce elevated levels of ROS (Lee et al., 1999). In our study, we used a PF6-AM probe to specifically detect the intracellular H_2O_2 level. The cells from Day 2, 4 and 6 post selection were stained with PF6 probe in living condition and live florescence images were obtained. The imaging results showed that the cells with RAS expression had higher level of ROS production as compared to the control cells. The production of ROS gradually increased as the senescence phenotype progressed (Figure 2.2A).

We also used an Amplex red assay to measure the ROS released into the media. In the presence of peroxidase, the Amplex Red reagent reacts with H_2O_2 in a 1:1 stoichiometry to produce the red-fluorescent oxidation product, resorufin. For the Amplex red assay, the IMR90

cells from different days post selection were seeded on to the plates at the same time and incubated overnight before the assay. The result from Amplex red assay showed that RAS-induced senescent cells released more ROS as compared to the control cells (Figure 2.2B).

2.3.3 ROS is important for oncogene-induced senescence

To determine whether the increased production of ROS was important for senescence, we cultured the RAS-expressing cells in media containing ROS scavenger N-acetyl cysteine. We examined the level of senescence phenotype at Day 6 by measuring the percentage of x-gal positive cells (Figure 2.3). Treating the RAS expressing cells with NAC decreased the percentage of senescent cells by half, which is consistent with the observation from Finkle group(Lee et al., 1999) . The result suggested that increased ROS level was necessary for RAS-induced senescence.

2.3.4 PTP1B is oxidized in senescent cells

We then used a cysteine labeling assay to identify the PTPs that were redox regulated in senescent cells. As mentioned in the introduction, cysteine labelling assay specifically enriches the proteins with reversibly oxidized low pKa cysteines. In the cysteinyl-labeling assay, the reversible oxidation proteins were labelled with a biotin tagged probe. After a biotin-streptavidin high-affinity purification, we resolved the enriched proteins by SDS-PAGE and visualized these proteins using an anti-biotin immunoblotting. The result showed that minimal biotin labeling was observed in normal fibroblasts; however, biotinylation was detected in lysates of RAS-expressing fibroblasts, with a ~50 kDa protein displaying pronounced reversible oxidation when compared to normal fibroblasts (figure 2.5A). Immunoblotting the streptavidin-

purified samples of the cysteinyl-labeling assay for PTPs known to possess a molecular mass of ~50 kDa revealed that PTP1B was targeted by H_2O_2 in RAS-induced senescent cells (Figure 2.5B).

We used N-acetylcysteine, a ROS scavenger, to treat the cells and demonstrated that the RAS-induced reversible oxidation of PTP1B occurred as a result of H_2O_2 production. We detected a time-dependent increase of PTP1B oxidation in RAS expressing cells; however, pre-treatment with NAC markedly decreased reversible oxidation of PTP1B (figure 2.6). The oxidation level of PTP1B gradually increased during the development of senescence phenotype.

RAS-induced senescent phenotype was established by artificially introducing oncogenic RAS into human diploid fibroblasts. One might argue that the production of ROS and PTP1B oxidation was a result of overwhelmingly expressed RAS being a burden to the cells. Here, we used replicative senescent cells as a more physiological model of senescence, wherein the senescent phenotype was induced by high level of population doubling. We tested whether PTP1B oxidation also occurs in replicative senescent cells. IMR90 cells kept beyond passage 20, were subject to cysteine labeling assay. The result showed that PTP1B underwent reversible oxidation in the replicative senescent cells (Figure 2.5C). The result indicated that PTP1B oxidation might be a general phenomenon in cellular senescence.

2.3.5 PTP1B overexpression attenuated RAS-induced senescent phenotype

We went on to determine whether PTP1B oxidation was the cause of senescence or a consequence of senescence. We over-expressed PTP1B in RAS expressing cells, as a compensation for the loss of activity of PTP1B because of ROS induced oxidation in senescent cells. Over 70% of RAS-expressing fibroblasts exhibited SA-β-gal activity. In contrast, cells

overexpressing the active phosphatase together with RAS displayed a 4-fold reduction in senescence, whereas the catalytically dead PTP1B C215S mutant or the trapping mutant PTP1B D181A did not affect the appearance of RAS-induced SA-β-gal activity (Figure 2.10).

2.3.6 Inhibition of PTP1B promoted OIS

Conversely, we treated the cells at Day 2 post selection with PTP1B inhibitor MSI1436 to mimic PTP1B oxidation and inactivation. At Day 2 post, 10% of the RAS-expressing cells were β-gal positive. PTP1B oxidation was low at Day2 as suggested by the time course cysteine-labeling assay. Therefore treating the cells with PTP1B inhibitor at Day2 was the optimal time point when we could exclude the inhibition effect caused by PTP1B oxidation and detect the maximum effect of PTP1B inhibition by MSI1436. Using x-gal staining we detected a 2-fold increase in the percentage of senescent cells in the RAS-expressing cells treated with MSI1436 (Figure 2.11 A and C), further supporting that PTP1B was an important regulator in RAS-induced senescence. The result was confirmed using a different PTP1B inhibitor CPT-157633 which has distinct structure and inhibitory mechanism from MSI1436 (Figure 2.11 B and D).

Furthermore, we treated the cells with NAC, which mimics the low ROS condition, together with the PTP1B inhibitor MSI1436. Previously we have shown that treating the cells with NAC attenuated RAS-induced senescence phenotype (Figure 2.3). Specifically inhibiting PTP1B with MSI-1436 in NAC-treated cells was sufficient to offset the NAC-inhibition of RAS-induced senescence. This demonstrated a critical role of the reversible oxidation and inhibition of PTP1B in triggering RAS-induced senescence (Figure 2.12).

2.3.7 Stoichiometry of PTP1B oxidation

We showed that overexpession of WT PTP1B attenuates the RAS-induced senescence phenotype (Figure 2.10). The question was raised why overexpressed WT PTP1B was able to attenuate senescence instead of being oxidized and inactivated in senescent cells. We found it would be helpful to measure the PTP1B activity and the stoichiometry of PTP1B oxidation under various conditions.

We used a DiFUMP assay to measure the activity of PTP1B immunoprecipitated from the samples expressing RAS only, RAS+PTP1B, PTP1B only, or control vectors. The result showed that the PTP1B phosphatase activity was higher in PTP1B/RAS co-expressing cells than that in RAS-expressing cells. It demonstrated that overexpressing the WT PTP1B in RAS expressing cells was able to compensate for the pool of ROS-inactivated enzyme (Figure 2.13 A).

Furthermore, we determined the stoichiometry of reversibly oxidized PTP1B using a single chain variable fragment antibody (scFv45) that recognizes selectively the reversibly oxidized (cyclic-sulphenamide form) of PTP1B (Haque et al. Cell 2013). We pre-coupled the purified, HA-tagged recombinant scFv45 with anti-HA agarose beads. Through incubating the scFv with cell lysates under anaerobic conditions, we were able to pull down the reversible oxidized PTP1B at the same time prevent post-lysis oxidation. We used scFv45 to demonstrate that the extent of reversible oxidation of endogenous PTP1B was ~50% in the cells only expressing RAS. However, in the cells that PTP1B was co-expressed with RAS, only ~30% of PTP1B was reversibly oxidized. The PTP1B protein level was increased 3 fold when it was overexpressed in RAS-expressing cells, however the amount of oxidized PTP1B only increased 1.5 fold, comparing to the cells expressing RAS alone (Figure 2.14 B). The result suggested that

overexpression of RAS might produce a finite amount of ROS and therefore the response does not have the capacity to inactivate the entire pool of PTP1B.

As further confirmation, we utilized a PTPox antibody which detects terminally oxidized PTPs to measure the extent of PTP1B oxidation. The cells were lysed under anaerobic condition with the presence of alkylating reagent IAA. PTP1B was immunoprecipiated from the lysate, followed by reduction and pervanadate-mediated oxidation. The treatment generated the terminally oxidized, sulfonic acid form of cysteine. The terminally oxidized PTP1B was resolved by SDS-PAGE and immunoblotted with PTPox. It showed that PTP1B protein level in RAS/PTP1B expressing cells was 3 fold compared to that in the cells only expressing RAS. However the amount of oxidized PTP1B in PTP1B/RAS cells only increased by 1.5 fold compared with RAS only cells. The result supported the observations we obtained using ScFv and DifMUP assay (Figure 2.14 C). These results taken together, suggested that there was a limit to the extent that ROS could oxidize PTP1B and erexpression of PTP1B may result in a greater extent of oxidation of the phosphatase in absolute terms, but there might be excess unmodified enzyme which was able to rescue RAS-induced senescence.

2.3.8 Optimization of cysteine labeling assay for mass spectrometry analysis

We planned to optimize the cysteine labeling assay. Our goal was to make it compatible with mass spectrometry analysis, so as to identify more reversibly oxidized PTP in senescent cells. To analyze the proteins enriched in cysteine labeling assay, we resolved the precipitant with SDS-PAGE and identified the differentially enriched bands using MS. We identified PTP1B enriched in the cysteine labeling assay.

We planned to directly digest the streptiavidin pull-down on-beads. Compared to in-gel digestion, on-beads digestion has less contamination and preserves more proteins from the pull-down. However, we hypothesized that there were non-PTP proteins with reactive cysteine present in high abundance in the cells. These hight abundance proteins might increase the complexity of the sample and mask the signal of low abundant PTPs during MS analysis. (Figure 2.7) To solve the problem, we decided to perform the trypsin digestion before streptavidin enrichment. In this way, we will only pull down the peptides that are labeled with IAP probe and therefore de-convolutethe sample and increase the chance of low abundant peptides to be detected. We performed a preliminary experiment with purified PTP1B directly labeled with IAP probe. We then precipitated the protein and performed trypsin digestion before streptavidin pull-down. The peptides pulled down by streptavidin beads were then eluted and analyzed with MS. The result showed that MS could detect IAP labeled peptide from as low as 1 pico mole starting material. A quantitative western blot showed that there was approximately 1 pico mole PTP1B in 50 micro gram of 293 cell lysate(Figure 2.9). Assuming (1) 10% of PTP1B in 293 cells is reversibly oxidizedl (2) the cysteine labeling assay can pull down 100% oxidized PTP1B and (3) there is no ion suppression effect during MS analysis, we need at least 500 microgram of cell lysate starting material for MS to detect labeled PTP1B. How well we can detect of other PTPs with reversible oxidation will be dependent on their abundance in the cells, the stoichoimetry of oxidation as well as how the peptide labeled with IAP probe behaves during the MS analysis.

2.4 Discussion

In this chapter, we detected elevated ROS production in oncogenic RAS-induced senescent cells. We identified that PTP1B was a target of ROS and underwent oxidative inactivation in senescent cells. We demonstrated that PTP1B function was in RAS-induced senescence. Overexpression of PTP1B attenuated and inhibition of PTP1B accelerated RAS-induced senescence.

2.4.1 PTP1B and RAS signaling

Studies using PTP1B KO mouse model show that PTP1B can act as a positive regulator of endogenous RAS signaling. PTP1B-deficient fibroblasts display increased expression of RAS GTPase-activating protein (p120RasGAP), which inactivates RAS (Dube et al., 2004). Moreover, phosphorylation of p62Dok is increased as a result of PTP1B deletion, which in turn contributes to the inhibition of RAS signaling (Dube et al., 2004). However in our study of oncogenic RAS-induced senescence, PTP1B is unlikely to further promote RAS function since the RAS protein expressed in the cells is constitutively active. In contrast, we observed that overexpression of WT PTP1B attenuated RAS-induced senescence, suggesting that PTP1B might act against RAS function by targeting downstream effectors of RAS. We were interested to study the signaling pathways regulated by PTP1B in RAS-induced senescence.

Oncogenic RAS was appreciated to trigger senescence through activation of ERK pathway which leads to aberrant proliferation signal; and activation of p38 which provokes the activation of p53/p21(DeNicola and Tuveson, 2009b). We hypothesize that PTP1B oxidation influences these downstream signaling pathways of RAS and regulates OIS. The best way to

identify the pathways regulated by PTP1B is by using a PTP1B substrate trapping strategy, which I will discuss in the next chapter.

2.4.2 PTP1B regulation of senescence

PTP1B can act as a tumor suppressor or as an oncogene depending on several factors such as the specific tissue and some modifier genes (Julien et al., 2011; Tonks and Muthuswamy, 2007). Interestingly, increased PTP1B expression has been reported in transformed human breast cells (Zhai et al., 1993) and ovarian carcinomas (Wiener et al., 1994). We observed that overexpression of PTP1B attenuated RAS-induced senescence. It indicates that PTP1B activity might contribute to the bypass of senescence and RAS-mediated transformation in tumor cells. Our study showed that inhibiting PTP1B accelerated senescence. Senescence is appreciated as a barrier to tumorigenesis. Therefore inhibition of PTP1B, which accelerates senescence, might prevent tumorigenesis.

Indeed, inhibition of PTP1B delays HER2-induced mammary tumorigenesis and cancer metastasis(Bentires-Alj and Neel, 2007). Our lab used a small molecule inhibitor MSI1436 against PTP1B to treat xenografts mouse model of HER-2 induced tumor. Inhibiting PTP1B prevented tumor growth (Krishnan et al., 2014). Our lab demonstrated that MSI1436 is an allosteric inhibitor of PTP1B. The binding of MSI1436 locks PTP1B in an inactive state (Krishnan et al., 2014). Given the cooperative role of PTP1B inhibition in RAS-induced senescence, it will be interesting to test whether treating with MSI1436 can delay the onset of cancer in the RAS-driven cancer mouse model, by promoting the RAS expressing cells to senescent state.

2.4.3 Source of ROS production

In this chapter, we showed that PTP1B was reversibly oxidized in RAS-induced senescent cells. The ROS generated in RAS-induced senescent cells might be from two sources: NOX proteins and mitochondria. RAS promotes the assembly of NOX protein complex, through the activation of RAS target Rac1, which is also one of the NOX protein activator(Sundaresan et al., 1996). Moreover, recent studies show that NOX proteins are unregulated in RAS-induced senescent cells and ablation of NOX by siRNAs blocked the senescent phenotype (Kodama et al., 2013; Weyemi et al., 2012). Early reports also found increased levels of mitochondrial ROS in during RAS-induced senescence (Lee et al., 1999; Moiseeva et al., 2009). RAS-induced PTP1B oxidation might be achieved by altering the NOX protein level or mitochondrial function. The future study that illustrates the source of ROS for PTP1B oxidation will help us further understand the mechanism involved in redox regulation of PTP1B.

ER membrane bound NOX4 protein was shown to regulate PTP1B oxidation in EGFR signaling (Chen et al., 2008). Chen et al, showed that NOX4 colocalized with PTP1B on the cytoplasmic surface of the ER membrane. The authors proposed that the localization of NOX protein, which determines the local ROS concentration, might contribute to the specific oxidative regulation of PTP1B.

In the future study, I propose to analyse the colocalization of oxidized PTP1B and the potential source of ROS such as NOX proteins or mitochondria. This study will help us identify the regulator of PTP1B oxidation. First, we should develop a method to detect the localization of oxidized PTP1B. It might be worthwhile to express scFv and PTP1B, both with fluorescent tags. When scFv binds to oxidized PTP1B, the fluorescent tags from each of the protein might be close enough to initiate Förster resonance energy transfer (FRET). Using the FRET technique, we

will be able to detect the localization of oxidized PTP1B in vivo. Furthermore, we should identify the localization of ROS in cells. Detecting NOX protein and mitochondria using immunofluorescence staining can provide us information of the localization of potential resource of ROS. I propose to visualize live ROS production using the live imaging super resolution microscopy technique with H_2O_2-specific fluorescent probe, such as PF6-AM. Analyzing the localized PTP1B oxidation and ROS production will provide us with a powerful tool to study the spatial and dynamic regulation PTP1B oxidation.

2.4.4 Optimization of cysteine labeling assay

The cysteine-labeling assay suggested that PTP1B was not the only protein reversibly oxidized in senescent cells. We hoped to find more PTPs that underwent reversible oxidation in senescent cells. There are several challenges using MS to identify reversibly oxidized PTPs enriched in cysteine labeling assay. First of all, the abundance of other PTPs in the cells might not be high enough to be detected by MS. Secondly, the IAP probe I was using is a sulfhydryl targeting probe, and it was able to react with other proteins that contain a reactive cysteine with low pKa, such as thioredoxin. The enrichment of high abundant proteins in the assay, such as thioredoxin, might mask the signal of PTPs in the following MS analysis. In order to pull down the PTPs selectively, we need to use a probe that reacts more specifically with the active form of PTPs. An α-bromobenzylphosphonate (BBP) activity-based probe generated from Zhang's group was available in our lab(Kumar et al., 2006). BBP mimics the structure of phosphotyrosine, and has higher specificity to PTPs than the IAP probe (Kumar et al., 2004). Using the BBP probe in cysteine labeling assay can limit the background of non-PTP proteins.

Due to the fact that the BBP probe is not commercially available and limited in amount, I was unable to apply this probe in a large scale cysteine labeling assay for MS analysis.

Although incorporating a trypsin digestion step before the streptavidin pull-down enabled us to specifically enrich the peptides with low-pKa cysteine and simplify the sample, there still is a lot of space orf improvement in the assay. First of all, given that the catalytic cysteine is the only one cysteine with low pKa in most of the PTP, with this protocol, we will technicallypull-down only one peptide from each PTP. Under this circumstance, it will be challenging for the MS analysis to identify the protein confidently, because at least two peptides are needed to identify a protein with good confidence. Secondly, the property of the active site tryptic peptide will affect how efficiently it flies in the MS instrument, especially with a biotin tagged, long probe attached to it. Thirdly, even if we could solve the technical problems, some PTPs may be expressed cells at very low levels and will therefore be hard to enrich for detection by MS analysis, especially when the stoichiometry of oxidation is low.

A systematic optimization is needed to establish a cysteine-labelling assay compatible with mass spec analysis.

We should test the sensitivity of the assay in vitro using recombinant proteins. Since recombinant proteins of several PTPs are readily available in the lab, it will be simple to measure lower limit of MS detection with those purified proteins. Meanwhile, we can estimate the cellular abundance of specific PTP by quantitative western blot or MS, using the recombinant protein as the standard.

We can test and optimize the selectivity of cysteine-labelling assay using a mixture of recombinant PTPs with other non-PTP proteins. From the initial attempt with MS identification

of proteins enriched in the assay, we observed Tubulin along with other high abundance proteins. Therefore it is reasonable and practical to mix PTPs with purified GAPDH and tubulin, which are commercially available. This in vitro system also brings the benefit that we can control the pH, salt condition and even apply different probes to increase the specificity of the assay. The optimization will improve the sensitivity and selectivity of the assay and make it more adaptable to the MS analysis.

2.4.5 Property of potential PTP1B substrates

We observed that WT PTP1B expression reversed RAS-induced senescence phenotype, whereas expression of catalytically dead mutant PTP1B C215S or trapping mutant PTP1B D181A was unable to reverse senescence phenotype. This result was quite interesting to us.

PTP1B trapping mutant contains a Asp181 to Ala mutation. Its catalytic activity is impaired however the substrate binding affinity is maintained. In the absence of Asp181, which acts as a general acid in the first step of catalysis, the tyrosyl-leaving group cannot be generated, therefore the substrate remains “trapped” to PTP1B trapping mutant once it enters the active site(Flint et al., 1997a).

Protein tyrosine phosphorylation can provide a binding site for pTyr binding motif such as SH2 domain. The tyrosine phosphorylation generally promotes the recruitment of SH2 domain containing proteins. PTP1B trapping with the substrates will prevent the SH2 protein engaging with these substrates. Therefore PTP1B D181A will attenuate the further function of its substrate, which is mediated by SH2 protein binding. Similarly, expression of WT PTP1B, which removes the phosphate group from target tyrosine residue, will impair the recruitment

of pTyr binding proteins to PTP1B substrate. Based on the hypothesis that phosphorylation of PTP1B substrate led to binding of SH2 proteins and promoting of signals, overexpression of WT PTP1B or PTP trapping mutant should result in similar impact on the substrate function, which should have led to similar phenotype. However, we observed that WT PTP1B expression attenuated senescence whereas PTP1B D181A expression did not affect senescence phenotype.

The phenotype of RAS/PTP1B D181A co-expressing cells suggests that the substrate through which PTP1B affects senescence has unique property, and there are two possible way that the phosphorylation affects the potential substrate's function:

1. The substrate is active in its dephosphorylated state and the activity of the substrate is to promote cells to bypass senescence. While it is phosphorylated or trapped by PTP1B substrate trapping mutant, it is unable to induce senescence bypass.

2. The substrate is active when it is phosphorylated and is able to induce senescence. The phosphorylation may lead to allosteric activation of the enzyme and expose its catalytic site. Under the circumstance, when the enzyme is trapped by PTP1B D181A mutant, the enzyme's catalytic activity may not be affected by the trapping. Therefore it is still able to induce senescence.

2.4 Table and Figures

Table 2.1 Comparison of the current methods to detect oxidized PTPs.

Method	Potential for MS	PTP Specific	Benefits	Limitations
Radiolabelled Assay	Yes	No	• First method to detect PTP oxidation	• Targeted method • Limited dynamic range
Modified In-Gel PTPase Assay	No	Yes	• Detects growth factor-induced oxidation • PTP-specific • Monitors all non-receptor PTPs	• Does not detect RPTPs • Does not identify oxidized PTP(s) • Not quantitative • Cannot be applied to MS
IAP-Biotin	Yes	No	• Detects growth factor-induced PTP oxidation • Identifies all oxidized proteins	• Not PTP-specific • High background of non-PTP proteins • Has not been applied to global MS approach
PTPox antibody	Yes	Yes	• Monitors all catalytically active PTPs • PTP-specific • Global MS approach • Quantifies PTP expression and oxidation	• Cannot distinguish reversible oxidation from higher order of oxidation
Conformation-sensing antibodies	Yes	Yes	• Measures sulfenylamide state *in vivo* • Quantifies fraction of PTP1B- OX	• Detects only PTP1B • Over-estimates

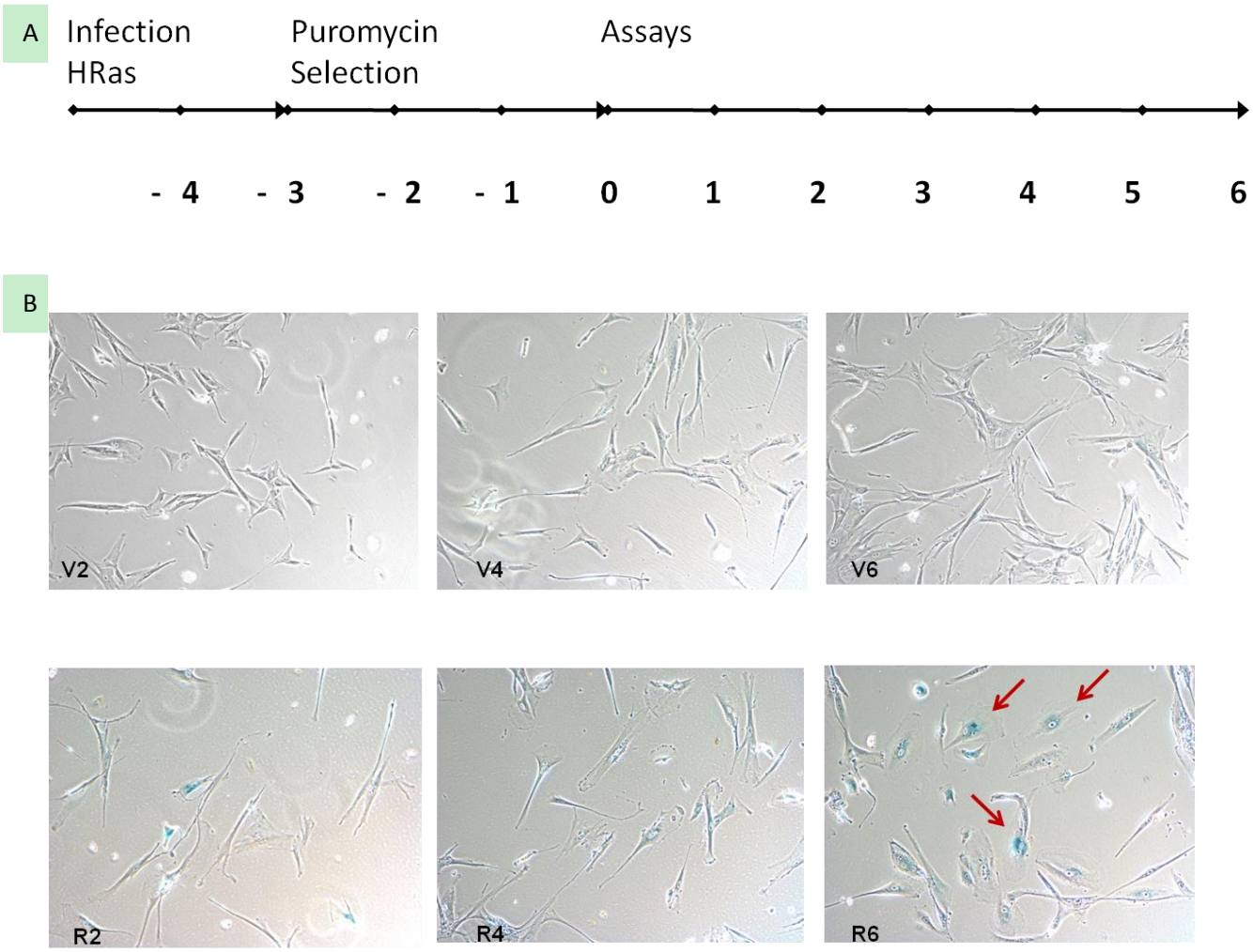

Figure 2.1 A. Scheme of establish senescent model. B. Representative photographs of IMR90 fibroblasts stained for SA- β-gal activity at Day 2, 4, 6 post puromycin selection. Photographs of cells in the absence (V) or presence (R) of oncogenic are at the same magnification.

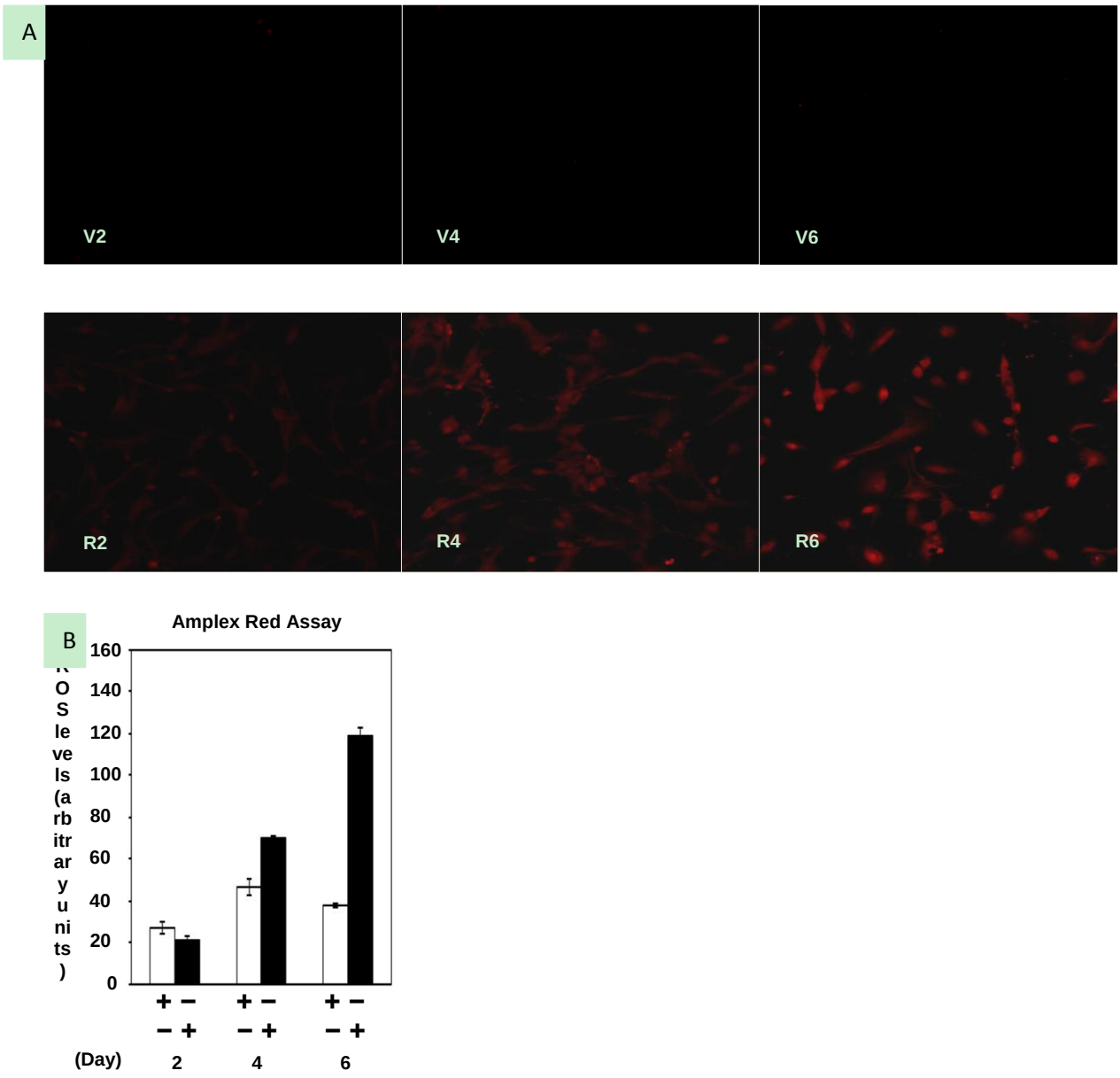

Figure 2.2 Elevated ROS production in RAS-induced senescence

A) H-RAS^{V12}-induced H_2O_2 production was assessed by molecular imaging using PF6-AM. Images of ROS-induced PF6 fluorescence are shown at magnification 400 X. (B) Levels of H_2O_2 released in the culture medium of *H-RAS^{V12}*-transformed cells were quantitated by Amplex Red.

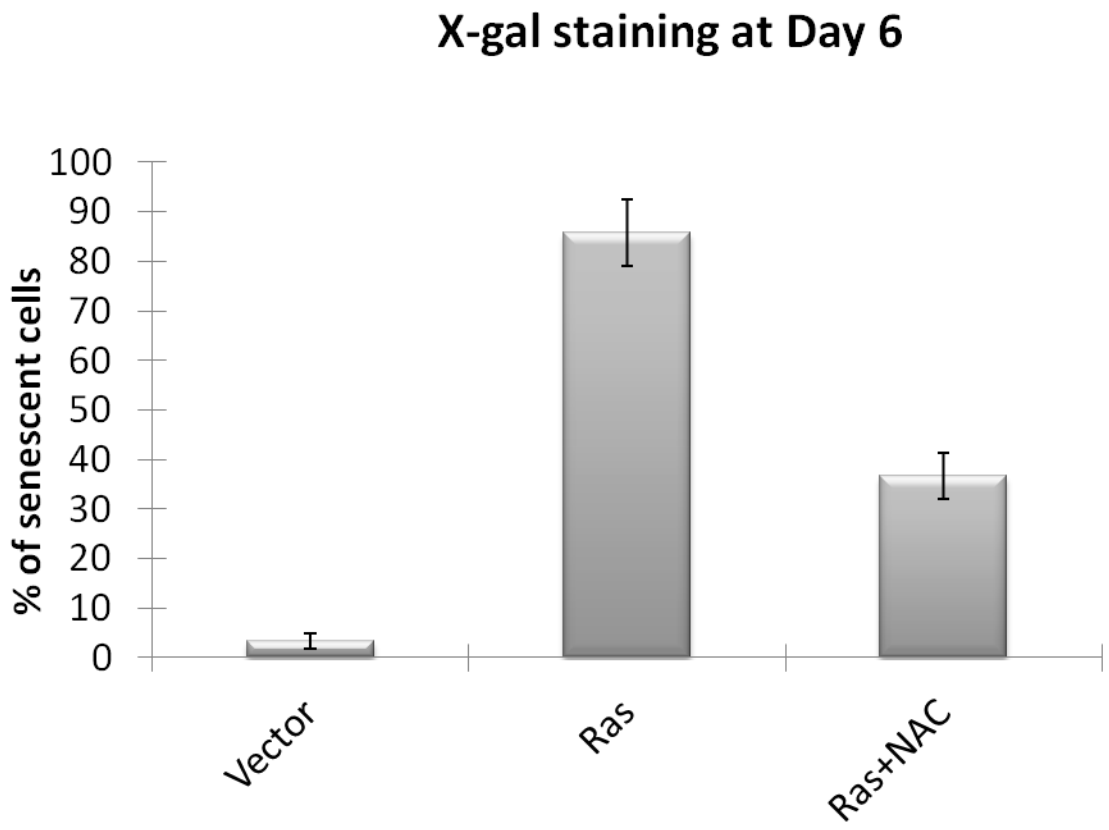

Figure 2.3 ROS production was important for senescence

Control or RAS-induced senescent cells and were cultured with or without 1 mM N-acetylcysteine (NAC) for 6 days, and were stained for β-gal**.** Senescent cells were counted as β-gal positive cells relative to the total number cells in 10 fields (10X magnification)

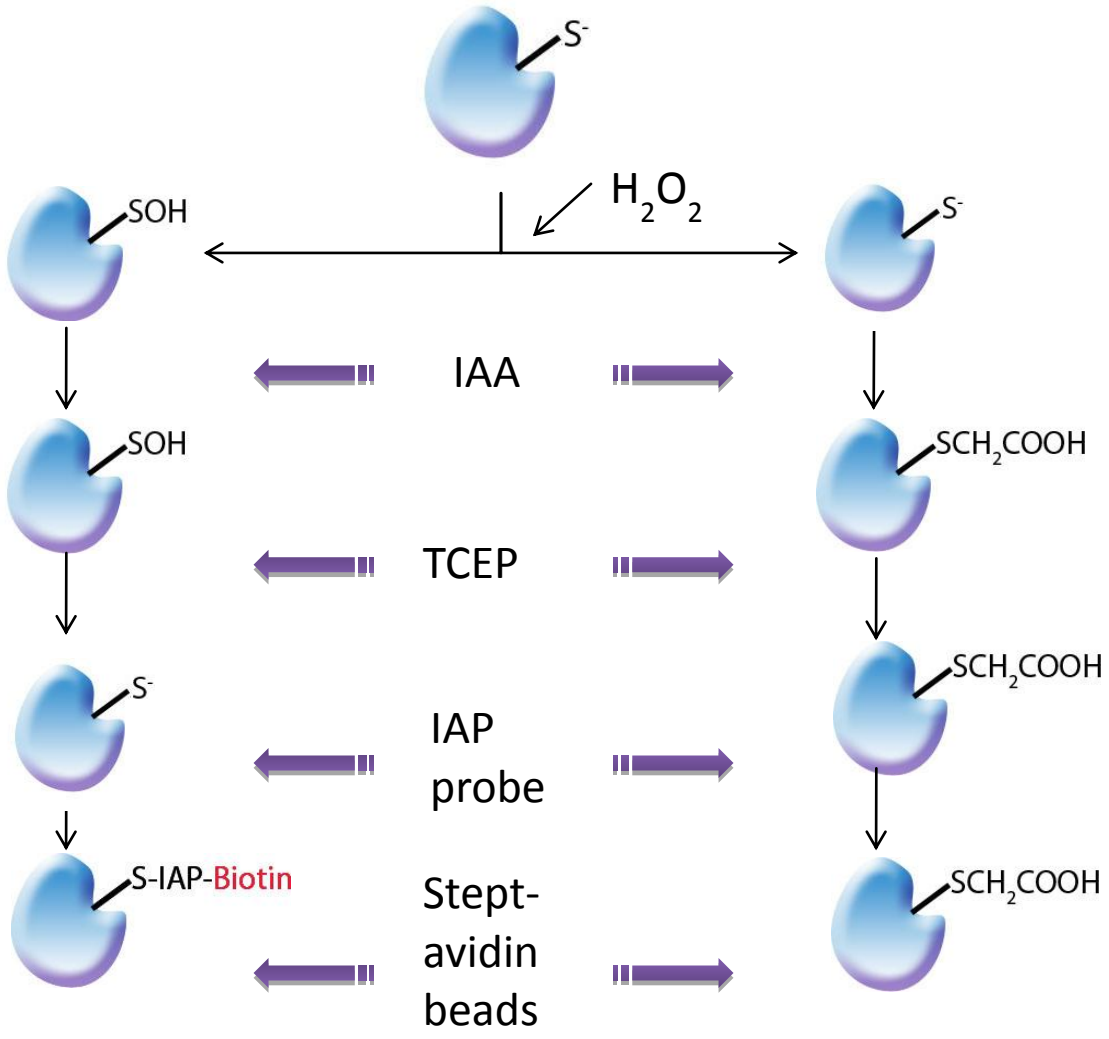

Figure 2.4 Scheme of cysteine-labeling assay

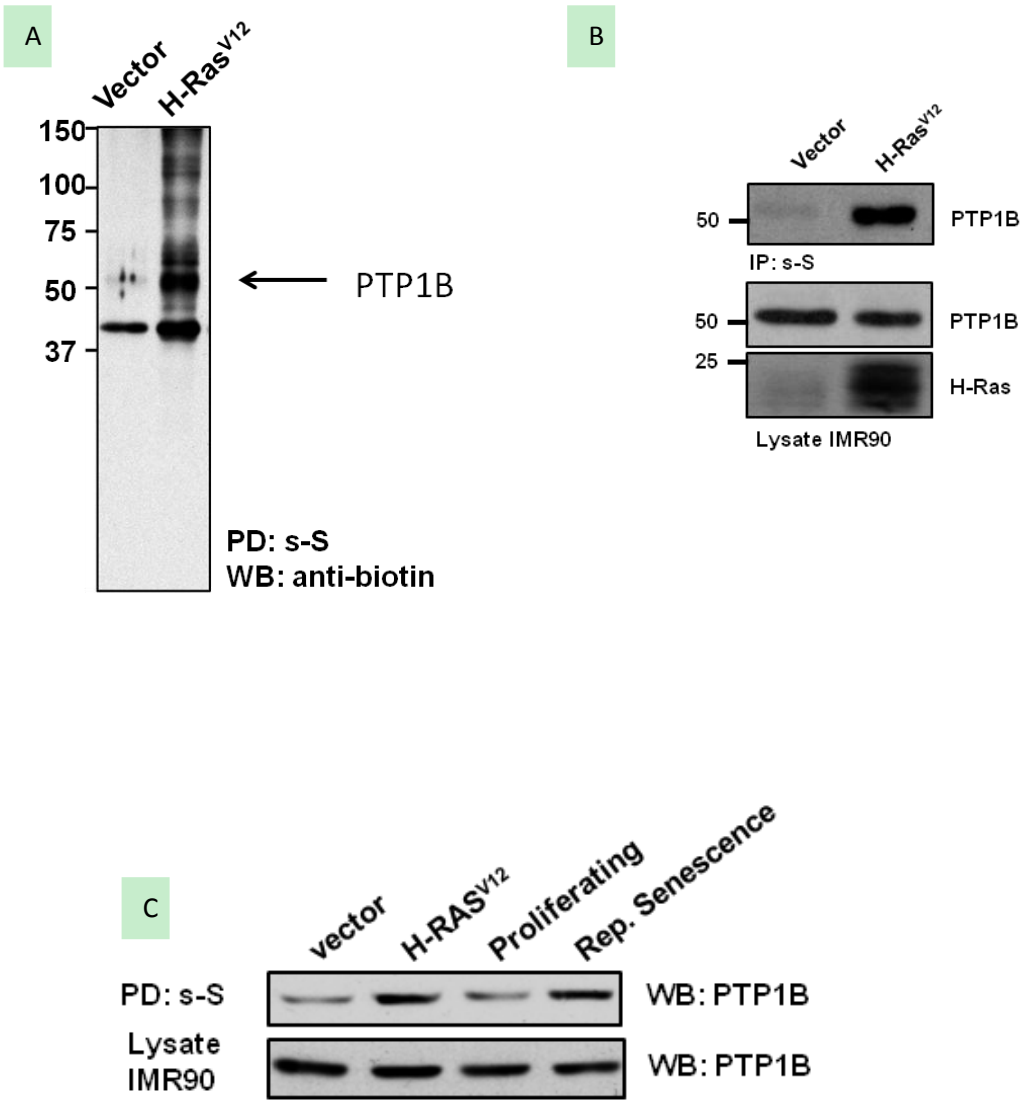

Figure 2.5 Cysteine labeling assay detected PTP1B reversible oxidation in senescent cells

A. Control or RAS-induced senescent cells were subjected to the cysteinyl-labeling assay, using biotinylated IAP at pH 5.5. Biotinylated proteins were purified on streptavidin–Sepharose beads, resolved by SDS/PAGE, and visualized using anti-Biotin-HRP. B. Proteins enriched in the cysteinyl-labeling assay were resolved by SDS/PAGE and immunoblotted using an anti-PTP1B antibody (FG6) (upper panel). Total PTP1B and RAS expression levels were measured by immunoblotting 5% of the lysate that was used in the cysteinyl-labeling assay. C. PTP1B oxidation in RAS-induced senescent cells and replicative senescent cells. PTP1B reversible

oxidation was measured in RAS-induced senescent cells, replicative senescent cells (population doubling > 40) and control IMR90 cells using the cysteinyl-labeling assay. The enriched, biotin-labelled, proteins were resolved by SDS-PAGE and immunoblotted for PTP1B

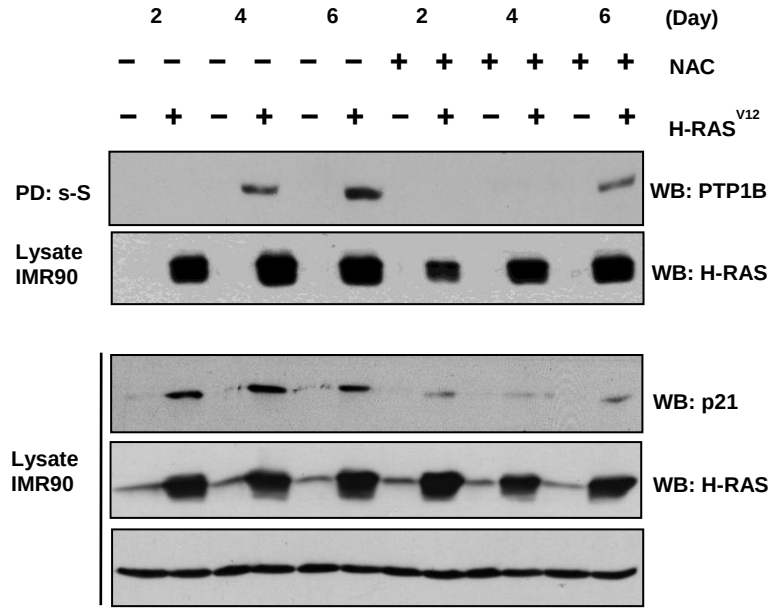

Figure 2.6 PTP1B oxidation during the progression of senescence phenotype

Control or RAS-induced senescent cells were cultured with or without 1 mM N-acetylcysteine (NAC) for 2, 4 or 6 days, then subjected to the cysteinyl-labeling assay. Reversibly oxidized PTP1B was visualized using FG6. Total RAS and p21 expression levels were measured by immunoblotting 5% of the lysate

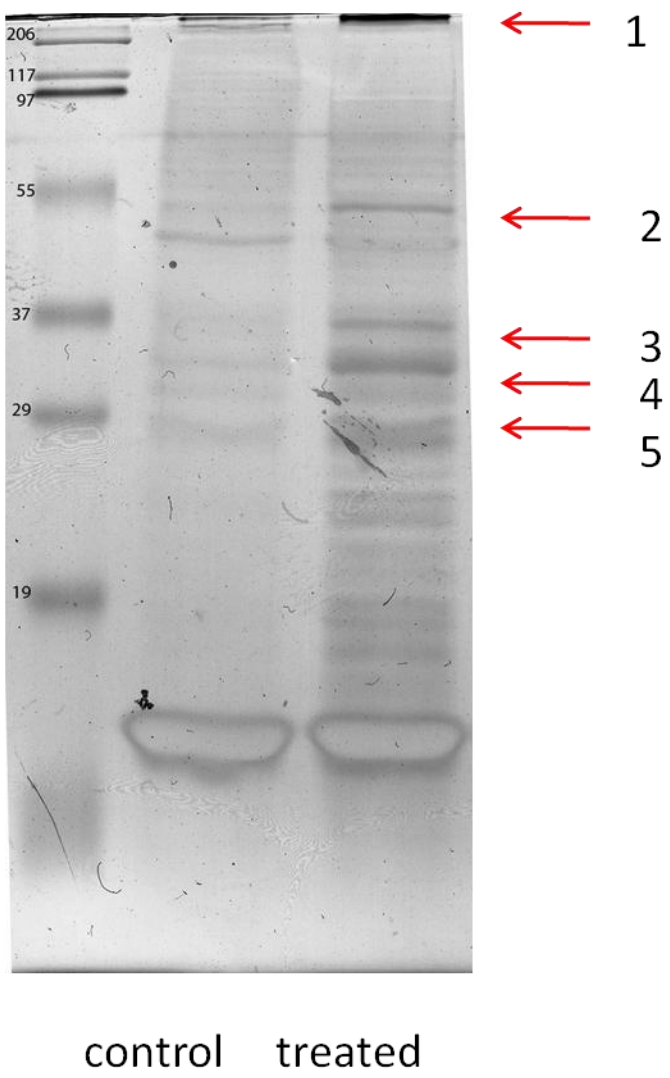

Figure 2.7 Identification of proteins enriched in cysteine labeling assay.

Control NIH3T3 or the cells treated with 1mM H_2O_2 for 10 mins were subject cysteine labeling assay. The enriched proteins were then resolved on SDS-PAGE and differentially enriched protein bands (labeled with arrows) were sent for MS protein identification. Protein ID for the indicated bands: 1.PTP1B 2: Tubulin 3:EF-1delta 4: 40S ribosomal protein S27 5: 60S ribosomal protein L23

A

PTN1_HUMAN Mass: 49935 Score: 40 Matches: 3(2) Sequences: 3(2) emPAI: 0.21

Tyrosine-protein phosphatase non-receptor type 1 OS=Homo sapiens GN=PTPN1 PE=1 SV=1

Query	Observed	Mr(expt)	Mr(calc)	ppm	Miss	Score	Expect	Rank	Unique	Peptide
4226	648.0696	2588.2492	2588.2476	0.62	0	20	0.093	1	U	R.ESGSLSPEHGPVVVHCSAGIGR.S
4349	706.5812	2822.2958	2822.2905	1.89	1	26	0.024	1	U	K.SGSWAAIYQDIRHEASDFPCR.V
4612	835.6710	3338.6548	3338.6441	3.22	0	22	0.05	1	U	R.EILHFHYTTWPDFGVPESPASFLNFLFK.V

B Matched peptides shown in ***bold red***.

```
  1 MEMEKEFEQI DKSGSWAAIY QDIRHEASDF PCRVAKLPKN KNRNRYRDVS
 51 PFDHSRIKLH QEDNDYINAS LIKMEEAQRS YILTQGPLPN TCGHFWEMVW
101 EQKSRGVVML NRVMEKGSLK CAQYWPQKEE KEMIFEDTNL KLTLISEDIK
151 SYYTVRQLEL ENLTTQETRE ILHFHYTTWP DFGVPESPAS FLNFLFKVRE
201 SGSLSPEHGP VVVHCSAGIG RSGTFCLADT CLLLMDKRKD PSSVDIKKVL
251 LEMRKFRMGL IQTADQLRFS YLAVIEGAKF IMGDSSVQDQ WKELSHEDLE
301 PPPEHIPPPP RPPKRILEPH NGKCREFFPN HQWVKEETQE DKDCPIKEEK
351 GSPLNAAPYG IESMSQDTEV RSRVVGGSLR GAQAASPAKG EPSLPEKDED
401 HALSYWKPFL VNMCVATVLT AGAYLCYRFL FNSNT
```

Figure 2.8 Mass spectormetry identification of the PTP1B peptides labeled with IAP probe.

Purified recombinant PTP1B was labeled with IAP probe in pH5.5 buffer and digested by trypsin. The tryptic peptides were enriched by neutron-avidin beads. The enriched peptides were then eluted and subject to MS analysis. An IAP-biotin modification on cysteine was added during peptide sequence search (A). Peptides identified by MS are labeled in red (B).

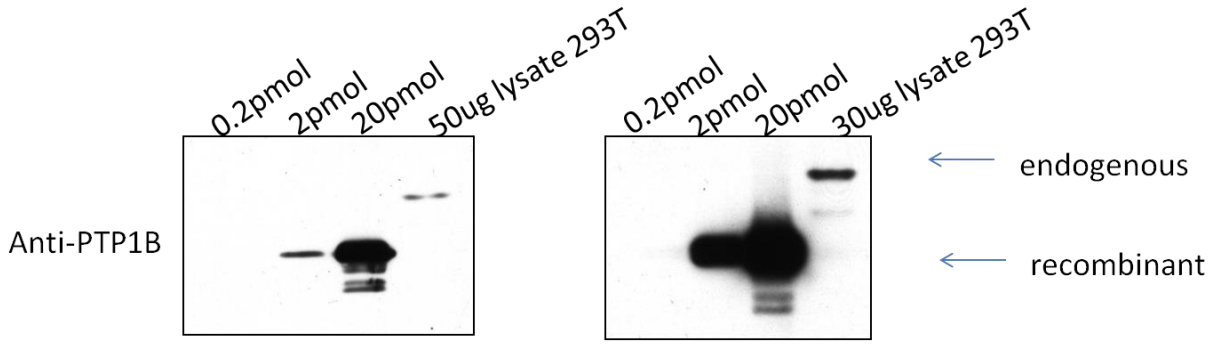

Figure 2.9 Quantitative western blot estimation of PTP1B quantity in 293T cells.

Different quantities of purified recombinant PTP1B and total cell lysate harvested from 293T cells were resolved by SDS-PAGE and visualized by immunobloting with PTP1B antibody. The arrows indicate endogenous or recombinant PTP1B.

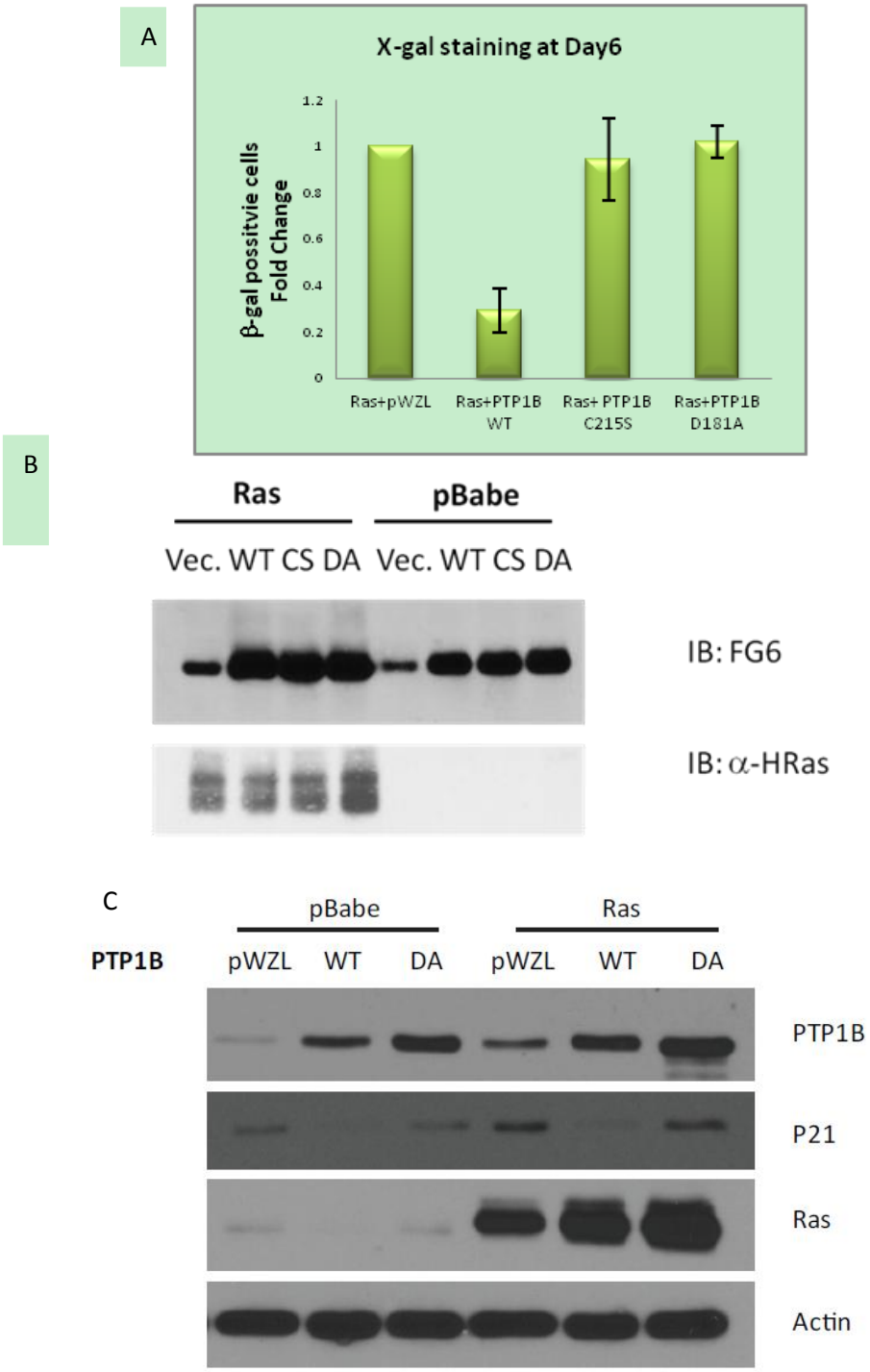

Figure 2.10 PTP1B expression attenuated RAS-induced senescence

(A) MR90 cells were infected for 2 day with mixture of virus and selected with puromycin for 3 days, followed by a 6-day hygromycin selection before x-gal staining. (B) The overexpression of

PTP1B was detected by PTP1B antibody FG6 and overexpressiong of HRASV12 was detected by anti-HRAS. (C) Empty vector (pWZL), PTP1B WT (WT) or PTP1B D181A mutant (DA) were co-expressed with control IMR90 cells (pBabe) or oncogenic RAS expressing cells (RAS). The lysates harvested from the samples were blotted with indicated antibodies.

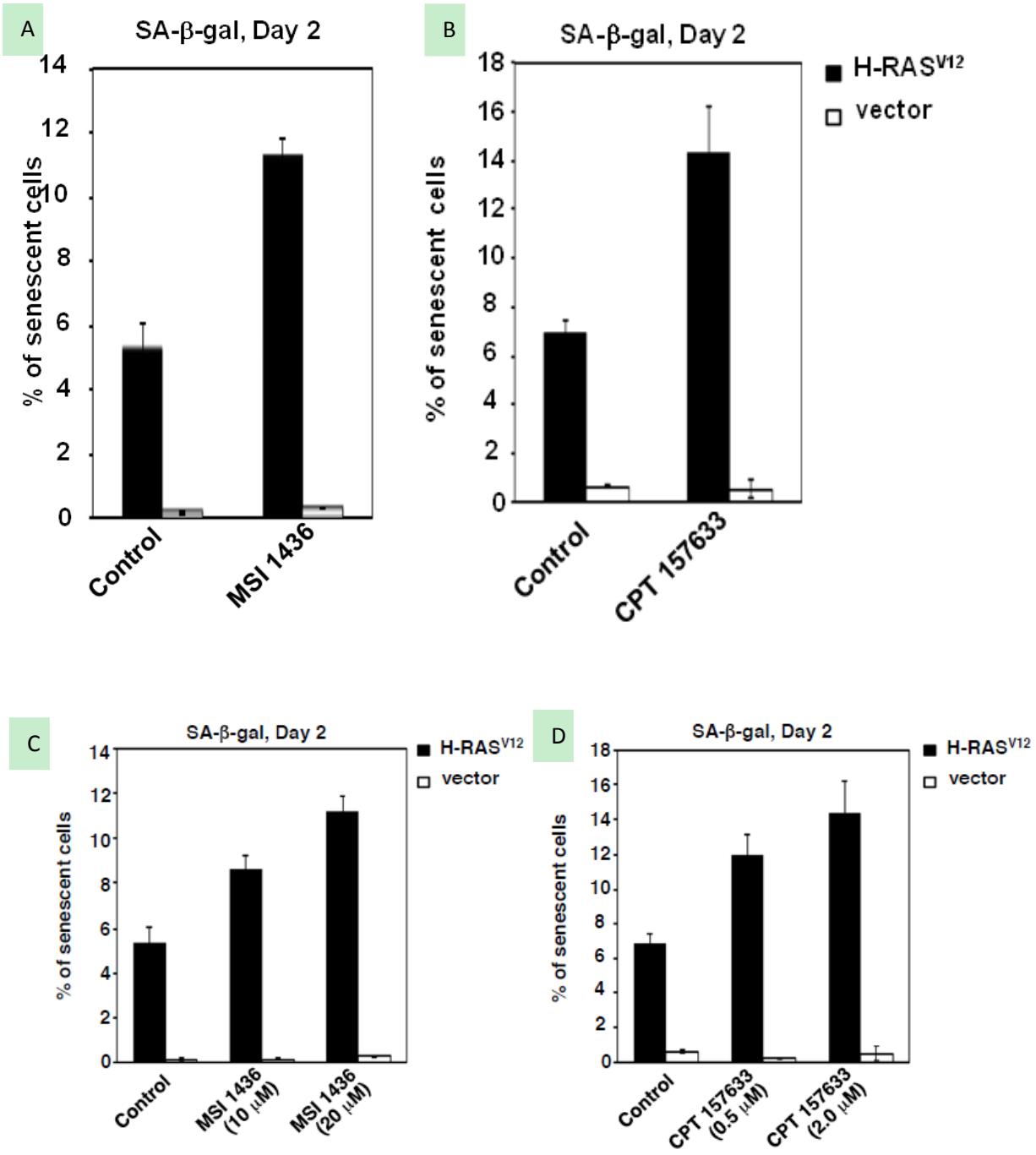
A
SA-β-gal, Day 2
% of senescent cells
14
12
10
8
6
4
2
0
Control
MSI 1436
B
SA-β-gal, Day 2
H-RAS^{V12}
vector
% of senescent cells
18
16
14
12
10
8
6
4
2
0
Control
CPT 157633
C
SA-β-gal, Day 2
H-RAS^{V12}
vector
% of senescent cells
14
12
10
8
6
4
2
0
Control
MSI 1436 (10 μM)
MSI 1436 (20 μM)
D
SA-β-gal, Day 2
H-RAS^{V12}
vector
% of senescent cells
18
16
14
12
10
8
6
4
2
0
Control
CPT 157633 (0.5 μM)
CPT 157633 (2.0 μM)

Figure 2.11 Inhibition of PTP1B accelerated senescence

A) Control (white bars) or RAS-expressing cells (black bars) were cultured in the presence or absence of the PTP1B inhibitor, MSI-1436 (20 μM). Cells were stained for β-gal activity 2 days post-puromycin selection. B) Inhibition of PTP1B with CPT 157633 caused a 2-fold increase in β-gal positive cells. Control (white bars) or RAS-expressing cells (black bars) were cultured in presence or absence of the PTP1B inhibitor, CPT-157633 (2μM). Cells were stained for β-gal activity 2 days post puromycin selection and β-gal positive cells were counted. C) Inhibition of PTP1B with two different concentrations of MSI-1436 and (D) two different concentrations of CPT 157633 caused an increase in β-gal positive cells.

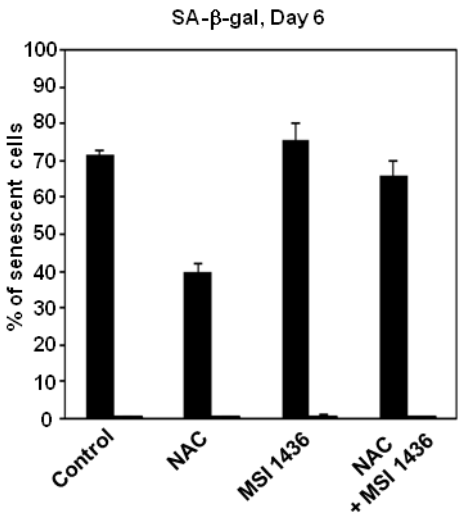

Figure 2.12 Oxidative inhibition of PTP1B was critical for RAS-induced senescence

Control (white bars) or RAS-expressing cells (black bars) were cultured in the absence or in the presence of 1 mM NAC, 20 μM MSI-1436, or both, for a 6 day-period post-selection.

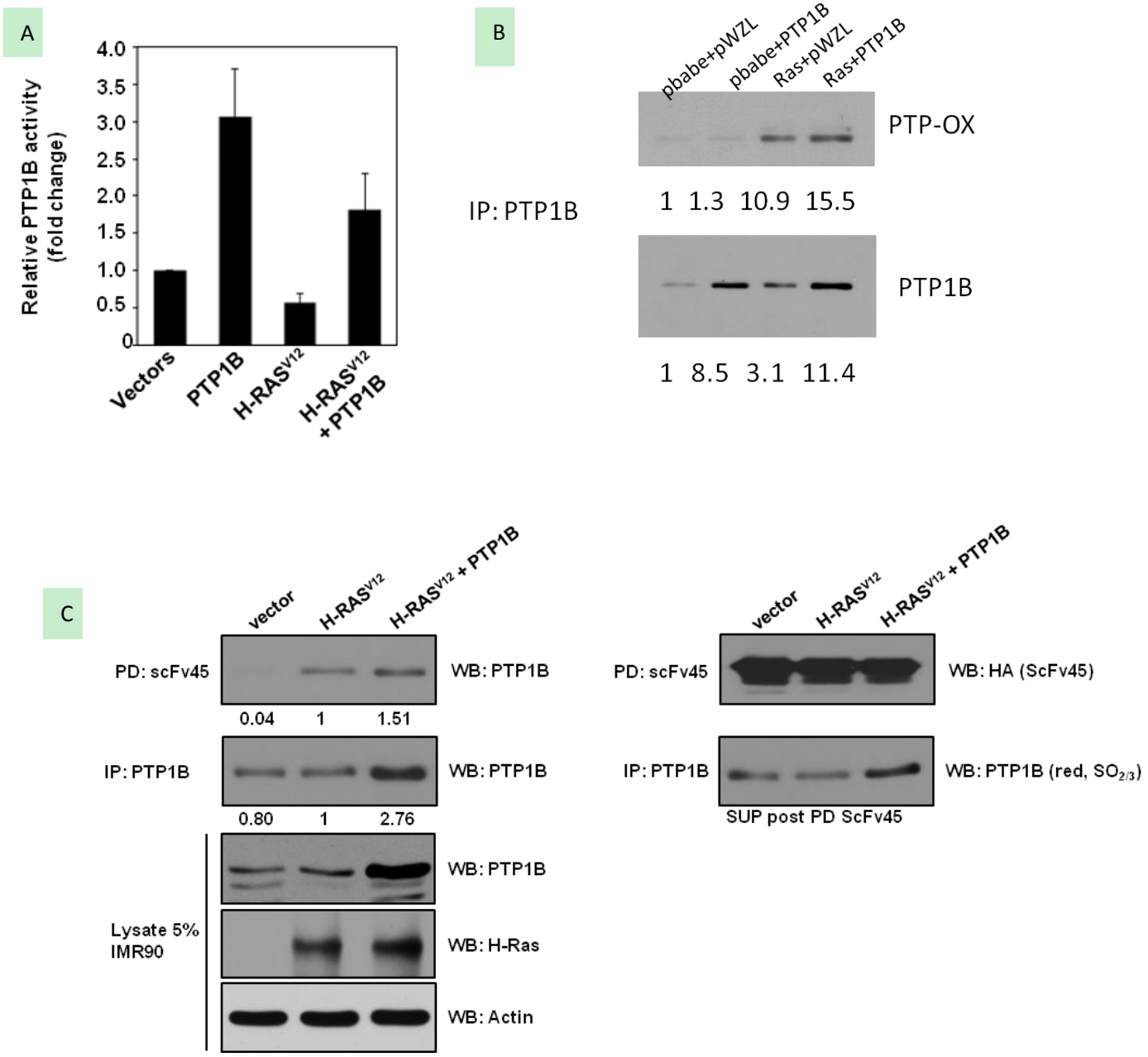

Figure 2.13 Overexpression of exogenous PTP1B compensated for the ROS mediated PTP1B activity loss

A) PTP1B overexpression compensated for RAS/ROS-mediated PTP1B decreased catalytic activity. PTP1B was immunoprecipitated from indicated IMR90 cell lysates and PTP1B activity was measured using DiFMUP. B) PTP1B oxidation detected by PTPox antibody. Cells expressing indicated proteins were lysed under anaerobic condition in present of IAA. PTP1B were precipitated from the lysate and subjected to reduction and pervanadate oxidation. The

precipitates were then blotted with PTPox antibody to exam the level of oxidation. C) Quantification of the reversible oxidation of PTP1B using scFv45. Reversibly oxidized PTP1B was pulled down indicated cell lysates using scFv45 (Haque et al., 2011a)(left top panel). An anti-PTP1B antibody (FG6) was used to immunoprecipitate PTP1B either from the scFv45 supernatant to quantify the non-reversible oxidized fraction (PTP1B red, $SO_{2/3}$) and from lysates to quantify the total fraction (PTP1B total).

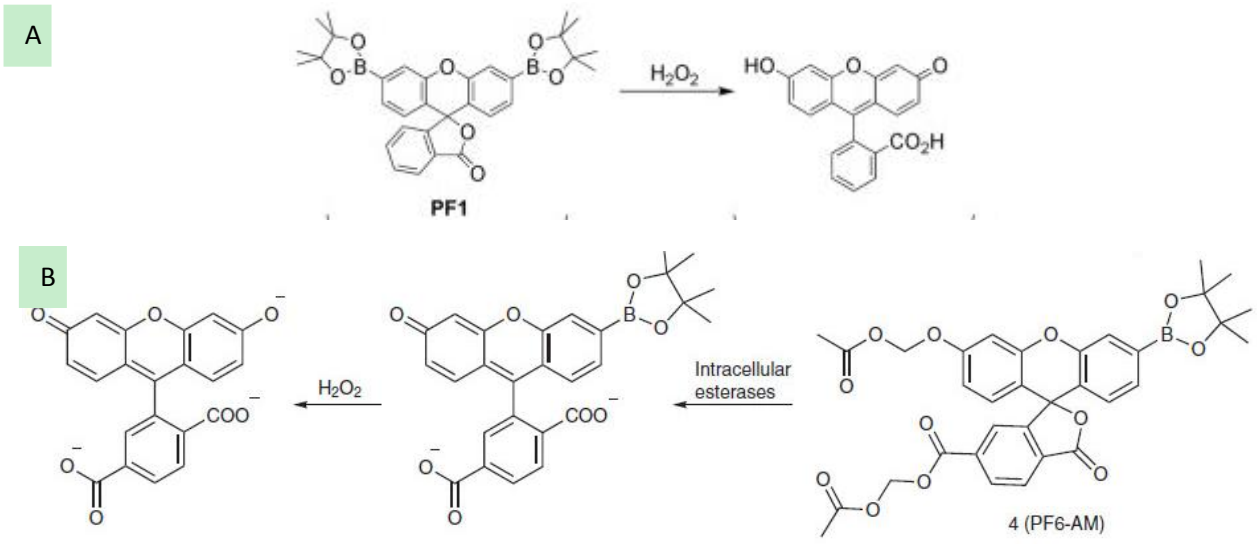

Figure 2.14 PF1 and PF6 probe.

A.Treatment of colorless, non-fluorescent Peroxyfluor-1 (PF1) with hydrogen peroxide yields bright green fluorescein (Miller and Chang, 2007). B, PF6-AM probe

Chapter3

3.1 Introduction

In chapter 2, we found that PTP1B is reversibly oxidized in RAS-induced senescent cells and that PTP1B is important in regulating OIS. We were interested to understand the signaling mechanism through which PTP1B oxidation affected OIS. We planned to identify the substrates of PTP1B in senescent cells, which would allow us to further dissect the signaling mechanism of how PTP1B regulates senescence through its substrates.

3.1.1 Trapping mutant assay

Our lab has developed a PTP substrate trapping strategy that enables the specific analysis and identification of the PTP substrates (Flint et al., 1997a). The substrate trapping mutant contains an Ala mutation at the conserved Asp residue shared throughout classical PTP members. As introduced in Chapter 1, the first step of the dephosphorylation involves the catalytic cysteine (Cys 215) that carries out the nucleophilic attack on the phosphate. This is coupled with protonation of the tyrosyl leaving group of the substrate by the conserved aspartic acid residue (Asp181 in PTP1B). In the trapping mutant, the Asp-181, which functions as a general acid in protonating the tyrosyl leaving group of the substrate, is changed to Ala in the trapping mutant. The mutant retains the binding affinity to its substrates in a cellular context but has impaired catalytic function. The K_m of trapping mutant to its substrate is comparable to the WT whereas the V_{max} is $1/10^5$ of that of the WT enzyme (Flint et al., 1997a; Tonks, 2006a). After expression *in vivo*, the trapping mutant will bind to its physiological substrates in the cell, protecting them from dephosphorylation by the endogenous PTPs. The

complex is relatively stable as the turnover rate is markedly reduced. It gives us the time window to isolate the PTP/substrate complex by co-immunoprecipitation and thereafter the substrates can be identified by mass spectrometry analysis or immuno blotting.

Combining PTP substrate trapping with mass spectormetry identification will provide a powerful tool for us to profile the proteins regulated by PTPs under different conditions. Chang et al have successfully applied this approach to identify the substrates of protein tyrosine phosphatase dPTP61 in Drosophila cells(Chang et al., 2008). We planned to use this method to study the substrates of PTP1B in RAS-induced senescent cells.

3.1.2 Quantitative mass spectrometry

In our study, we planned to use quantitative mass spectrometry to analysis the protein enrich by PTP1B trapping mutant. In recent years the notion of performing protein-protein interaction studies using quantitative MS measurements has gained wider appreciation(Westermarck et al., 2013). Quantitative MS approaches can identify changes in the compositions of protein complexes and can distinguish background contaminants in protein complex purifications from true interacting partners(Oeljeklaus et al., 2009). Quantitatively comparing the proteins co-precipitated with PTP1B trapping mutant in senescent cells with the proteins co-precipitated with PTP1B in control samples, which would distinguish the real substrates of PTP1B from non-specific binding proteins.

Quantitative mass spectrometry can be divided into two major categories: the isotopic labeling approaches and the label free approaches. The commonly used isotopic approaches include: 1. Chemical labeling, where the isotopic labeled probes are chemically incorporated

onto the peptides. The examples are isobaric tags for relative and absolute quantitation (iTRAQ)(Ross et al., 2004) and isotope-coded affinity tags (ICAT)(Gygi et al., 1999). 2. biological or metabolic labeling, where stable isotope-containing amino acids are added in the cell culture media or chow food in place of normal amino acid. Labeling of the peptide/protein is achieved in the culturing/growing step (SILAC)(Ong et al., 2002). Label-free methods do not need isotopic labeling of the samples. In label free methods, highly sensitive and accurate LC-MS or LC-MS/MS experiments are compared with each other and analyzed for similarities and differences between samples(Neilson et al., 2011).

Labeling strategies are often considered to be more accurate in quantitating protein abundances; however, these techniques require expensive isotopic reagents, specific software, and expertise in analyzing data. Additionally, the number of samples that can be analyzed in a single experiment is limited and some labeling strategies cannot easily be applied to all types of samples. In recent years, the label free approach, which is based on the correlation between protein abundance and peak areas (Bondarenko et al., 2002; Chelius and Bondarenko, 2002) or number of MS/MS spectra (Liu et al., 2004a) is increasingly accepted in the field of quantitative proteomics.

3.1.3 Label-free quantitation

In our study to identify PTP1B substrates in OIS, the cells stop proliferating after RAS-induced senescence, it results in low cell density in tissue culture and low yield of protein harvested per plate. The SILAC method is not feasible for our project because of the large

amount of cell culture media needed. In our study, we used label free quantitation approach for MS identification of PTP1B substrates.

Label-free quantitation can be divided into two distinct groups: (1) area under the curve (AUC), which measures the signal intensity based on precursor ion spectra and (2) spectral counting, which is based on counting the number of peptides assigned to a protein in an MS/MS experiment(Neilson et al., 2011)(Figure 3.7).

In the AUC approach, usually the peptide ion peak area is integrated as a measurement of peptide quantity. This allows the quantity of protein to be compared between different samples or with standard curve built with synthetic peptide(Tate et al., 2013). This method requires high mass accuracy mass spectrometer to minimize the interfering signals of similar but distinct mass. Moreover, the right balance between acquisition survey and fragment spectra has to be found. Extensive peptide sequencing by MS2 will certainly benefit protein identification, whereas multiple sampling at MS1 is the prerequisite of a better quantitative reading. It means that even for the fast sampling instrument, better quantitation accuracy will inevitably lead to lower proteome coverage and vice versa(Neilson et al., 2011).

The peptide spectral counting approach is based on the empirical observation that more of the particular protein present in the sample, the more spectra can be detected for the peptides from that protein(Liu et al., 2004a). Hence by comparing the spectra counting between samples, we can perform the relative quantitation of proteins. In contrast to comparing the AUC, which requires integration of peptide ion intensity from MS1, spectra counting will actually benefit from extensive MS2 data acquisition (Tate et al., 2013).

Comparing the Exponentially Modified Protein Abundance Index (emPAI)(Ishihama et al., 2005) is one of the peptide spectrum counting approaches and in our study we used this approach in the identification of PTP1B substrates. emPAI score is calculated as emPAI$= 10^{\frac{N_{observed}}{N_{observable}}} - 1$, in which $N_{observed}$ is the number of unique peptide identified in MS analysis and $N_{observable}$ is the number of peptide which theoretically detected in MS. The emPAI has been shown to have good correlation with protein abundance(Ishihama et al., 2005).

Several groups carried out independent studies to compare the label free approaches and the isotopic labeling approaches (Bantscheff et al., 2007; Patel et al., 2009; Ryu et al., 2008; Turck et al., 2007). The studies suggest that with the improvement of instruments, the accuracy of label free approach is comparable to isotopic labeling approach. Moreover, label free quantitation has the following advantages over the isotopic labeling approaches: The time and resource consuming steps of incorporating isotope onto peptides is omitted; label free approach provides higher dynamic range and better proteome coverage than other approaches(Bantscheff et al., 2007).

Both AUC method and spectra counting method (emPAI score) were used in our experiments to quantitatively compare the protein amounts between different samples.

3.2 Method

3.2.1 PTP1B substrate trapping

Protein A/G Plus agarose beads (Santa cruz), Protein A Dynabeads and Protein G Dynabeads (Invitrogen) were used for immunoprecipitation. As previously described(Flint, Tiganis et al. 1997), the cells expressing PTP1B D181A and control cell lines were lysed in trapping buffer (50mM Tris, 5mM EDTA, 150mM NaCl, 1% Triton, 5mM IAA, 10mM Sodium phosphate, 10mM NaF), with 10micorM RNase A. The lysate were then incubated with PTP1B antibody-bound protein G Dynabeads for 1.5hr in 4C. The immuno-precipitated proteins were then analyzed by mass spectrometry or western blot.

3.2.2 MS identification of PTP1B substrates after on-beads digestion

PTP1B trapping mutant assay was carried out with the cells expressing PTP1B DA+RAS, PTP1B WT+RAS and PTP1B DA+vector control. The PTP1B immunoprecipitates were collected and directly subject to on-beads digestion and MS analysis.

18 uL of 100mM TEAB and 2uL of ProteaseMAX™ Surfactant (Promega) were added to the beads from each sample. Tris (2-carboxyethyl) phosphine (Sigma-Aldrich) was added to final concentration of 5mM and the samples were heated at 55°C for 20 min. Samples were then cooled to room temperature and Methyl methanethiosulfonate (Thermo Scientific) was added to final concentration of 10mM. After incubating at room temperature for 20 minutes, 2ug of sequencing grade trypsin (Promega) were added to each sample. Samples were digested overnight at 37°C with gentle shaking. Samples were spun in a centrifuge for 5 minutes at

13,000 x g and the supernatant was removed and dried to completeness. The samples were then re-suspended in 20uL of mobile phase A prior to LC/MS analysis.

An Orbitrap XLmass spectrometer (Thermo Scientific), equipped with a nano-ion spray source was coupled to an EASY-nLC system (Thermo Scientific). The nano-flow LC system was configured with a 180-µm id fused silica capillary trap column containing 3 cm of Aqua 5-µm C18 material (Phenomenex, Ventura, CA), and a self-pack PicoFrit™ 100-µm analytical column with an 8-µm emitter (New Objective, Woburn, MA) packed to 15cm with Aqua 3-µm C18 material (Phenomenex). Mobile phase A consisted of 2% acetonitrile; 0.1% formic acid and mobile phase B consisted of 90% acetonitrile; 0.1% formic acid. 10uL of sample were injected through the autosampler onto the trap column. Peptides were then separated using the following gradient: 8% B for 5 min, 8% B to 35% B over 80 min, 35% B to 70% B over 5 min, held at 70% B for 5 min, 70% B to 5% B over 2 min and the final 15 min held at 5% B. The flow rate was 300 nL/min for the duration of the method.

Eluted peptides were directly electrosprayed into the Orbitrap XL mass spectrometer with the application of a distal 2.3 kV spray voltage and a capillary temperature of 275°C. Each full-scan mass spectrum (380-1700 *m/z*) was followed by MS/MS spectra for the top 6 masses. Collision-induced dissociation (CID) was used with a normalized collision energy of 35% for fragmentation. Duration of 70 seconds was set for the dynamic exclusion parameters with an exclusion list size of 500. We used monoisotopic precursor selection for charge states 2+ and greater. MS data was collected in profile mode while MS/MS data was collected in centroid mode.

Peaklist files were generated by Mascot Distiller (Matrix Science) and searched using Mascot against the Uniprot human database (88,378 sequences). Peptide mass tolerance was set to 20 ppm while the fragment ion tolerance was set to 0.6 da. The results were adjusted to have a false discovery rate (FDR) of 0.93%.

emPAI scores were used as the quatitation of protein abundance in the samples. The emPAIs in each sample were normalized to the emPAI of PTP1B in individual sample. The fold changes were calculated using the normalized emPAI of corresponding proteins.

3.2.3 MS identification of PTP1B substrate after vanadate elution

IMR90 cells co-expressing Ras + PTP1B D181A, Ras + PTP1B WT, and pBabe + PTP1B D181A were lysed in trapping mutant buffer (50 mM Hepes pH 7.5, 1 mM EDTA, 150 mM NaCl, 1% Triton X-100, 10 mM Sodium phosphate, 10 mM NaF, and 5mM IAA, 10 µg/ml leupeptin, 10 µg/ml Aprotinin). Protein content of lysates was measured by Bradford assay, and equal amounts of lysates were incubated with FG6 coupled to the Protein-G magnetic beads (Dynabeads, Invitrogen) for 2 h at 4 °C. The supernatant fluids were then removed and the beads were washed twice in trapping mutant buffer and twice in PBS. The beads were incubated with 30 µL of 2.5 mM Na_3VO_4 at RT for 10 min to elute PTP1B substrates. The supernatant fluids were collected and loaded onto an SDS-PAGE gel. The electrophoresis was stopped when proteins just entered the resolving gel to remove non-protein components. The gel was stained by Coomassie blue and the gel bands were excised and reduced, alkylated, and digested in-gel with sequence grade modified trypsin (Promega). After digestion, peptides were

extracted by 50% acetonitrile in 5% formic acid, dried in a speedvac, and desalted using StageTips packed with C18 before analysis by MS.

A nanoflow HPLC instrument, EASY nLC 1000, was coupled directly to a Q Exactive mass spectrometer (Thermo Fisher Scientific) with a nanoelectrospray ion source (Proxeon Biosystems, now Thermo Fisher Scientific). Chromatography columns were packed in-house with PeproSil-Pur C18-AQ3 µm resin (Dr. Maisch GmbH). Peptides were loaded onto a C18-reversed phase column (15 cm long, 75 µm inner diameter) and separated with a linear gradient of 3 to 30% acetonitrile in 0.1% formic acid at a flow rate of 250 nL/min over 120 min.

The Q Exactive was operated in data-dependent mode. The method dynamically chose the top 10 most abundant precursor ions from the survey scan (300 – 1650 Th) for HCD fragmentation. Dynamic exclusion duration was 45 s. Survey scans were acquired at a resolution of 70,000 at m/z 200. Resolution for HCD spectra was set to 17,500 at m/z 200. Normalized collision energy was 27 eV.

The data analysis was performed with MaxQuant software (Version 1.2.7.0, Max Planck Institute of Biochemistry) supported by the Andromeda search engine. Data were used to search a UniProt Human fasta database encompassing 71, 434 protein entries. Mass tolerance for searches was set to maximum 7 ppm for peptide masses and 20 ppm for HCD fragment ion masses. Searches were performed with carbamidomethylation as a fixed modification and protein N-terminal acetylation and methionine oxidation as variable modifications. A maximum of 2 missed cleavages was allowed while requiring strict trypsin specificity. Peptides with a

minimum sequence length of 7 were considered for further data analysis. Peptides and proteins were identified with a false discovery rate (FDR) of 1%.

The protein quantitation data generated by MaxQuant were analyzed using Perseus (1.4.1.3). A two-sample t-test with multiple hypothesis correction was performed with FDR = 0.01.

3.2.4 Estimation of the percentage of Ago2 trapped by PTP1B

Lysate was harvested from the samples expressing RAS +PTP1B WT or RAS +PTP1B D181A, or PTP1B D181A alone and incubated with anti-Ago2-bound protein A/G plus beads in presence of RNasA. The precipitates were then resolved on SDS-PAGE and blotted for PTP1B. Lysate was harvested from the samples expressing RAS +PTP1B WT or RAS +PTP1B D181A, or PTP1B D181A alone. Trapping mutant assay was carried out in 50% of each lysate, and immunopercipitation of Ago2 is carried out in the other 50% of the lysate. Immunoprecipitances were blotted with anti-Ago2 antibody. The supernatant from IP and same amount of lysate was resolved by SDS/PAGE and blotted with anti-Ago2 and anti-PTP1B to compare the IP efficiency.

3.2.5 Reverse trapping by Ago family protein

Lysates from HEK293 cells expressing PTP1B (DA) alone, RAS and PTP1B (DA) or RAS and PTP1B (WT) were prepared in trapping LB and lysates were immunodepleted using an AGO2 antibody. The supernatants, recovered after the immunoprecipitation, were incubated with a pan-AGO antibody. Pan-AGO immunoprecipitates were blotted for AGO2, PTP1B and for the AGO 1, 3 and 4 isoforms using a pan-AGO antibody.

3.3 Result

3.3.1 Identification of PTP1B substrates by MS

Our hypothesis is that PTP1B oxidation in RAS-induced senescent cells caused hyperphosphorylation of PTP1B substrate and altered signaling pathways. To identify the PTP1B substrate, we employed an *in vivo* PTP1B substrate trapping mutant strategy. We stably co-expressed RAS and PTP1B D181A, the substrate trapping mutant of PTP1B, in IMR90 cells to establish an *in vivo* PTP1B trapping model to look for the substrates regulated by PTP1B during RAS-induced senescence. Cells expressing RAS with WT PTP1B and expressing only PTP1B D181A were chosen as controls to rule out the proteins interacting with PTP1B through non-active site or the proteins that were phosphorylated in non-senescence condition.

We performed MS identification for PTP1B substrate in senescent cells. PTP1B was immunoprecipitated from cellular extracts of IMR90 cells expressing RAS and a substrate-trapping mutant PTP1B (DA) or a catalytically competent PTP1B. The protein complex was digested on-beads and the digest was analysed by liquid chromatography-tandem mass spectrometry (LC-MS/MS). The exponentially modified protein abundance index score (emPAI) was obtained in the MS analysis. emPAI score offers approximate, label-free, quantitation of proteins in a mixture (Ishihama et al.,2005). Based on the emPAI score of proteins co-purifying with PTP1B (normalized to PTP1B for each sample), Argonaute 2 (Ago2) was approximately 4-fold enriched in the PTP1B (DA) trapping mutant sample when compared to PTP1B (WT) results. No interaction was detected in cells not expressing RAS. The data also suggested that Ago2 was the most enriched protein by PTP1B trapping mutant in senescent cells (Table 3.1).

To confirm that the interaction between Ago2 and PTP1B trapping mutant is through the binding at PTP1B active site, we treated the lysate with RNase to exclude the possibility that Ago2 binds to PTP1B in an RNA mediated manner. Moreover, we used sodium orthovanadate (Na_3VO_4) to elute the proteins from PTP1B trapping mutant co-precipitation. Sodium orthovanadate is a competitive inhibitor of PTPs and is generally believed to interact with PTPs as a transition state analogue (Denu et al., 1996; Huyer et al., 1997). Chang, et al have shown that vanadate can efficiently elute substrates from PTP trapping mutant without dissociating non-substrate proteins from the PTP(Chang et al., 2008). We collected the eluates and performed an MS label free quantitaion of the proteins eluted from different samples. Ago2 was the most abundant protein found in a complex with the substrate-trapping mutant in RAS-expressing fibroblasts compared to the WT enzyme (Table 3.2). A similar enrichment of Ago2 bound to PTP1B DA (> 8 fold) was also observed when comparing lysates of cells in the presence and absence of RAS (Table3.3). We immune-blotted the precipitates harvested in trapping mutant assay with Ago2 antibody. The western blot result also confirmed that Ago2 was a substrate of PTP1B. Ago2 was trapped by PTP1B D181A expressed in the RAS-induced senescent cells. Minimal level of Ago2 interacted with WT PTP1B, or with PTP1B D181A in the proliferating cells (Figure 3.1).

We estimated the percentage of Ago2 binding to PTP1B D181A over total Ago2 in the cells. We used the same amount of lysate to perform PTP1B trapping mutant assay and the same time with a total Ago2 immuno-precipitation. Comparing the supernatant after IP with the total cell lysate, we illustrated that there was >85% immunodepletion of Ago2 and PTP1B. We compared the signal intensity of Ago2 co-precipitated in PTP1B trapping mutant assay with

total Ago2 precipitated by Ago2 antibody, 34% of total Ago2 associated with PTP1B D181A in RAS expressing cells (Figure 3.1).

3.3.2 Ago2 was selectively targeted by PTP1B

Ago2 is found in complex with Dicer and TRBP to form the RISC loading complex (RLC)(Chendrimada et al., 2005). Interestingly, we did not detect Dicer in PTP1B trapping mutant assay and TRBP was not specifically enriched by trapping mutant in RAS expressing cells. This suggested that neither Dicer nor TRBP was a substrate of PTP1B and Ago2 might dissociate from RLC when it was trapped by PTP1B (Figure 3.2 B).

There are four members in the mammalian Argonaute protein family: Ago1, 2, 3 and 4. All four of them share very high sequence similarity (Figure 3.6). It was interesting for us to find out whether or not the other 3 Argonaute proteins were substrates of PTP1B. The challenge was that there are no good antibodies for Ago3 and Ago4. However, we have good antibodies against Ago2 and a pan-Ago antibody that detects all 4 members of human Ago family. We performed a reverse trapping mutant assay to detect PTP1B interaction with Ago 2 versus other Ago family members. We first immune-precipitated Ago2 from the cell samples expressing RAS+WT PTP1B, RAS+ PTP1B D181A and vector+PTP1B D181A. The post-AGO2 IP supernatant was then incubated with a pan-Ago antibody coupled beads for a pan-Ago IP. We detected that Ago2 was 90% depleted from the lysate (Figure 3.2A), therefore the pan-Ago IP would presumably only precipitate Ago1, 3 and 4. By blotting with PTP1B, we could detect PTP1B co-precipitated with Ago2 in the trapping mutant condition (RAS+ PTP1B D181A), but not in the

pan-Ago IP of the supernatant (Figure3.2 A). The result suggested that PTP1B selectively targeted Ago2 but not Ago1, 3 or 4.

3.3.3 Ago2 phosphorylation was regulated by PTP1B

To confirm PTP1B dephosphorylated Ago2, we co-expressed PTP1B and RAS in IMR90 cells and used anti-Ago2 antibody to precipitate Ago2 proteins. Immunoblotting the precipitates with anti-phospho-tyrosine antibody demonstrated that RAS expression enhanced Ago2 tyrosine phosphorylation. In contrast, PTP1B expression attenuated Ago2 tyrosine phosphorylation (Figure 3.3 A). When we precipitated tyrosine phosphorylated proteins and detected amount of Ago2 precipitated with the pY antibody, we saw a similar result: increased amount of Ago2 was detected in RAS expressing samples whereas PTP1B co-expression lowered Ago2 phosphorylation (Figure 3.3 B).

In replicative senescent cells, we detected elevated Ago2 tyrosine phosphorylation. The level of Ago2 tyrosine phosphorylation was similar to that in RAS-induced senescent cells (Figure 3.4). Note that PTP1B oxidation also existed in replicative senescent cells, shown in Chapter 2 (Figure 2.5). The result indicated the PTP1B/Ago2 pathway might be a common feature of cellular senescence.

3.3.5 Ago2 was a major substrate of PTP1B

The MS analysis suggested that Ago2 was the most enriched protein by PTP1B in RAS-expressing cells. To further test whether Ago2 was a major target of PTP1B in senescent cells, we performed phosphotyrosine IP from lysates harvested from cells expressing RAS with PTP1B

WT, RAS with PTP1B D181A or PTP1B D181A alone. The PTP1B trapping mutant binds to its substrates and protects the substrates from being dephoshporylated by active phosphatases. The expression of PTP1B trapping mutant can enhance the phosphorylation of PTP1B substrates. Blotting the precipitates with anti-phosphotyrosine antibody demonstrated the enhanced phosphorylation of a protein at 100kDa, showing a prominent band in the sample that PTP1B DA and RAS were coexpressed. When we immune-deplete Ago2 from the lysate before pTyr IP, the 100KDa band was significantly decreased (Figure3.5). The MS analysis showed that Ago2 was the most abundant protein enriched by PTP1B trapping mutant in senescent cells. Taken together, the results suggested that Ago2 is a major substrate of PTP1B.

3.4 Discussion

In this chapter, we identified that Ago2 was a substrate of PTP1B in senescence cells. Ago2 phosphorylation was enhanced in RAS-induced senescent cells and PTP1B expression attenuated Ago2 phosphorylation. Moreover, we demonstrated that Ago2 was specifically targeted by PTP1B, whereas Ago1,3,4 were not substrates of PTP1B.

3.4.1 PTP1B dephosphorylates Ago2 in senescent cells

PTP1B has been shown to dephosphorylate a wide range of proteins *in vitro*, leading to the argument that PTPs might not be very selective on their substrates. However, it has been shown that PTP1B targets at specific substrate *in vivo* (Flint et al., 1997a) In our study, we found using mass spectrometry analysis that 8 proteins were significantly enriched in senescent cells by PTP1B trapping mutant when compared to that by WT PTP1B, while 16 proteins were enriched by PTP1B trapping mutant from senescent cells as compared to that from control cells. ERK and p38MAPK are known to be tyrosine phosphorylated and activated in OIS(DeNicola and Tuveson, 2009b), however MS analysis did not detect either of these proteins enriched by PTP1B trapping mutant. The result further supports that PTP1B displayed substrate specificity *in vivo.*

In this chapter, we identified Ago2 as a substrate of PTP1B in senescent cells. As introduced in Chapter 1, the localization of PTPs, determined by their non-catalytic sequences, contribute to the PTP substrate specificity. PTP1B is an ER bound protein, with the C-terminus tail anchoring it to the ER and the catalytic domain facing the cytosolic side. Ago2 is found majorly in the cytosol. A recent report found that mi- and si-RNA loaded Ago2, Dicer and TRBP

almost exclusively co-sedimented with the markers of the rough ER membranes (Stalder et al., 2013), where PTP1B is also localized (Frangioni et al., 1992) The colocalization of PTP1B and Ago2 may be important for PTP1B specifically targeting Ago2.

3.4.2 Ago2 phosphorylation and senescence

Ago2 is the core enzyme of RNA induced silencing complex (RISC). Ablation of Ago2 activity impairs microRNA mediated gene silencing (Liu et al., 2004b). Tyrosine phosphorylation has been shown to regulate Ago2 funcion. The tyrosine phosphorylation of Ago2 on Y529 residue was reported to abolishmiRNA loading on Ago2 (Rudel, Wang et al. 2011). The function of Y393 phosphorylation was characterized in 2013. It was shown that Y393 phosphorylation disrupted interaction between Ago2 and Dicer, inhibited the maturation of miRNAs, enhanced cell survival and invasiveness, and correlated with poor survival in breast cancer patients (Shen et al., 2013b).

Ago2 phosphorylation was not previously known to regulate senescence. We hypothesized that PTP1B regulates senescence through affecting Ago2 phosphorylation. We planned to identify the PTP1B target site on Ago2 and study how phosphorylation affected Ago2 function. Furthermore, we planned to investigate the role of Ago2 in RAS-induced senescence. These will be discussed further in the next chapter.

3.4.3 Other potential targets of PTP1B

The two distinct mass spectrometry analysis from different instruments were consistent with each other, showing that Ago2 was significantly enriched by PTP1B trapping mutant

expressed in senescence cells, and that Ago2 was a major substrate of PTP1B. The variation in lower abundant hits might be due to the difference in sample preparation.

In addition Ago2, which is top on the list, some of the other potential PTP1B substrates identified in the MS analysis are worthwhile for further investigation as well. I am going to focus my discussion on two of them, which should be given the top priority in the future study.

3.4.3.1 Transforming growth factor beta-1-induced transcript 1 protein:

It is also called hydrogen peroxide-inducible clone-5 (HIC-5). It was originally isolated as an H_2O_2-inducible cDNA clone whose product was normally found at focal adhesions (Thomas et al., 1999). It was first characterized as a TGF-beta-inducible gene and proposed to be a transcription factor involved in senescence (Shibanuma et al., 1994). HIC-5 induces senescence when overexpressed in human diploid fibroblasts, and HIC-5 expression is lost in K-RAS-transformed cells and in several human tumor cell lines(Shibanuma et al., 1994). These results have led to the proposal that this protein may be involved in growth arrest or cellular senescence (Shibanuma et al., 1994).

In addition to Ago2, which showed as a 100kDa band in PTP1B DA/RAS expressing sample, we detected a 50kDa protein with enhanced tyrosine phosphorylation, suggesting that this 50kDa protein might be the substrate of PTP1B (Figure 3.5). Interestingly, the molecular weight of HIC-5 is 50kDa, making it a strong candidate for PTP1B target in senescent cells. Furthermore, HIC-5 has known tyrosine phosphorylation site, Y60. It has been shown that CAKβ or Fyn promotes the tyrosine phosphorylation of coexpressed HIC-5. HIC-5 phosphorylated on tyrosine 60 is bound specifically by the SH2 domain of Csk (Ishino et al., 2000). The authors

proposed that the phosphorylation might activate a feedback loop, bringing Csk to close proximity to Src Family kinase and CAKβ to terminate the signal. Phosphorylation on Y60 is also observed to inhibit the effect of EGF signalling (Hetey et al., 2005).

The function of HIC-5 fits well in the RAS/PTP1B pathway in oncogene-induced senescence. PTP1B oxidation and inactivation can lead to HIC-5 activation, which may in turn induce senescence. It will be interesting to determint whether HIC-5 is a substrate of PTP1B in OIS and elucidate how the tyrosine phosphorylation on HIC-5 affects its activity in the context of RAS-induced senescence.

3.4.3.2 S100A8

S100A8 (also known as calgranulins A) is a member of the S100 multigene sub-family of cytoplasmic EF-hand Ca2+-binding proteins. It is a small protein with a molecular weight of ~10kDa. When visualizing the pTyr proteins in RAS+PTP1B DA sample, we did not detect a band running a 10kDa. However, it is probably because the gel we used for SDS-PAGE was 10%, which is unsuitable for resolving a 10kDa protein.

However, the property of S100A8 makes it an interesting potential target for the further study. It activates NADPH-oxidase by facilitating the NOX enzyme complex assembly at the cell membrane, transferring arachidonic acid, an essential cofactor, to the enzyme complex (Kerkhoff et al., 2005). S100A8 also contributes to the enzyme assembly by directly binding to NCF2/P67PHOX (Kerkhoff et al., 2005). S100A8/A9 function is also implicated in regulating cell cycle progression. In head and neck squamous cell carcinoma (HNSCC), S100A8/A9 is downregulated at both mRNA and protein levels. S100A8/A9 expression leads to the

inactivation of Cdc2/cyclin B1 complex and thereby causes G2/M cell cycle arrest (Khammanivong et al., 2013).

The specific tyrosine phosphorylation site on S100A8 is unknown. However, tyrosine phosphorylation of S100A8 was found significantly higher in the tumour tissue in cervical cancer compared to normal tissue (Robinson-Bennett et al., 2008). Furthermore, tyrosine phosphorylated S100A8 was demonstrated to translocate to the membrane and facilitate the organization of NOX2 complex and NOX protein activation (Schenten et al., 2010). Taken together, these findings imply that S100A8 tyrosine phosphorylation may regulate important signaling pathways and affect several cellular functions.

The role of S100A8 in NOX protein organization places it upstream of ROS production, while the ROS produced by NOX proteins are believed to be one of the sources causing PTP1B oxidation. However, the mass spec data suggested that S100A8 was a substrate of PTP1B, making it a downstream effector of PTP1B. We propose that S100A8 might serve in a feed forward loop that augment the NOX activity; or there were different waves and sources of ROS that causes PTP1B oxidation in different kinetics; or different pool of S100A8 were carrying out distinctive functions in the cells. It will be particularly interesting to characterize the function of S100A8 in OIS and where in the signaling pathways it stands.

3.4.4 Future characterization of PTP1B substrates

In the future study, we should first use immunoblotting to confirm whether these proteins are trapped by PTP1B D181A trapping mutant in senescent cells. Furthermore, we will test whether the tyrosine phosphorylation of these potential substrates is affected by PTP1B

expression. Once we can confirm that these proteins are real substrates of PTP1B in senescent cells, we can proceed to further understand the role of these substrates in regulating OIS. We should identify the phosphorylation sites on these substrates that are regulated by PTP1B. Furthermore, we study how phosphorylation affects the function of PTP1B and how PTP1B-mediated regulation of these substrates affects OIS. Characterizing multiple pathways regulated by PTP1B will give us a more comprehensive view of the role of PTP1B in OIS.

3.4 Tables and Figures

Table 3.1 Protein enriched by trapping mutant PTP1B vs WT PTP1B in senescent cells, the emPAI score of proteins were normalized to that of PTP1B. Fold change was calculated by dividing the normalized emPAI scores from trapping mutant PTP1B sample by those from WT PTP1B sample.

Protein Name	RAS+PTP1B DA Norm emPAI (RD)	RAS+WT PTP1B Norm emPAI (RB)	Fold Change RD/RB
Protein argonaute-2	0.210366	0.06	3.50
Core histone macro-H2A.1	0.189024	0.06	3.15
Heterogeneous nuclear ribonucleoproteins C1/C2	0.29878	0.14	2.13
Histone H2B type 1-J	2.442073	1.15	2.12
Histone H2B type F-S	2.396341	1.13	2.12
Histone H2A.Z	0.445122	0.23	1.93
Poly [ADP-ribose] polymerase 1	0.17378	0.09	1.93
Serine/arginine-rich-splicing factor 1	0.170732	0.09	1.90
Histone H2A type 1	0.814024	0.47	1.73
Nucleophosmin	0.189024	0.11	1.71
Heterogeneous nuclear ribonucleoprotein A1	0.185976	0.11	1.69
Myosin regulatory light chain 12A	0.45122	0.27	1.67
Vimentin	1.045732	0.7	1.49
Myosin-9	0.265244	0.18	1.47
Tubulin alpha-1B chain	0.167683	0.13	1.29
Actin, cytoplasmic 1	0.643293	0.51	1.26
Histone H1.3	0.307927	0.25	1.23
Heterogeneous nuclear ribonucleoproteins A2/B1	0.246951	0.23	1.07
Myosin light polypeptide 6	0.240854	0.23	1.04
Heterogeneous nuclear ribonucleoprotein M	0.237805	0.23	1.03
Tyrosine-protein phosphatase non-receptor type 1	1	1	1

Table 3.2 Vanadate eluted proteins from RAS+PTP1B D181A mutant sample vs RAS+PTP1B WT sample

Protein IDs	Sequence Coverage [%]	Peptides	PEP (probability of protein identification)	protein Name	Fold change	log t-test p value
Q9UKV8	22.4	18	2.64E-69	Protein argonaute-2	8.1	5.04
P62995	10.1	2	1.93E-08	Transformer-2 protein homolog beta	3.5	1.66
P05109	39.8	4	4.06E-45	Protein S100-A8	3.1	1.67
P38919	29.4	11	7.81E-77	Eukaryotic initiation factor 4A-III	2.8	1.04
Q13435	9.1	7	1.20E-16	Splicing factor 3B subunit 2	2.8	1.57
O00461	6	3	5.79E-09	Golgi integral membrane protein 4	2.7	1.97
Q9NR30	7	5	8.57E-12	Nucleolar RNA helicase 2	2.4	2.05
O75533	7	7	7.28E-17	Splicing factor 3B subunit 1	2.2	1.62

Table 3.3 Vanadate eluted proteins from RAS+PTP1B D181A mutant sample vs Vector+PTP1B D181A sample

Protein IDs	Sequence Coverage [%]	Peptides	PEP (probability of protein identification)	protein Name	Fold Change	log t-test p value
Q9UKV8	22.4	18	2.64E-69	Protein argonaute-2	8.3	3.24
Q08188	13.7	9	1.78E-33	Protein-glutamine gamma-glutamyltransferase E	5.6	3.96
P05121	26.1	11	1.37E-82	Plasminogen activator inhibitor 1	5.2	3.57
O75083	36.5	18	1.25E-172	WD repeat-containing protein 1	4.7	3.90
Q02413	9.4	8	1.16E-25	Desmoglein-1	4.5	3.07
P05089-2	12.4	4	5.47E-10	Arginase-1	4.3	3.47
P15924	17.7	57	0	Desmoplakin	4.3	3.66
O43294	20.8	6	4.90E-36	Transforming growth factor beta-1-induced transcript 1 protein	4.2	3.05
A8MUS3	26.8	7	3.84E-32	60S ribosomal protein L23a	4.1	1.44
Q9NZN4	29.7	15	5.22E-158	EH domain-containing protein 2	4.1	1.75
O14908	28.2	7	6.77E-55	PDZ domain-containing protein GIPC1	4.0	2.07
P05109	39.8	4	4.06E-45	Protein S100-A8	4.0	2.51
P50454	39	17	2.45E-145	Serpin H1	3.9	2.49
Q9NVI7-2	42	7	1.57E-113	ATPase family AAA domain-containing protein 3A	3.9	3.00
Q3SYB4	7.3	3	1.81E-08	Serpin B12	3.8	3.67
P08758	14.4	6	2.73E-14	Annexin A5;Annexin	3.7	2.49
P21589	32.4	19	0	5-nucleotidase	3.6	2.40
B7Z6Z42	28.6	6	4.58E-30	Myosin light polypeptide 6	3.6	2.69

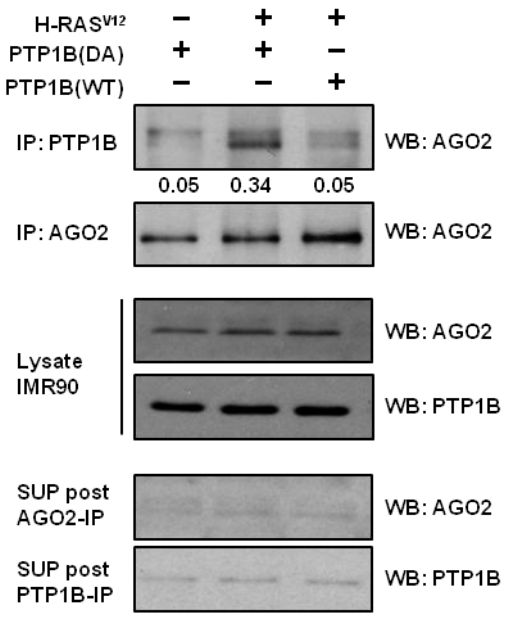

Figure 3.1 Ago2 associated with PTP1B trapping mutant in senescent cells

Lysates were prepared from cells expressing PTP1B (DA), RAS and PTP1B (DA), or RAS and PTP1B (WT). PTP1B was immunoprecipitated from half of each lysate, whereas total AGO2 was immunoprecipitated from the second half. Immunoprecipitates were blotted with an anti-AGO2 antibody, to estimate the stoichiometry of association between AGO2 and PTP1B. 5% of the supernatant recovered after the immunoprecipitation (Post-IP) and same amount of lysate were resolved by SDS-PAGE and blotted for AGO2 and PTP1B to illustrate the efficiency of immunoprecipitation.

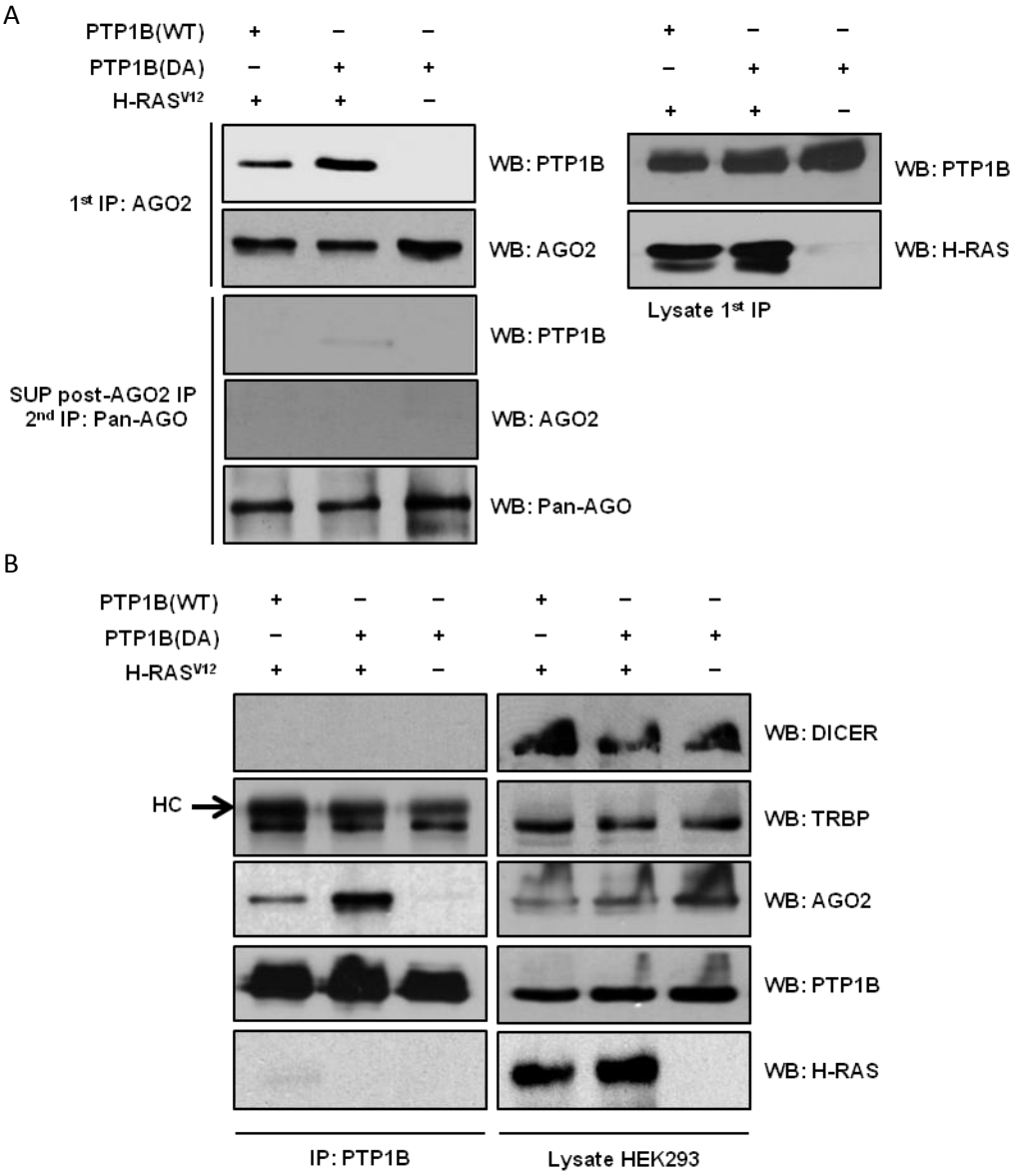

Figure 3.2 PTP1B trapping mutant did not enrich Dicer, TRBP or Ago1,3,4

A) Lysates from HEK293 cells expressing PTP1B (DA) alone, RAS and PTP1B (DA) or RAS and PTP1B (WT) were immunodepleted using an AGO2 antibody. The supernatants, recovered after the immunoprecipitation, were incubated with a pan-AGO antibody. Pan-AGO immunoprecipitates were blotted for AGO2, PTP1B and for the AGO 1, 3 and 4 isoforms using a pan-AGO antibody. **(B)** PTP1B was immunoprecipitated from lysates of HEK293 cells expressing PTP1B (DA), RAS and PTP1B (DA) or RAS and PTP1B(WT). Immune-complexes were blotted for DICER, TRBP, AGO2, PTP1B and H-RAS. HC designates antibody Heavy Chain

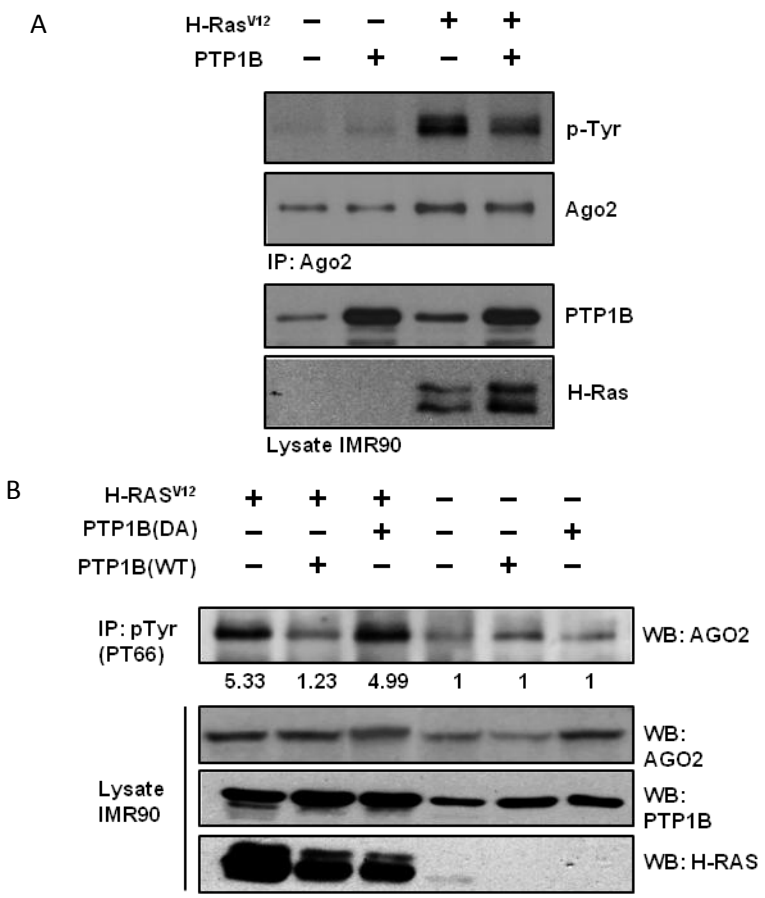

Figure 3.3 PTP1B regulated Ago2 phosphorylation

(A) AGO2 was immunoprecipitated from 10% of the lysates to illustrate AGO2 tyrosine phosphorylation and total levels. 5% of the input lysates were blotted for AGO2 and H-RAS.(**B)** pTyr-proteins were immunoprecipitated from lysates of cells expressing the indicated combination of RAS and PTP1B proteins using the PT-66 antibody. The precipitates were then resolved and blotted for AGO2. Lysates were blotted for the total expression of AGO2, PTP1B (WT or DA), and H-RAS. Images were analyzed using ImageJ

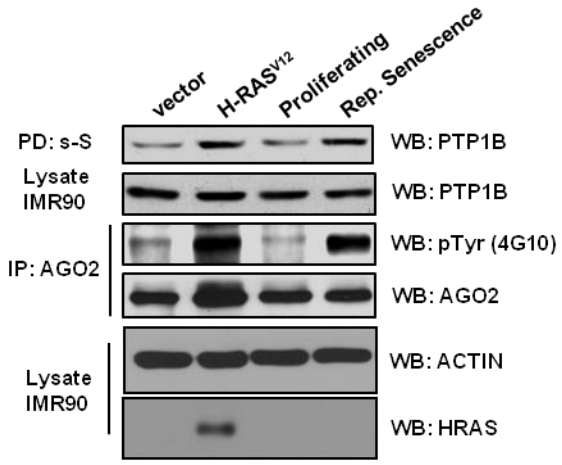

Figure 3.4 Ago2 phosphorylation and PTP1B oxidation were detected in senescent cells

Reversible oxidation of PTP1B was measured using the cysteinyl-labeling assay in lysates of RAS-induced senescent cells, replicative senescent cells (population doubling > 40) and control IMR90 cells. The enriched, biotin-labeled, proteins were resolved by SDS-PAGE and immunoblotted for PTP1B (upper panel). The total level of PTP1B was determined by immunoblotting cell lysates (middle panel). AGO2 was immunoprecipitated from these lysates and tyrosine phosphorylation was detected with anti-pTyr antibody 4G10 (lower panels).

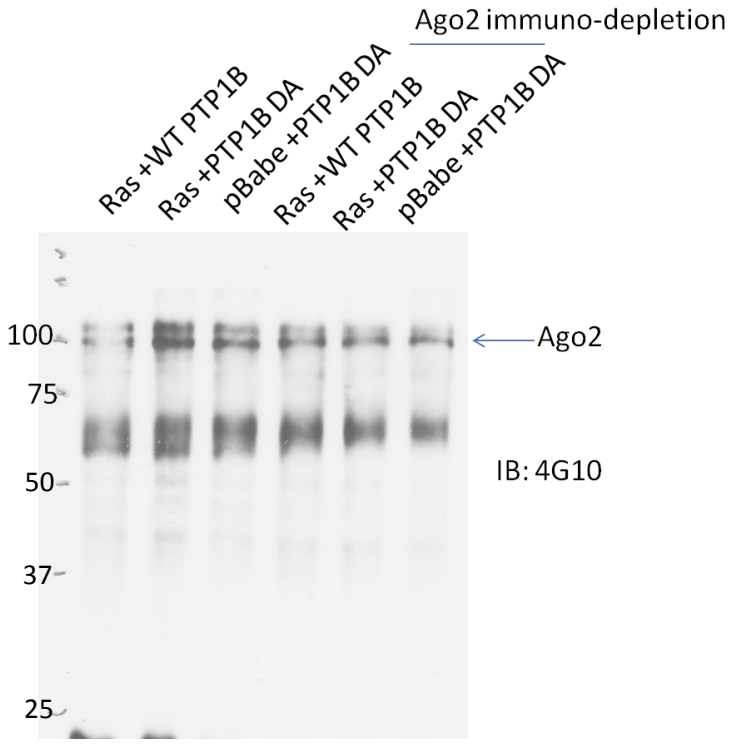

Figure 3.5 Tyrosine-phosphorylated proteins fromPTP1B/RAS coexpressing cells

Lysate from cells expressing RAS+WT PTP1B or HRAS+PTP1B DA or PTP1B DA alone were collected and were split into two equal parts. Half of the lysates were directly subjected to immunoprecipitation with a cocktail of pY antibody (4G10, PT66, P-100). The other half of the lysates were first incubated with Ago2 antibody-bound beads to deplete Ago2, then followed by pTyrosine IP. The precipitates were resolved by SDS-PAGE and blotted with anti-pTyr antibody (4G10)

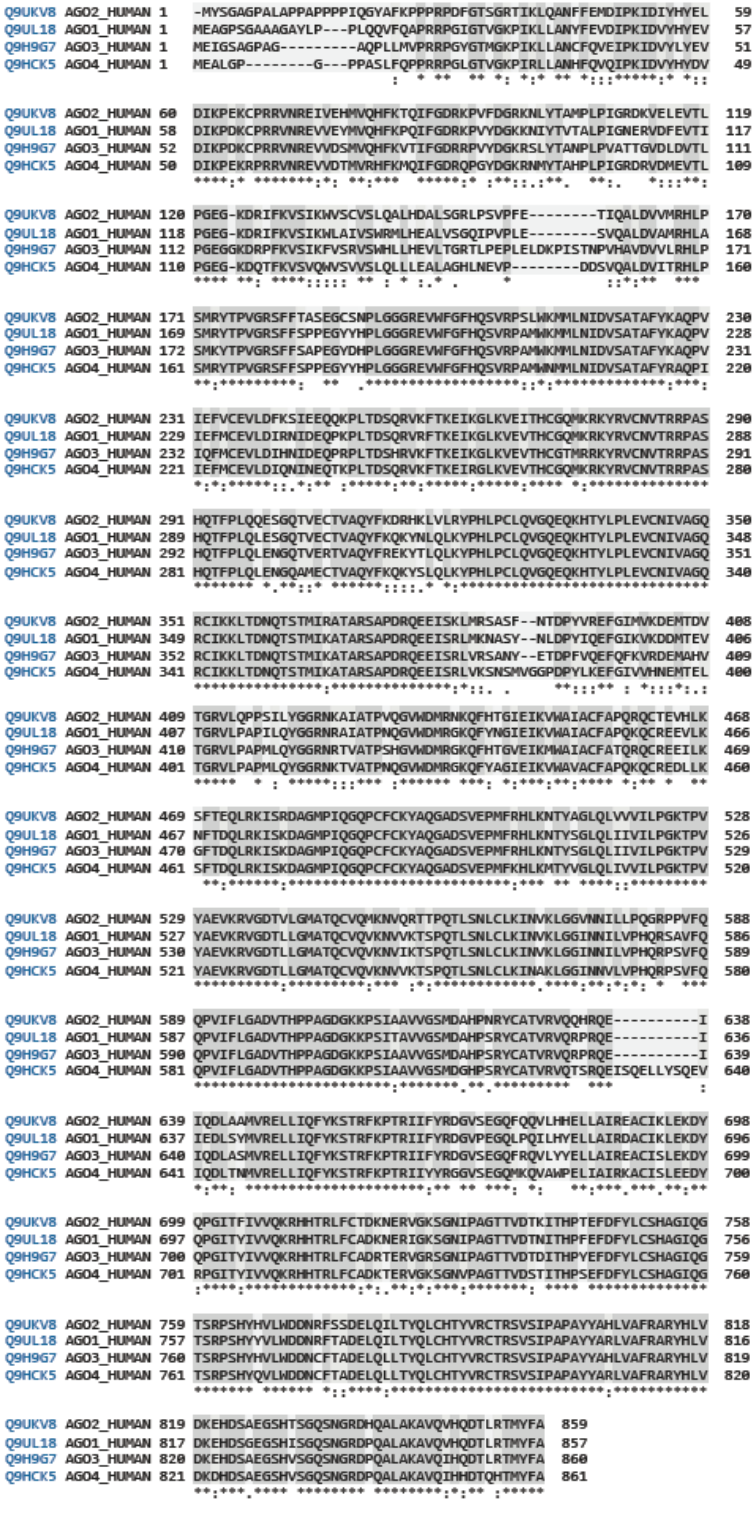

Figure 3.6 Protein sequence alignment of Ago1,2,3,4

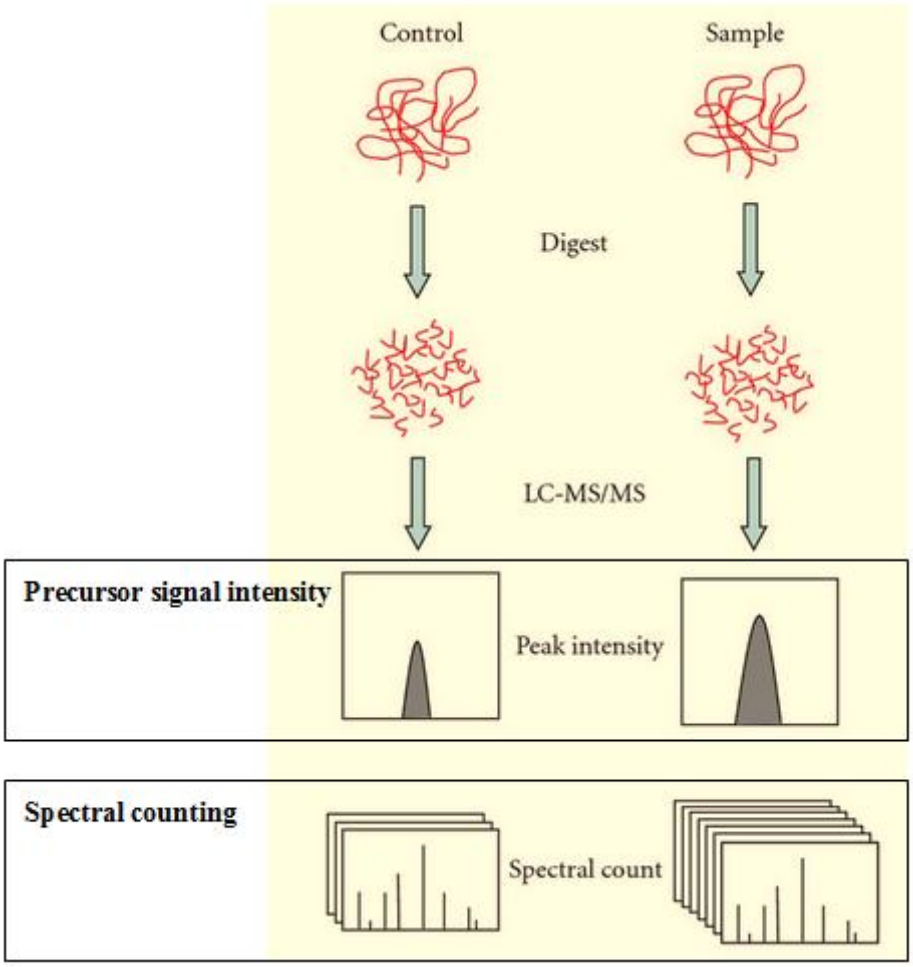

Figure 3.7 Label-free quantitation

Two different approaches of label free quantitation are: 1. area under the curve (AUC), which is based on the precursor ion intensity in MS1 scaning 2. spectral counting, which is based on counting the number of peptides assigned to a protein in an MS2 experiment. [Adopted from Zhu, et al 2010]

Chapter 4

4.1 Introduction

In Chapter 3, we identified Ago2 as a major substrate of PTP1B in OIS. We showed that Ago2 was hyperphosphorylated in senescent cells and PTP1B expression attenuated Ago2 phosphorylation. Ago2 has two tyrosine residues reported to undergo phosphorylation: Y393 and Y529(Rüdel et al., 2011; Shen et al., 2013a).Phosphorylation on Y393 was shown to affect microRNA biogenesis(Shen et al., 2013a), and Y529 phosphorylation impairs Ago2 microRNA loading(Rüdel et al., 2011). Our goal was to identify the phosphotyrosine residue on Ago2 that was regulated by PTP1B and to understand how tyrosine phosphorylation of Ago2 affects its function in OIS.

4.1.1 Ago2 in microRNA pathway

Ago family proteins are core enzymes in small RNA mediated gene silencing complex (RISC)(Liu et al., 2004b). The function of Ago proteins are important for microRNA mediated gene silencing and microRNA biogenesis (Cheloufi et al., 2010).

Mature microRNAs are 19-23 nt in length. The first microRNA lin-4 was isolated from C. elegans in 1993(Lee et al., 1993). In recent years, the number of microRNAs discovered has increased substantially through the rapid development of next generation sequencing technology. Mature mirRNAs are bound by the Ago family proteins to form functional RNA mediated gene silencing complexes (RISCs). In the RISC complex microRNA functions as a guide molecule and leads the RISC to mRNA via base pairing. The RISC binding to target mRNAs leads

to the silencing of the mRNAs(Rand et al., 2005).The functions of microRNA include regulation of heterochromatin formation(Kim et al., 2008), destabilization of mRNA, and translational regulation(Chu and Rana, 2007). microRNA thus regulates a vast variety of biological processes including development, cell proliferation, and metabolism.

4.1.1.1 microRNA biogenesis

microRNA biogenesis is a multiple step process which requires several enzyme complexes (Figure 4.11). The transcription of most microRNA (miRNA) is mediated by RNA polymerase II(Lee et al., 2004), which generates primary-miRNAs. The primary-miRNA is usually several kb in length and contains a stem-loop structure. Cleavage of the primary miRNA is exerted by an RNase III type enzyme Drosha(Lee et al., 2003). Drosha interacts with other proteins to form a large protein complex called microprocessor. The microprocessor recognizes the substrates and assists Drosha to cleave the primary-miRNA at 11bp away from the ss-RNA-ds-RNA junction (Denli et al., 2004; Gregory et al., 2004; Han et al., 2004; Landthaler et al., 2004) (Figure 4. 11). The cleavage at the stem releases a hairpin structure RNA, called pre-miRNA.

The pre-miRNAs are exported to the cytosol following nuclear processing by Drosha. This export is mediated by exportin-5(EXP5). EXP5 recognizes the dsRNA stem that is longer than 14bp and with a short 3’ end overhang. This is a characteristic structural feature of pre-miRNAs(Kim, 2004). The length of the double-stranded stem and the 3´ end overhangs is important for successful binding to Exportin-5, ensuring the export of correctly processed pre-miRNAs (Figure 4.11)(Zeng and Cullen, 2004).

Dicer is responsible for cleaving the pre-miRNA at the terminal loop, once the pre-miRNA is transported into the cytoplasm(Bernstein et al., 2001). This cleavage generates ~ 22nt microRNA duplexe with a phosphate group at the 5' end and a 2-nucleotide overhang at the 3' end. In mammalian cells, Dicer associates with TRBP, which facilitates Dicer in pre-miRNA processing and the subsequent miRNA loading to Argonaute proteins (Ago)(Figure 4.11)(Chendrimada et al., 2005; Haase et al., 2005; Lee et al., 2006).

4.1.1.2 microRNA loading

The RISC loading complex (RLC), containing Dicer, TRBP and Ago protein, functions to facilitate miRNA loading (Gregory et al., 2005; MacRae et al., 2008). Dicer contains two different RNA-binding sites: one that positions pre-miRNA for cleavage, and one that rebinds the cleaved miRNA with the help of TRBP, a dsRNA-binding domain protein (Figure 4.12A) (Gregory et al., 2005; Maniataki and Mourelatos, 2005; Meister et al., 2005). In mammals, TRBP interacts with Dicer, positions the pre-miRNA in the right orientation for Dicer mediated cleavage and transfers the cleaved RNAs to Ago(Haase et al., 2005; Noland et al., 2011; Tomari et al., 2004). HSP70 and HSP90 facilitate the transfer of double-stranded miRNA to Ago by keeping Ago in an "open" conformation, allowing it to accommodate the RNA duplex (Figure 4.12 B) (Iwasaki et al., 2010). Hence, a minimal RISC loading complex requires Dicer, a dsRNA-binding protein (TRBP in case of mammalian cells), the HSC70–HSP90 system and an Ago protein. The interruption of RISC loading complex formation will affect the loading of Ago, thus impairing the formation of a functional RISC complex.

Following miRNA loading, the RNA duplex is unwound. The guide strand of the miRNA duplex remains in Ago, whereas the other strand, called the passenger strand, is removed (Schwarz et al., 2003). It was shown that the endogenous RNase activity of Ago proteins is responsible for the removal of passenger strand of siRNA and some of miRNA duplexes (Diederichs and Haber, 2007; Matranga et al., 2005). Perfectly paired siRNA or miRNA duplexes are cleaved by catalytically active Ago proteins, such as Ago2, and can be efficiently unwound. Ago proteins that lack catalytic activity are loaded as well but are less efficient in removing the passenger strand (Rand et al., 2005). The N-terminal domain, which has the RNA helicase activity of Ago protein is likely to support the unwinding and removal of the passenger strand(Kwak and Tomari, 2012) (Figure 4.12 B).

4.1.1.3 miRNA mediated translation repression

miRNA mediated translation repression is a complex process. Several mechanisms are proposed on how RISC mediates translation repression in mammalian system: RISCs have been proposed to inhibit initiation or post-initiation stages of translation by interfering with 40S small ribosomal subunit recruitment (Wang et al., 2008) or by preventing translation elongation(Petersen et al., 2006). Other evidence suggests that recruitment of RISC to target mRNA can stimulate deadenylation and exonucleolytic mRNA decay(Wu et al., 2006)(Figure 4.13). In addition, RISCs are shown to direct mRNA to P-Body where the RNAases are enriched for further degradation(Fabian and Sonenberg, 2012)

4.1.2 Regulation of miRNA mediated silencing

miRNA mediated silencing is controlled at several levels. The amount of miRNAs is controlled by the transcription of primary miRNAs and its post-transcriptional processing (Winter et al., 2009). Altered miRNA quantity directly affects the activity of RISC, hence influencing gene silencing(Leung and Sharp, 2010). The enzymes participating in miRNA pathways are also subject to regulation. The expression of Drosha and Dicer can be controlled by miRNA mediated feedback circuit. High levels of a particular miRNAs, such as miR-103/107 and let-7 silence the expression of Drosha or Dicer and therefore impair miRNA biogenesis (Kim et al., 2009; Martello et al., 2010). Moreover, it is increasingly appreciated that post-translational modification of the members of the RNAi pathway such as Drosha, TRBP and Ago2, plays an important role in regulating miRNA function(Herbert et al., 2013; Meister, 2013; Paroo et al., 2009; Tang et al., 2010). I am going to focus on the structure and regulation of Ago2 in the following sections.

4.1.3 Ago2 structure, function and regulation

In mammalian cells, there are 4 members of the Argonaute family: Ago1, 2, 3 and 4. Ago2 is the only one with nuclease activity and is shown to be the catalytic engine of RNA induced gene silencing (Liu et al., 2004b). Ago2 knock-out causes embryonic lethality whereas individual knockout of the other 3 human Ago proteins causes no obvious defects in mice(Cheloufi et al., 2010).

Ago2 protein comprises 4 domains: N-domain, PAZ, MID and PIWI domain. PAZ domain is responsible for recognizing the 2-nucleotide 3' terminal overhang of the miRNA duplex and provides a pocket to accommodate the 3' terminus of miRNA(Lingel et al., 2004). The MID

domain anchors the 5’ end of the miRNA. It provides a binding pocket in which the miRNA 5’ terminal base engages in stacking interaction with the tyrosine 529(Frank et al., 2010). In addition, several hydrogen bonds contribute to correct 5’ end binding. The N domain is thought to assist in unwinding the small RNA duplex(Kwak and Tomari, 2012). The PIWI domain has a structure that is similar to RNase H and has been shown to have endonuclease activity. It can cleave the small RNA duplex that is fully complementary (Parker et al., 2004).

The activity of Ago2 can be regulated by post-translational modification. It is shown that the proline 800 can be hydroxylated by type I collagen prolyl-4-hydroxylase and the proline hydroxylation stabilizes Ago2(Qi et al., 2008). Under cellular stress conditions, Ago2 can be modified by poly(ADP-ribose). This modification is added by specific poly(ADP-ribose) polymerases, such as PARP13. The poly ADP-ribosylation impairs miRNA-guided repression (Leung et al., 2011). Ago2 can also be ubiquitylated and targeted to proteasome mediated degradation. TRIM71 (also known as LIN41) has been reported as a potential E3 ubiquitin ligase responsible for Ago2 ubiquitination and turnover (Rybak et al., 2009).

The phosphorylation on different residues of Ago2 is related to its subcellular localization or regulation of small RNA binding. The phosphorylation on serine 387 is implicated in facilitating the recruitment of Ago2 to the P-body (processing body), where the RNAs are degraded. The serine 387 phosphorylation reportedly enhances RNAi function (Zeng et al., 2008b). Phosphorylation on tyrosine 529 interferes with microRNA loading. The tyrosine 529 is located inside the miRNA 5’ phosphate binding pocket in the MID domain. Y529 phosphorylation creates an electrostatic repulsion against the 5’ end phosphate on the RNAs

thus attenuating miRNA binding (Rudel et al., 2011). EGFR signaling under hypoxic condition causes Ago2 phosphorylation at Y393. Y393 resides on the back of the enzyme, at the Ago2 interacting surface with Dicer. Y933 phosphorylation destabilizes the Ago2/Dicer interaction and is shown to impairs miRNA maturation(Shen et al., 2013a).

In last chapter, we demonstrated that Ago2 tyrosine phosphorylation was upregulated in senescent cells and PTP1B dephosphorylated Ago2. We aimed to identify the tyrosine site on Ago2 that was targeted by PTP1B and understand how phosphorylation on this particular site affected Ago2 function.

4.1.4 RNAi pathway and senescence

Various miRNAs modulate the expression of the genes essential for senescence (Gorospe and Abdelmohsen, 2011). Up-regulation of miRNAs such as the miR-106b family was shown to overcome RAS-induced senescence by silencing p21 and other cell cycle regulators in human mammary epithelial cells (Borgdorff et al., 2010). It is found that in oncogenic E7-induced senescent Hela cells, miR-29, miR-30 are upregulated in an Rb-dependent manner. Overexpression of miR-29 and miR-30 in proliferating cells suppress the expression of B-Myb, an oncogene that promotes in cell-cycle progression (Martinez et al., 2011).

Reports have shown that Ago2 activity can affect OIS. It was shown that Argonaute 2 expression is critical for stem cells to escape senescence (Kim et al., 2011). Impaired RNA silencing activity was also observed in replicative senescent IDH4 fibroblast(Chang et al., 2010b). However, it was also observed that depletion of Ago2 delays senescence arrest in WI38 fibroblasts cultured under 3% O2 condition(Benhamed et al., 2012). These obviously

contradictory observations made us interested in characterizing the role of Ago2 in RAS-induced senescence.

4.2 Method

4.2.1 Preparation of MEFs

MEFs were prepared from 10.5 day embryos. The head and the red organs were removed, and the torso was minced and dispersed in 0.1% trypsin the Ago2 KO MEFs was generated as previous described (Yang and Maurin et al. 2010.)In brief, Flox/flox mice were bred to C57BL/6J mice that carry Cre-recombinase fused to T2-ER1α (allowing binding to tamoxifen but not estrogen) at the Rosa26 locus. Deletion was induced by administration of 4-hydroxytamoxifen (Sigma-Aldrich) at 10-nM concentration over two 3-d intervals for a total of 6 d. The cells were frozen after two passage in DMEM plus 10% FBS and pen/strep growth media.

4.2.2 DNA constructs and infection

The mammalian expression vectors pCDNA3.1 and pCDNA3.1–*H-RAS*^{V12} and the retroviral vector pBabe–*H-RAS*^{V12}-Puro were generous gifts from Dr. Linda Van Aelst (Julien et al., 2011; Lin et al., 1998). pCDNA3-myc-*AGO2*, pMT2-*PTP1B*, pMT2-*PTP1B* D181A were generated as described previously (Flint et al., 1997b; Liu et al., 2004c). AGO2 mutants (Y55/57F, Y393F, Y529F, Y741F, and D598A) expression constructs were generated by site-directed mutagenesis using the QuickChange Kit and pCDNA3-myc-*AGO2* (WT) as a template. pWZL–*PTP1B*-Hygro WT, DA and CS mutants were generated as described previously (LaMontagne et al., 1998). pWZL–*AGO2*-hygro was generated by subcloning wild type *AGO2* from pCDNA3-myc-*AGO2* constructs into the pWZL-Hygro vector.

Viruses were generated using Phoenix cells and fibroblasts were incubated with virus-containing media or a mixture of two different virus-containing media 36 hours post primary-

infection, the infected cell populations were selected using 2 μg/ml puromycin (H-RASV12) for 48hrs, and 100 μg/ml hygromycin for an additional 6 days in experiments necessitating a double infection (H-RASV12 and PTP1B or AGO2).

4.2.3 qRT-PCR of mRNA binding to Ago2

qRT-PCR of Ago2 binding mRNA was performed following the method of Beitzinger and Meister with a few modifications. (Beitzinger and Meister 2011). Briefly, RNA extracted from lysate and immune-precipitated Ago2 using Trizol reagent (invitrogen) were treated with RNase free DNase (Roche) and cDNA were synthesized using cDNA synthesis kit (Bio-rad). Obtained cDNA were used for qRT-PCR, with sybergreen master mix (Apply Biosystem). Primers used in the qRT-PCR are (p21, Gapdh as the internal control), p21: TGTCCGTCAGAACCCATG and GCCTCCTCCCAACTCATC. p16 : CAACGCACCGAATAGTTACG and GGTTCTTTCAATCGGGGAT. p53 TACAGTCAGAGCCAACCTCAG and AGATGAAGCTCCCAGAATGCC. GAPDH: TGCACCACCAACTGCTTAGC and GAGGGGCCATCCACAGTCTTC

4.2.4 Detection of Ago2 phosphorylation

To analyze Ago2 phosphorylation, the cells were lysed in RIPA buffer and incubated with Ago2 antibody-bond A/G agarose beads for 4hrs in 4°C. The immune-precipitated proteins were then analyzed by western blot. Ago2 pY393 antibody was generated by Cell Signaling Technology and validated using Ago2 WT or Ago2 Y393F mutant co-expressing with RAS.

4.2.5 Ago2 mutant analysis

Ago2-Myc pCDNA3 Y55/57F, Y393F, Y529F and Y728F were generated using site-directed mutagenesis. To analyze the phosphorylation of Ago2 mutants, the constructs were transfected into 293 cells with or without RAS. The lysates were harvested and incubate with anti-Myc (9E10)-coupled protein A/G agarose beads for 6 hr in 4°C. The precipitates were resolved on SDS/PAGE and transferred to nitrocellulose membrane and blotted with anti-pTyr antibody (4G10). To identify the tyrosine residue on Ago2 targeted by PTP1B, the Ago2 mutants were co-expressed with RAS and PTP1B D181A. The trapping mutant assay was preformed as described before and the precipitates were immuno-blotted with anti-Myc antibody.

4.2.6 Detection of Ago2 Y393 phosphorylation

The Ago2 pY393 antibody was generated from Cell Signaling technology. The anti-serum was validated by Ago2 Y393F mutant co-expressed with RAS. To test Ago2 phosphorylation in RAS-induced senescent cells, Ago2 was immune-precipitated from cell lysate and resolved with SDS-PAGE, followed by immunoblotting with Anti-Ago2 pY393 antibody. To estimate the stoichiometry of Ago2 phosphorylation in senescent cells, lysate was first subject to immune-depletion with Ago2 pY393 antibody for 6 hours. The supernatant were then incubated with Ago2 antibody-precoupled beads for 6 hours at 4°C. The precipitates were then resolved and blotted with Ago2 antibody and the signal intensity were compared to determine the stoichiometry of Ago2 pY393 phosphorylation.

4.2.7 Detection of Ago2 microRNA loading

As described previously(Mourelatos, Dostie et al. 2002) , prior to cell collection Ago2 antibody were conjugated on protein A Dynabeads magnetic beads (Sigma) using Rabbit anti-mouse

bridging antibody. The cells were lysed in Ago2 IP buffer (10mM Hepes, 100mM KCl, 5mM MgCl2, 0.5% NP-40,1% Triton,10% glycerol,1mM DTT,100u/ml RNASIN), and then 1mg of lysates were incubated with antibody bond beads for 4hrs in 4C. The beads were then collected using a magnetic stand and wash twice with NT2 buffer (50mM Tris pH 7.4,150mM NaCl, 1mM MgCl2, 0.05% NP40,100U/ml RNASIN, 1mM DTT) for 10-15min and two additional times with a higher salt NT2 buffer (300mM). Tubes were changed for the last wash. 10% of lysate were saved for total RNA extraction. 30μg of lysate were saved for western blot.

RNA were extracted from both lysate and immuno-precipitate using Trizol reagent (Invitrogen). 5' phosphate of the RNAs were removed by CIP and after acidic phenol extraction, the 5' phosphate was then replaced with radio-active phosphate p32 using gamma-p32 ATP and PNK. The 5' labeled RNA were then resolved by 15% Urea-PAGE and radiograph was detected using Fuji phospho-imager.

4.2.8 RNA isolation and microarray analysis

Total RNA was harvested using Trizol reagent from IMR90 cells expressing H-RAS^{V12} alone, control IMR90 cells 6 days post puromycin selection. Microarray analysis was performed in the CSHL microarray facility, using the GeneChip miRNA 2.0 Array (Affimetrix) following the manufacturer instruction. In brief, Poly(A)-tailing and FlashTag Biotin HSR Ligation was performed on the samples using FlashTag Biotin HSR RNA labeling kit (Affymetrix). The labeled RNA samples were than hybridized on to arrays at 48C for 16hrs. The array were then washed and stained before scanning.

Only the 5617 human miRNA probe sets were considered for further analysis, log2 value was used to compare the differences between samples, and the Δlog2 value of the miRNAs in control sample were normalized to 0. A heatmap was generated using the Heatmap tool from the CSHL Galaxy platform. Euclidean distance was used for hierarchical clustering of miRNA hits

4.2.9 Quantitation of AGO2-bound miRNAs and mRNAs

qRT-PCR of AGO2-bound mRNAs was performed following the method of Beitzinger and Meister with minor modifications (Beitzinger and Meister, 2011). Briefly, RNAs from immunoprecipitated AGO2 and lysates were extracted using Trizol and treated with RNase free DNase. Following DNase treatment, cDNAs were synthesized using a cDNA synthesis kit. The cDNA library was then used as template for qRT-PCR using a SYBR Green master mix. Primers used in the qRT-PCR were: p21: TGTCCGTCAGAACCCATG and GCCTCCTCCCAACTCATC. GAPDH: TGCACCACCAACTGCTTAGC and GAGGGGCCATCCACAGTCTTC. GAPDH was used as an internal control. For miRNA quantitation, each miRNAs and U6 snRNA were reverse transcribed and cDNAs were used for qPCR, using Taqman microRNA assay following the manufacturer's instruction (Applied Biosystems). Briefly, the probes used in the experiments were #000580 for miR-20a, 1014 for miR-20b, 442 for miR-106b, and 001973 for U6 snRNA. U6 snRNA was used as internal control and quantitation of miRNAs was determined by calculating the -ΔCt value of each miRNA over U6. The relative binding of each miRNA to AGO2 was normalized to the vector control of the most abundant miRNA (miR-106b).

4.2.10 Analysis of EGFR activity in senescent cells

IMR90 cells were lysed in RIPA buffer and EGFR was immunoprecipiated by anti-EGFR coupled protein A/G agarose bead. The precipitates were blotted first with anti-pY antibody to detect EGFR phosphorylation and then with EGFR antibody for equal loading.

4.3 Result

4.3.1 PTP1B dephosphorylated Ago2 at Y393

We introduced Y to F mutation on Ago2 by site-direct mutagenesis on the Y55/57, Y393, Y529 and Y741 sites to generate the phospho-resistant form of Ago2 and measured the tyrosine phosphorylation of Ago2 in RAS-expressing HEK293 cells. Phosphorylation on Y393 and Y529 residues have been reported by other groups(Rudel et al., 2010; Shen et al., 2013b). Y55, Y57 and Y741 are predicted phosphorylation site on Ago2(Figure 4.1A) We transfected 293 cells with myc-tagged Ago2 WT or mutants together with RAS. Immunoprecipitating myc-tagged Ago2 and blotting the precipitants with anti-pTyr antibody showed that either mutation of Y393 or Y529 residue caused decrease of tyrosine phosphorylation of Ago2, suggesting that Y393 and Y529 were two main tyrosine phosphorylation sites on Ago2 (Figure 4.1 B). Furthermore, we generated a phospho-specific antibody that targets the Ago2 pY393 site. We demonstrated RAS-induced phosphorylation of Ago2 Tyr 393 in senescent cells (Figure 4.1 D).

To identify the Ago2 tyrosine phosphorylation site targeted by PTP1B, we co-expressed the myc-tagged Ago2 mutants together with PTP1B D181A and RAS in HEK293 cells and performed the PTP1B substrate trapping mutant assay. We found that the interaction between Ago2 Y393F and PTP1B D181A was impaired whereas all the other mutants remained associated to PTP1B trapping mutant as well as the WT Ago2 (Figure 4.1 C). This result suggested that Y393, but not Y529 was the target site of PTP1B.

4.3.2 Ago2 phosphorylation impaired Ago2/Dicer interaction

Tyr 393 of Ago2 locates close to the binding surface between Ago2 and Dicer. Phosphorylation of this residue has been shown to impair Ago2 binding to Dicer (Shen et al., 2013a; Tahbaz et al., 2004; Wang et al., 2009). We induced Ago2 phosphorylation by overexpressing oncogenic RAS in HEK293 cells. Coexpressing various amounts of PTP1B in these cells could affect the level of Ago2 phosphorylation. Indeed, we observed that the Ago2-Dicer interaction was impaired in RAS expressing cells (Figure 4.2) and that overexpression of PTP1B, which led a decrease of RAS-induced Ago2 phosphorylation, favored the association between Dicer and Ago2.

4.3.3 Ago2 phosphorylation caused microRNA unloading

As mentioned in the introduction, Dicer, TRBP and Ago2 form a RISC loading complex (RLC) which loads miRNA duplex processed by Dicer onto Ago2. Since disruption of RLC affects miRNA loading onto Ago2(Chendrimada et al., 2005), we decided to test whether Ago2 miRNA loading was affected by Ago2 phosphorylation and dissociation with Dicer. We immunoprecipitated Ago2 from the cells expressing RAS, RAS+PTP1B, PTP1B, or the control vectors and extracted RNAs from the precipitants. We then utilized the CIP/Kinase method to incorporate a radioactive 5’ phosphate group on to the RNAs isolated from the precipitants. The RNAs were then resolved by urea-PAGE. Using auto-radiography, we detected the RNA species at ~22 nt, which represent the miRNAs loaded onto Ago2. The loading of small RNAs with Ago2 observed in untransformed cells was markedly reduced in RAS-expressing cells. Overexpression of PTP1B in RAS-expressing cells rescued miRNA loading onto Ago2 (Figure 4.3A).

Previously we showed that PTP1B dephosphorylated pY393 on Ago2 (Figure 4.1C). We hypothesized that Ago2 phosphorylation on Y393 affected miRNA loading. We generated Y393D mutant of Ago2 to introduce negative charge to the residue thus mimicking the phosphorylated state. Y393F mutant was generated as the phospho-resistant mutant of Ago2. We co-expressed Ago2 or Ago2 Tyr 393 mutants with RAS in *Ago2-null* MEFs. We immuno-precipitated Ago2 from MEFs and analyzed the miRNA loading on the different mutants or WT Ago2 by radiolabeling. Our data showed that whereas WT and Y393F mutant Ago2 were associated with endogenous small RNAs, such association with the Y393D mutant was dramatically decreased. In the cells expressing RAS, which caused Ago2 WT phosphorylation, the miRNA loading to WT Ago2 was impaired as compared to the one under no-RAS condition. miRNA loading to Ago2 Y393F was not affected by RAS expression. The results illustrated that the increased phosphorylation of Ago2 on Y393 led to decreased Ago2 miRNA loading, suggesting that dephosphorylation at Y393 was required for efficient loading (Figure 4.3 B).

4.3.4 Ago2 function was important for RAS-induced senescence

Our previous results indicated that in senescent cells Tyr 393 of Ago2 was hyperphosphorylated in response to PTP1B inactivation and phosphorylation on Tyr393 impaired Ago2 function. We went on to test whether the loss of Ago2 activity affected RAS-induced senescence. We co-expressed Ago2 in the RAS expressing cells, to compensate for the inactivating tyrosine phosphorylation of Ago2. By assaying for SA-beta-gal at Day 6 selection, we measured that introducing exogenous Ago2 into RAS-expressing cells significantly attenuated senescence (Figure 4.5 B). Ago2 expression also decreased the protein level of p21,

a key regulator of senenscence. This result further supported that Ago2 activity was important to attenuate RAS-induced senescent phenotype (Figure 4.5 A).

4.3.5 Ago2 Y393 phosphorylation facilitated RAS-induced senescence

To determine the importance of tyrosine phosphorylation of Ago2 in its ability to suppress senescence, we overexpressed WT or Y393 mutants (Ago2 Y393D, Ago2 Y393F) in RAS-expressing *Ago2* null (*Ago2* -/-) MEFs prepared from Day 11 mouse embryo. We quantitated the effects of Ago2 mutants on RAS-induced senescence. The Ago2 Y393D mutant possesses an additional negative charge, which would partially mimic the phosphorylated form of Ago2 that would occur when PTP1B was inactivated. As expected, overexpression of the Ago2 Y393D mutant did not prevent RAS-induced senescence. In contrast, overexpression of the Ago2 mutant (Ago2 Y393F), which cannot be phosphorylated, prevented the appearance of senescence to a similar extent to the WT enzyme (Figure 4.6). This suggests that Ago2 phosphorylation on Y393 is necessary and sufficient for RAS-induced senescenece.

4.3.6 Ago2 was downstream of PTP1B in RAS-induced senescence

To test whether PTP1B regulates senescence through influencing Ago2 phosphorylation and function, we verified whether PTP1B could attenuate RAS-induced senescence in *Ago2* null (*Ago2* –/–) mouse embryonic fibroblasts (MEFs) and in *Ago2* heterozygous (*Ago2* +/–) MEFs. X-gal staining of the cells at Day6 showed that overexpression of PTP1B only prevented RAS-induced senescence when Ago2 was expressed in the cell (Figure 4.9). The result indicated that PTP1B exerted its function through Ago2. This is consistent with a ROS-PTP1B-Ago2 pathway that is responsible for RAS-induced senescence.

4.3.7 Regulation of Ago2 affected prevented silencing of p21 in senescent cells

We used microarray analysis to further examine the effect of oncogenic RAS-expression on gene silencing. Total RNAs from IMR90 fibroblasts and IMR90 fibroblasts expressing RAS were hybridized to microarrays that report the expression status of 1105 human miRNAs. Transformation of human diploid fibroblasts with RAS resulted in induction of oncogenic miRNAs. Members of the oncogenic miR-17~92 cluster and its two paralogs, the miR106a~363 and miR106b~25 clusters (18a, 19b, 20a, 20b, 106b), were among the top 20 up-regulated miRNAs (i.e. log2-ratio values normalized to control cells) (Figure 4.7B). These miRNAs have been shown to promote cell cycle progression and to possess oncogenic properties by cooperative down-regulation of p21CIP/CDKN1A mRNA to regulate the G1-to-S cell cycle progression (Conkrite et al., 2011; Ivanovska et al., 2008; Wu et al., 2010).

Our previous results indicated that p21 protein was upregulated in RAS-induced senescent cells (Figure 2.6). Therefore, we investigated the effect of oncogenic miRNAs on p21 mRNA levels in RAS-transformed cells. Previously we observed that overexpression PTP1B or Ago2 in RAS-expressing cells lowered p21 expression (Figure 2.10A and 4.5). We hypothesize that PTP1B-mediated regulation of Ago2 function affected miRNA pathways and as a result controlled p21 expression. To this end, we immunoprecipitated Ago2 from control IMR90 cells, or from IMR90 cells expressing RAS in the presence and absence of co-expressed PTP1B, and quantitated the level of Ago2-associated miR-20a, miR-20b and miR106b by qPCR. In accordance with our observations on global Ago2 loading with small RNAs (Figure 4.4), the

association of Ago2 with these miRNAs was decreased by RAS signalling. Co-expression of wild type PTP1B recovered loading of Ago2 with all three miRNAs (Figure 4.7A).

To evaluate the effects on Ago2-p21 mRNA interactions, we immunoprecipitated Ago2 and performed qPCR on p21 mRNA from control IMR90 cells, or from IMR90 cells expressing RAS in the presence and absence of co-expressed PTP1B. Ago2-p21 mRNA interaction was maximal in control IMR90 cells, whereas expression of RAS decreased this interaction by more than 90% (Figure 4.8). Furthermore, p21 mRNA levels were 8-fold increased in RAS-expressing cells compared to untransformed fibroblasts (Figure 4.8, right panel). Overexpression of PTP1B together with RAS led to recovery of the interaction between Ago2 and p21 mRNA to ~40% of the level observed in non-senescent cells, suggesting re-establishment of an active RNA-induced silencing complex. Accordingly, levels of p21 mRNA were silenced to a similar extent as in control IMR90 cells.

p21 is a major regulator of Ras-induced senescence and we have shown in the previous chapter that PTP1B repressed p21 expression. We demonstrated that p21 protein level was reduced when Ago2 was co-expressed with RAS. The result suggested that inhibition of Ago2 activity in senescent cells facilitated the expression of senescence regulator p21. Taken together, our data suggests a mechanism regulating RAS- induced senescence that involves de-repression of p21 mRNA translation due to the inhibition of miRNA silencing as a consequence of PTP1B oxidation by ROS.

4.3.8 Study of the kinase which phosphorylates Ago2

In the process of looking for the kinases responsible for Ago2 phosphorylation, we referred to the work of Shen, et al(Shen et al., 2013a). They demonstrated that under hypoxic conditions, EGF treatment caused Ago2 hyperphosphorylation. EGFR was shown to directly phosphorylate Ago2, prompting us to test whether EGFR was the kinase that caused Ago2 phosphorylation in RAS-induced senescent cells. We immunoprecipitated EGFR from RAS-induced senescent cells and used a pTyr antibody to blot for EGFR phosphorylation. The result showed that there was no increase of EGFR phosphorylation in senescent cells as compared to control cells, indicating EGFR activity was not increased in senescent cells (Figure 4.10). Hence it was unlikely for EGFR to cause Ago2 hyperphosphorylation in OIS. Furthermore, we overexpressed EGFR or RAS in 293 cells to compare the extent of Ago2 phosphorylation induced by these two different stimuli. Ago2 phosphorylation level is higher in presence of oncogenic RAS, as compared to that in EGFR overexpressing cells (Figure 4.10). The result suggested that RAS might trigger Ago2 phosphorylation through different pathways.

4.4 Discussion

In this chapter, we identified Ago2 pY393 as a PTP1B target site. We demonstrated that Ago2 phosphorylation at Y393 impaired miRNA loading and Ago2 function. Our result showed that Ago2 phosphorylation and loss of function was important for oncogenic RAS to induce senescent phenotype and Ago2 was a downstream effector of PTP1B in OIS**.**

4.4.1 Ago2 phosphorylation at Y393 attenuated Ago2 activity

As mentioned before, reports have shown that Ago2 Y393 undergoes reversible phosphorylation (Rudel et al., 2010; Shen et al., 2013b). Y393 residue resides at the linker region between MID domain and PAZ domain. The linker region folds with the N-domain of Ago2 and together lies in the back of the enzyme, away from the RNA binding region. Structural studies show that Y393 resides at the binding interface between Ago2 and Dicer (Iwasaki, Kobayashi et al. 2010). Ago2 association with Dicer has been shown to play an important part in loading mature miRNAs on to Ago2 (Chendrimada et al., 2005). We found that phosphorylation of Y393 attenuates Ago2 miRNA loading. This was consistent with the previous observation from Shen, et al that Ago2 Y393 phosphorylation impairs Ago2 function (Shen et al., 2013b).

We showed that Ago2 phosphorylation on Y393 disrupted Ago2/Dicer association, which impaired miRNA loading and subsequently miRNA mediated gene silencing. Here we propose a model that PTP1B D181A trapping of Ago2 in senescent cells can also disrupt Ago2/Dicer interaction, which in turn impairs Ago2 function. Whereas PTP1B WT, which dephosphorylates Ago2, can restore Ago2 function. In Chapter 2, we observed that overexpressing PTP1B WT, but

not PTP1B D181A or PTP1B C215S, attenuated the senescence phenotype (Figure 2.10A). As discussed in Chapter 2, we proposed that the potential substrate of PTP1B would be inactivated by phosphorylation or by trapping with PTP1B trapping mutant. Our finding that Y393 phosphorylation impairs Ago2 function was consistent with the previous observation.

In this chapter, we showed that PTP1B mediates Ago2 dephosphorylation and activation. EGFR was previously reported to mediate Ago2 phosphorylation and inactivation (Shen et al., 2013b). However in our study, EGFR phosphorylation was not enhanced in senescent cells, which suggested that EGFR activity was not increased and was unlikely to be responsible for the hyperphoshorylation of Ago2 in the context of RAS-induced senescence. Further studies to identify the kinase that phosphorylates Ago2 will complete our understanding of the regulation of Ago2 phosphorylation in OIS.

4.4.2. Regulation of RNAi pathway was important in RAS-induced senescence

Increasing evidence has shown that the proteins involved in the RNAi pathway are important for senescence induction. Dicer ablation was found to trigger senescence in primary cells, accompanied by high levels of both p53 and p19ARF (Mudhasani et al., 2008; Srikantan et al., 2011). Furthermore, prevention of Ago2 association with p21, p16 mRNA was also shown to promote senescence (Chang et al., 2010a; Kim et al., 2012). Our study support that modulation of RNAi pathway had significant impact on oncogene-induced senescence.

In our study we demonstrated that Ago2 loading with some p21 targeting miRNAs (mir20a, mir20b, mir106b) was impaired and unloading of these miRNAs facilitated p21 expression. However, the mir-20a, 20b and 106b might not be the only miRNAs affected

because of Ago2 phosphorylation. Our microarray analysis showed that the expression of other microRNAs were affected in senescent cell (Figure 4.7). Shen, et al suggested that Ago2 phosphorylation on Y393 preferentially inhibits the maturation of the pre-microRNAs with longer stem loops. It will be interesting to analyse the structure of the microRNAs upregulated in senescent cells, to test whether the precursor of these microRNAs have specific stem loop structure.

Furthermore, these microRNAs might target other mRNAs in the senescent cells, in addition to the p21 mRNA. For example, miR-106b and miR-20a also target WEE1, RB1, and RBL1/2. The scope and the specificity of PTP1B/Ago2 pathway thus merit future investigation. I propose to perform a CLIP-seq (cross-linking immunoprecipitation-sequencing) experiment to analyse the RNAs associated with Ago2 in senescent cells. In the CLIP-seq experiment, we will crosslink RNAs associated with Ago2 by UV irradiation. The RNAs will be co-immunoprecipitated with Ago2 from the samples and subjected to RNA sequencing. This method will provide us a global view of which RNAs are specifically affected by Ago2 phosphorylation in senescent cells. Investigation on whether or not microRNAs were selectively unloaded, what specific targets are affected and what factors are involved in determine the specificity of PTP1B/Ago2 pathway will advance our understanding on the regulation of RNAi pathways.

4.4 Figures

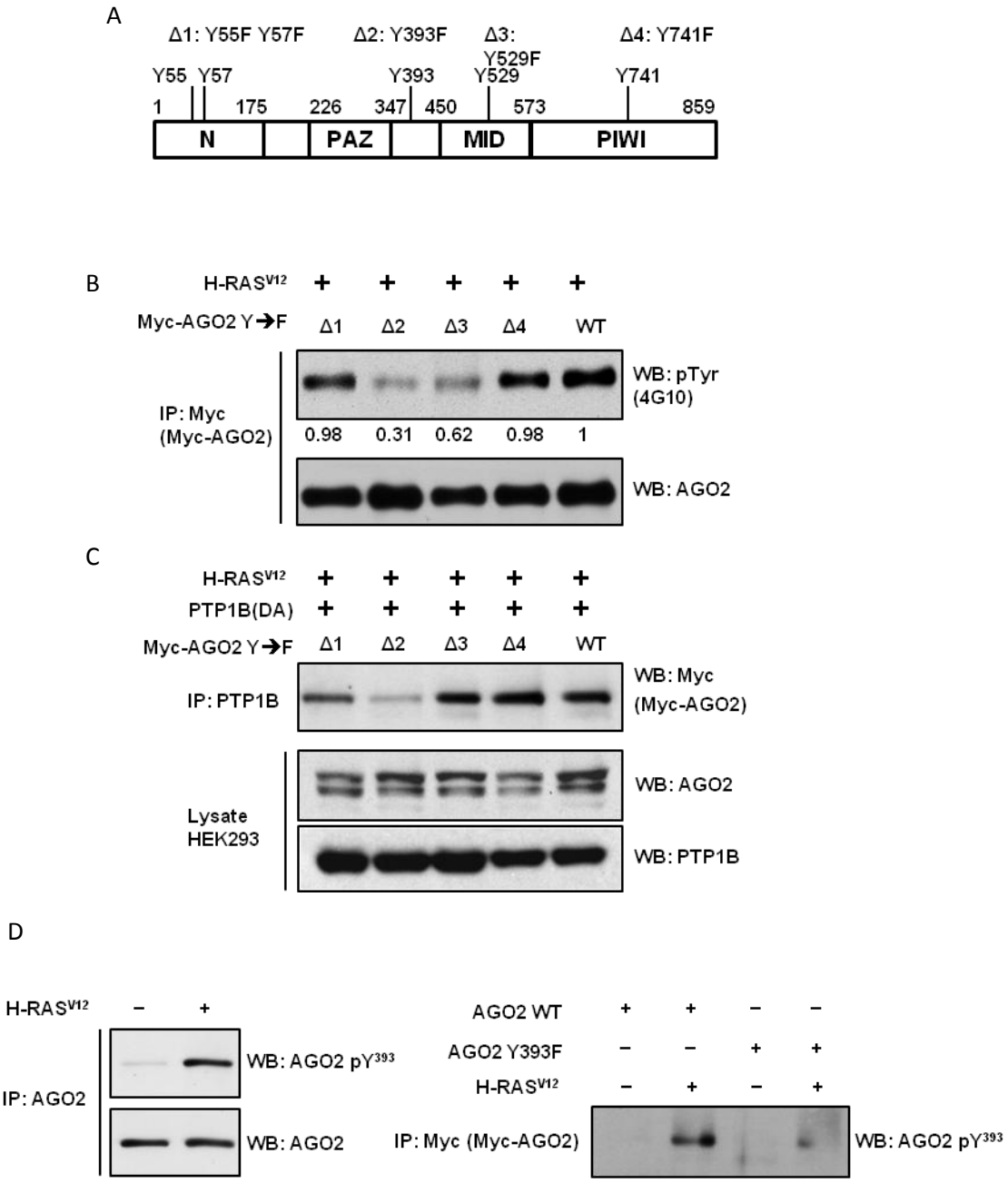

Figure 4.1 PTP1B regulates Ago2 phosphorylation at Y393

A)Schematic representation of Ago2 domains identifying the five tyrosine residues that were mutated to phenylalanine. **B)** Myc-tagged Ago2, either WT or phosphorylation site mutants [(1)Y55F,Y57F; (2)Y393F; (3)Y529F; (4)Y741F], was expressed in HEK293 cells together with RAS, then immunoprecipitated using an anti-Myc antibody and blotted for the presence of

phosphorylated tyrosine using 4G10. The membrane was stripped and reblotted for total Ago2. **(C)** Immunoblot of Myc-tagged Ago2, either wild type (WT) or phosphorylation site mutants [(1)Y55F,Y57F; (2)Y393F; (3)Y529F; (4)Y741F] to demonstrate interaction with the PTP1B (DA) substrate-trapping mutant in RAS-expressing HEK cells. Lysates were resolved by SDS-PAGE, transferred and blotted for Ago2 and PTP1B to illustrate equal expression of the mutant proteins. **(D)** Immunoprecipitation of Ago2 was performed using lysates from IMR90 cells expressing RAS or control vector (left panels). The immunoprecipitated proteins were resolved by SDS-PAGE, transferred onto nitrocellulose and blotted with an Ago2-pY393 antibody (Cell Signaling). The membrane was stripped and reprobed for total Ago2 (Abnova, lower panel).

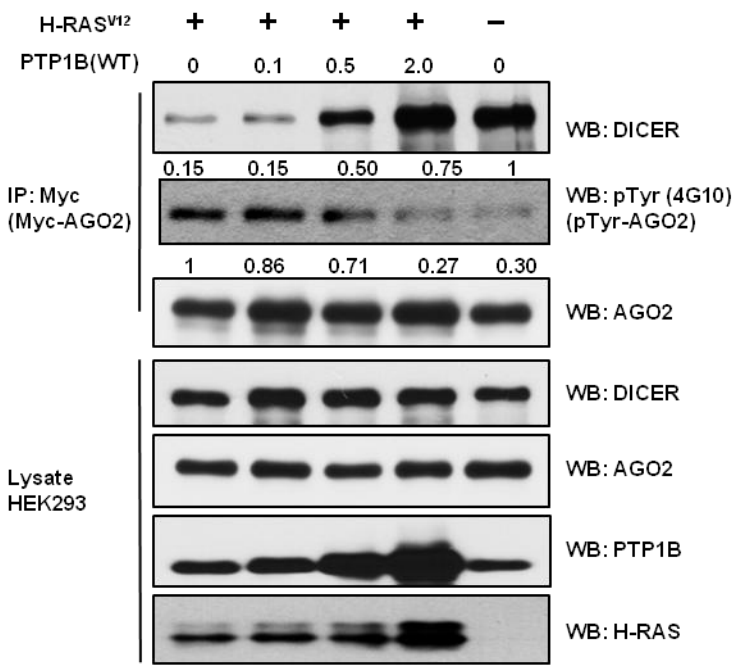

Figure 4.2 Ago2 phosphorylation disruptes the interaction between Ago2 and Dicer

Myc-tagged Ago2 was immunoprecipitated from cell lysates of untransfected HEK293 or from HEK293 cells co-transfected with *RAS* and 0, 0.1, 0.5 or 2.0 μg of *PTP1B* (WT) expression plasmid, resolved by electrophoresis and blotted for DICER, Ago2 tyrosine phosphorylation (4G10) and total Ago2. Lysates were also blotted for PTP1B and H-RAS.

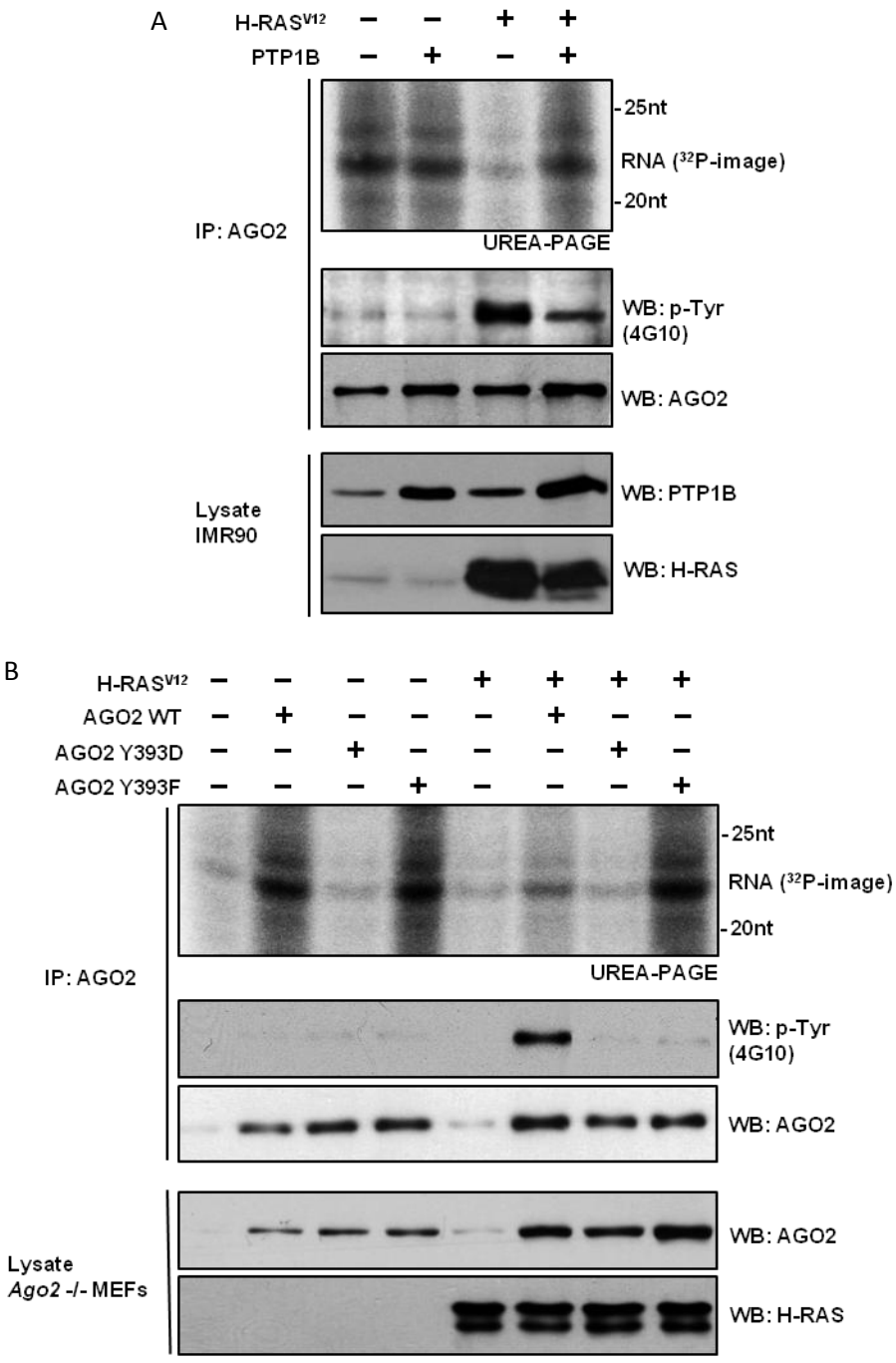

Figure 4.4 Ago2 phosphorylation at Y393 impairs Ago2 microRNA loading

A) Ago2 was immunoprecipitated from lysates of control IMR90 cells, cells expressing RAS, cells expressing PTP1B, or both RAS and PTP1B, and associated RNAs were extracted, 5'-end-labeled with [γ-^{32}P]-ATP and resolved by electrophoresis. Labeled miRNAs were visualized by autoradiography (top panel). B) Ago2 was immunoprecipitated from lysates of immortalized

Ago2 -/- MEFs infected with *Ago2* WT or mutants (Y393D, Y393F) with or without *RAS* and associated RNAs were extracted, 5'-end-labeled with [γ-^{32}P]-ATP, resolved by electrophoresis and labeled miRNAs were visualized by autoradiography (top panel). Ago2 was immunoprecipitated from 10% of the lysates to illustrate Ago2 tyrosine phosphorylation and total levels. 5% of the input lysates were blotted for Ago2 and H-RAS.

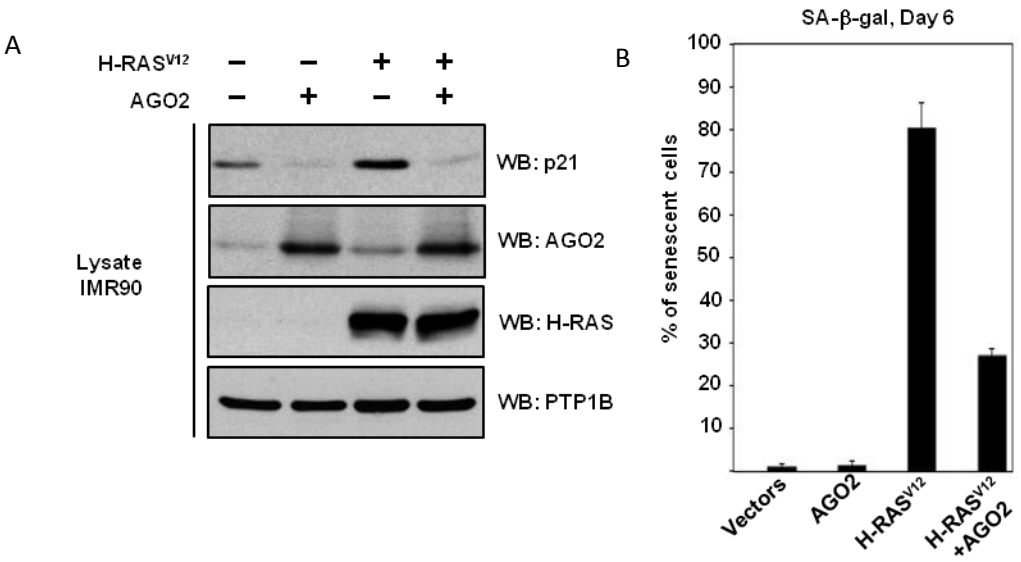

Figure 4.5 Ago2 is important for RAS-induced senescence

A)IMR90 cells infected with the control vector, *Ago2*, *RAS* or both were lysed and blotted for p21, Ago2, H-RAS and PTP1B. β-gal activity was measured in IMR90 cells infected with the control vectors, *Ago2*, *RAS* or both. Senescent cells were counted as β-gal positive cells relative to total cells. B) Non-immortalized *Ago2* knockout (*Ago2* -/-, black bars) and heterozygous (*Ago2* +/-, white bars) MEFs co-infected with control vectors, *PTP1B*, *RAS* or with *RAS* and *PTP1B* were cultured for 6 days post-selection and stained for β-gal activity. Senescent cells were counted as beta-gal positive cells relative to the total cells. Images were quantitated by image J. Error bars represents SEM. N=3

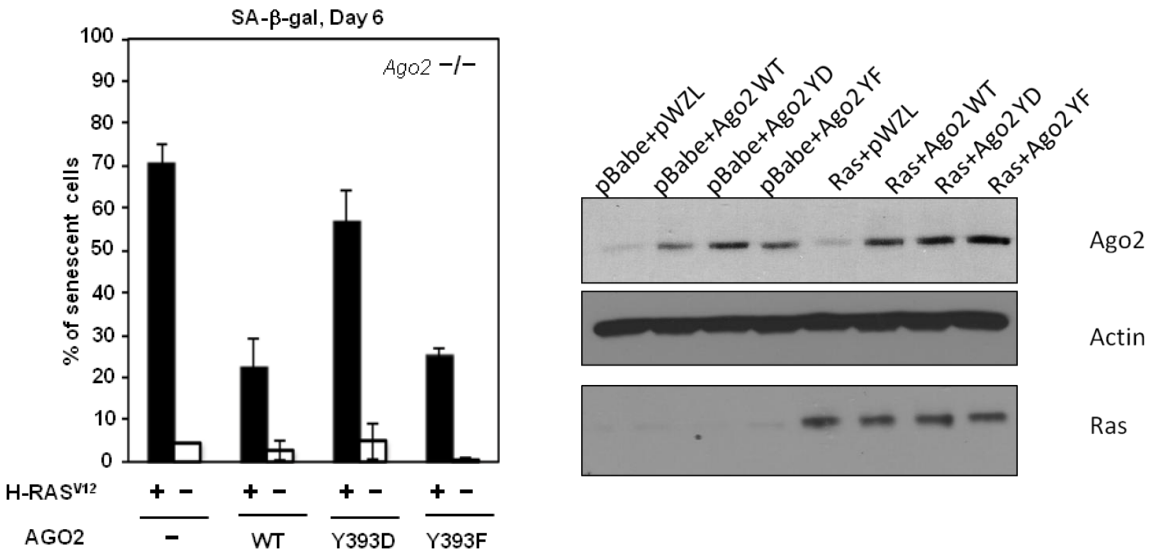

Figure 4.6 Phosphorylation on Ago2 Y393 facilitates RAS-induced senescence

Non-immortalized *Ago2* -/- MEFs infected with *RAS* (black bars) or the control vector (white bars) were co-infected with a control vector, *Ago2* WT or mutants (Y393D, Y393F), cultured for 6 days post-selection and stained for beta-gal activity. Senescent cells were counted as beta-gal positive cells relative to the total cells. Proteins from lysates of non-immortalized *Ago2* knockout (*Ago2* -/-) MEFs infected with *RAS* or the control vector were co-infected with a control vector, *Ago2* WT, *Ago2* Y393D or *Ago2* Y393F mutants, cultured for 6 days post-selection and resolved by SDS-PAGE, transferred onto nitrocellulose membranes and blotted for Ago2 and H-RAS expression, Error bars represents SEM. N=3

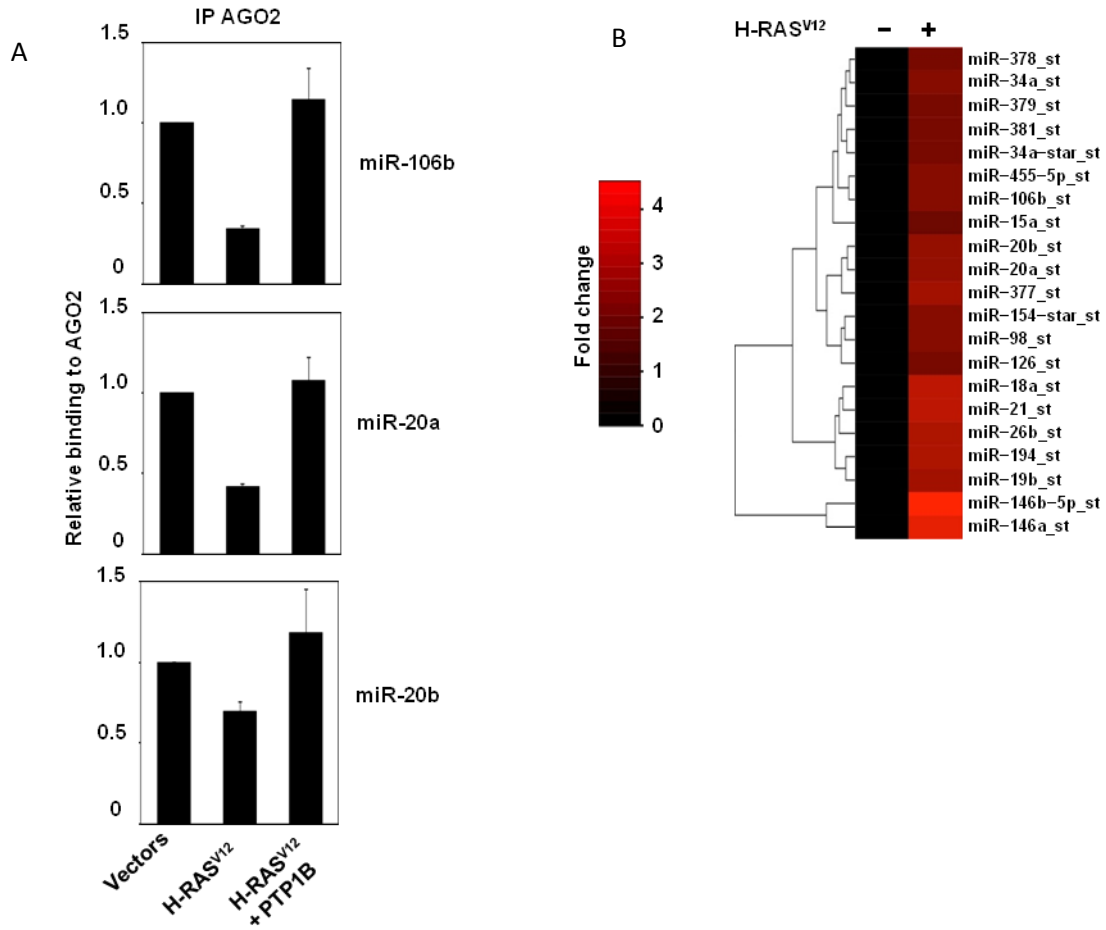

Figure 4.7 Loading of oncogenic miRNAs to Ago2 is impaired in senescent cells

(A)miRNA populations were extracted from IMR90 cells infected with a control vector or with *RAS*. Ago2 was immunoprecipitated from lysates of IMR90 cells, and Ago2-associated miRNAs were extracted. After cDNAs were synthesized, miR-20a, -20b and -106b were assessed by qRT-PCR. Enrichment of miRNA was normalized to 1 in IMR90 fibroblasts. (B)IMR90 cells were infected with a control vector or with *RAS* and miRNA populations were extracted. The RNAs were then analyzed on an Affymetrix miRNA Array. The heat map shows normalized $\log_2$-ratio values for each data set, with black representing the normalized expression levels in IMR90 cells and red representing the relative increase. The top 20 most up-regulated miRNAs were visualized in a heat map generated by Galaxy. Error bars represents SEM. N=3

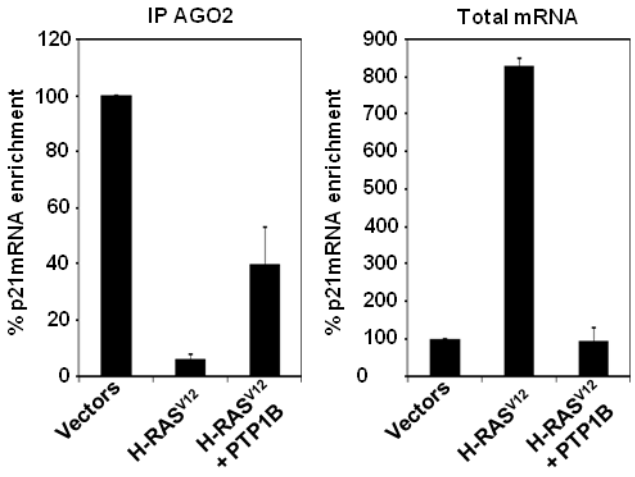

Figure 4.8 p21 mRNA association with Ago2 is impaired in senescent cells

Ago2 was immunoprecipitated from lysates of IMR90 cells infected with control vectors, *RAS* alone or co-infected with *PTP1B* WT. Ago2-associated RNAs were extracted, cDNA was synthesized and used for qRT-PCR to detect p21. Enrichment levels of p21 mRNA were normalized to 100% in IMR90 fibroblasts. Error bars represents SEM. N=3

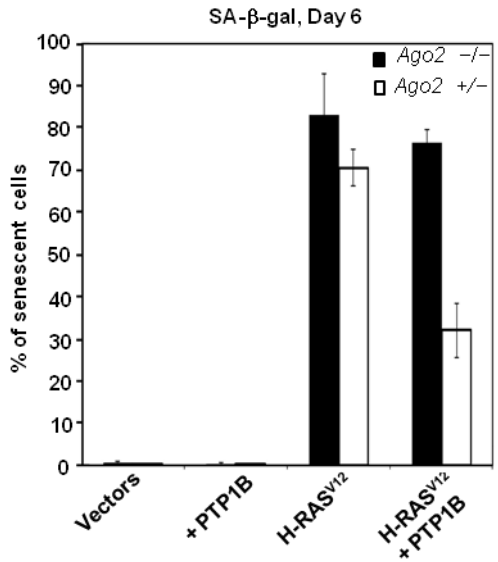

Figure 4.9 Ago2 is needed for PTP1B to attenuate RAS-induced senescence phenotype

Non-immortalized *Ago2* knockout (*Ago2* -/-, black bars) and heterozygous (*Ago2* +/-, white bars) MEFs co-infected with control vectors, *PTP1B*, *RAS* or with *RAS* and *PTP1B* were cultured for 6 days post-selection and stained for β-gal activity. Senescent cells were counted as β-gal positive cells relative to the total cells. Error bars represents SEM. N=3

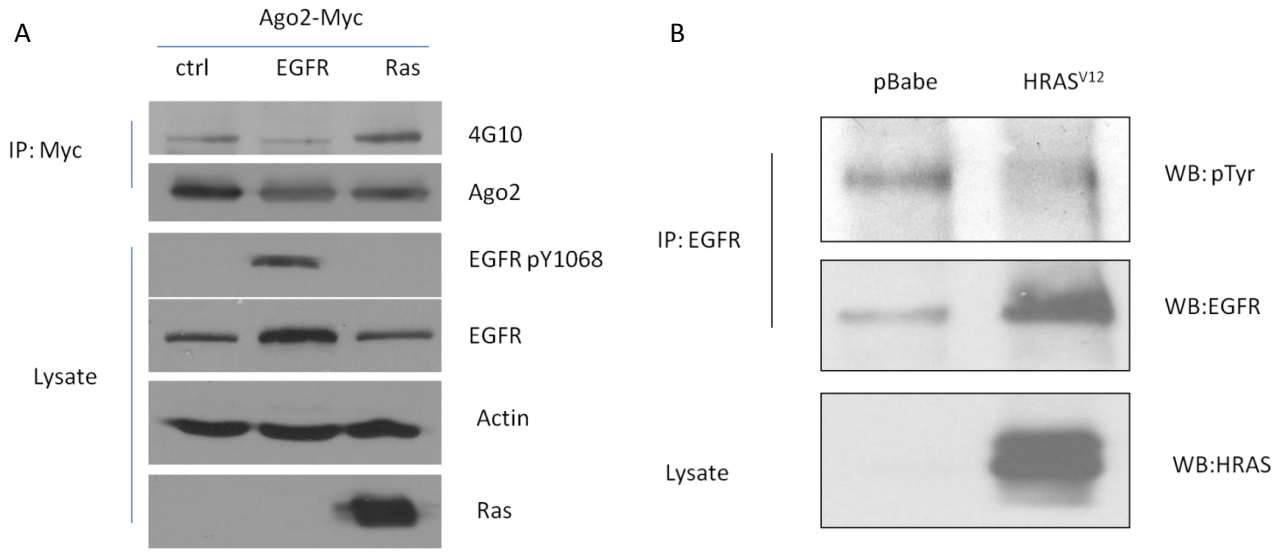

Figure 4.10 EGFR is unlikely to cause Ago2 phoshorylation in senescent cells

A) Ago2-MYC was co-expressed with control vector or $HRAS^{v12}$ or EGFR in HEK 293 cells. The lysates were harvested and Ago2 was immuneprecipitated and blotted with anti-pY antibody (4G10), and reblotted with Ago2 antibody. The lysate were blotted with phospho-EGFR (pY1068), total EGFR, actin and HRAS. B) EGFR was immunoprecipitated from IMR90 cells expressing control vector or $HRAS^{v12}$, the precipitates were blotted with anti-pTyr antibody (4G10) as measurement of EGFR activation, and then reblotted with EGFR antibody.

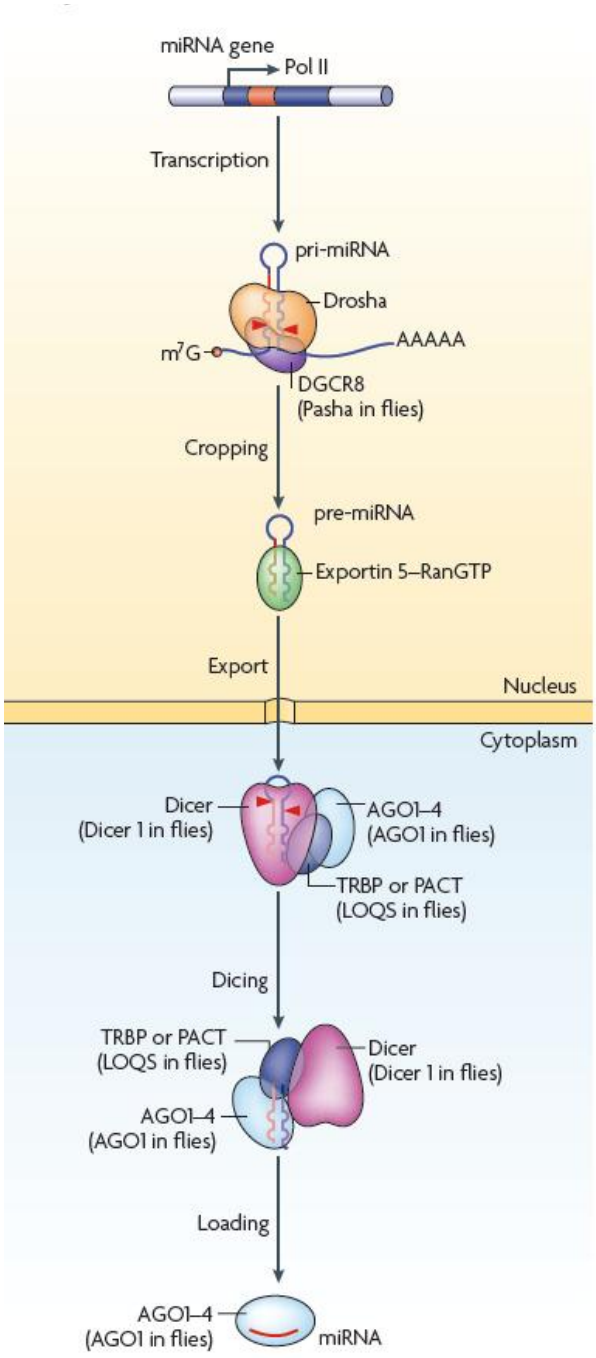

Figure 4.11 microRNA biogenesis pathway. Drosha cleaves primary RNA at 11bp away from the single strand RNA-double strand-RNA junction (indicated with red arrows). Dicer cleaves the terminal loop of precursor microRNA (pre-miRNA) and generates a miRNA duplex with phosphate group at 5' end and 2-nucleotide overhang at 3' end. miRNA duplex is loaded to Ago2 and unwound to from mature RISC [Adopted from (Kim, 2009)].

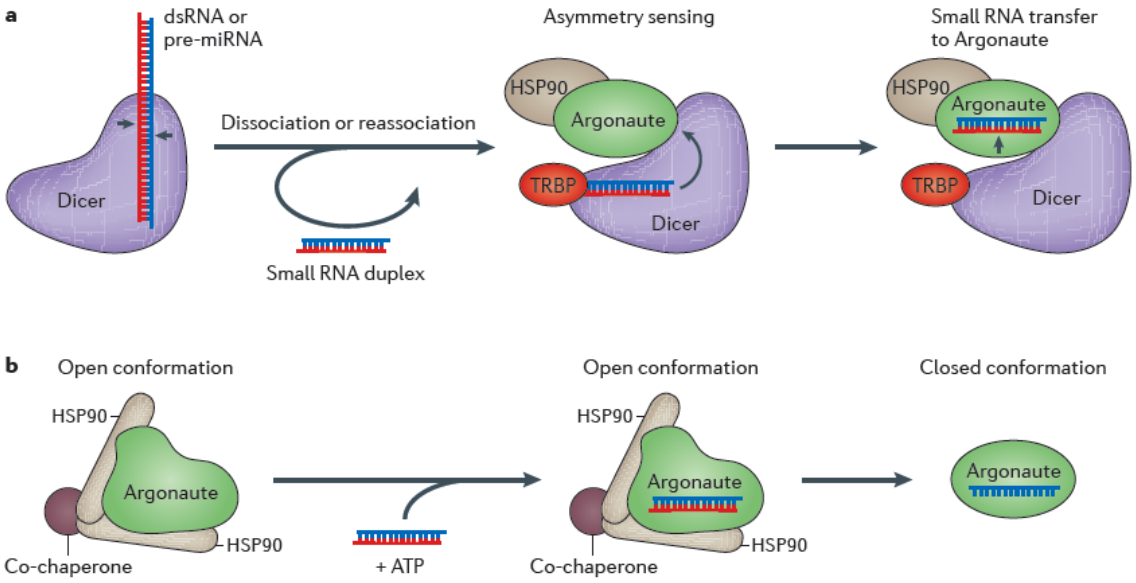

Figure 4.12 microRNA loading

(A) Dicer binds long double-stranded RNAs (dsRNAs) or precursor microRNAs (pre-miRNAs) and uses its two RNase III domains to cleave both strands (indicated by the two arrows), generating a ~21 nt dsRNA. This short dsRNA dissociates from and reassociates with Dicer at a different position. TRBP positions the RNA in an orientation, allowing correct loading. In the next step, the dsRNA is transferred to a bound Argonaute protein that is kept in an open conformation by heat shock protein 90 (HSP90) [Adopted from (Meister, 2013)].(B) An HSP90 dimer binds unloaded Argonaute proteins and holds them in an open conformation. After small RNA binding, the passenger strand is removed, HSP90 hydrolyses ATP, and the AGO protein loaded with the single-stranded RNAtransitions into a closed conformation. HSP90 and potential co-chaperones leave the complex.

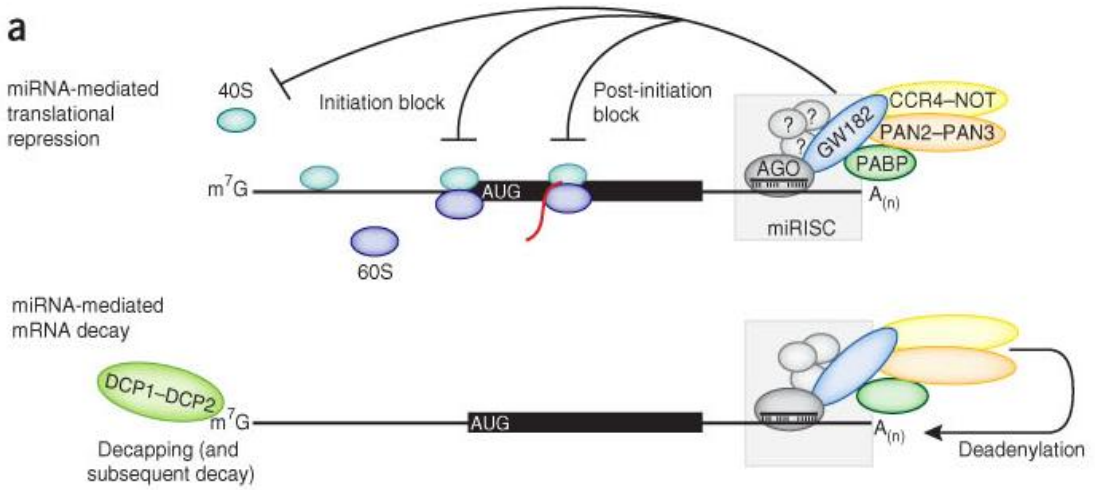

Figure 4.13 microRNA mediated translation repression and mRNA degradation

The RISC inhibits translation initiation by interfering with eIF4E-cap recognition and 40S small ribosomal subunit recruitment. The RISC might inhibit translation at post-initiation steps by inhibiting ribosome elongation. The RISC interacts with deadenylase complexes to facilitate deadenylation of the poly(A) tail (indicated by $A_{(n)}$). Following deadenylation, the 5-terminal cap (m^7G) is removed by the decapping the DCP1–DCP2 complex.[Adopted from (Fabian and Sonenberg, 2012)]

Chapter 5

5.1 Conclusion

Elevated expression of the *RAS* oncogene initiates a premature senescence program in cultured cells and *in vivo* that limits the mitogenicity of excessive RAS signalling (Collado and Serrano, 2010; Ferbeyre, 2007; Serrano et al., 1997). We addressed the potential role of PTPs in oncogenic senescence by assaying their reversible oxidation utilising a cysteinyl-labeling assay (Boivin et al., 2010b; Boivin et al., 2008). Our results demonstrated that RAS-triggered generation of ROS was an integral part of the signalling events leading to oncogene-induced cell-cycle arrest by causing the inactivation of PTP1B. Importantly, the reversible oxidation and inactivation of PTP1B resulted in enhanced phosphorylation and inactivation of Ago2 in our system of OIS. In turn, the inactivated Ago2 was uncoupled from DICER, and consequently unloaded of miRNAs, which was a direct cause of elevated expression of p21. Therefore, RAS expression provokes ROS production and caused redox regulation of PTP1B which overrode the *RAS* oncogenic program and led to senescence via inactivation of Ago2. Considered together, our results shed new light on the role of PTP1B in senescence and on how ROS-induced signalling is tightly linked to miRNA-mediated post-transcriptional regulation (Figure5.1).

5.1 Redox regulation of PTP1B is important for RAS-induced senescence

Induction of senescence by oncogene expression was shown as a result of the production of ROS. Culturing oncogene overexpressing cells in antioxidants or in low oxygen

conditions prevented the onset of senescence(Lee et al., 1999). How ROS mediate signalling pathways that regulate OIS was previously unknown.

We established the system of oncogene-induced senescence using human primary fibroblasts expressing a constitutively activated form of RAS: $HRAS^{V12}$. We detected an elevated but limited production of ROS in these cells and used the RAS-expresssing cells as the system to study ROS signalling. We detected PTP1B oxidation in the senescent cells and showed that the level of PTP1B oxidation gradually increase with the progress of senescence. Furthermore, we demonstrated that this oxidative inactivation of PTP1B is important for OIS. Overexpessing PTP1B WT attenuated, and inhibiting PTP1B promoted, RAS-induced senescence.

5.1.1 Targets of ROS in oncogene-induced senescence

In Chapter 2, we utilized a modified cysteine labelling assay and identified that PTP1B underwent reversible oxidation in the context of RAS-induced senescence. In this assay, we showed that PTP1B was a major protein oxidized in senescent cell. We illustrated the gradual increase of PTP1B oxidation during the development of senescence phenotype. Treating the cells with N-acetyl cysteine, a ROS scavenger, significantly reduced the extent of PTP1B oxidation.

Although we showed that PTP1B is a major target of ROS, we do not exclude the possibility that other proteins might also be regulated by ROS signalling in senescence. While PTP1B inhibition accelerates senescence, inhibition alone cannot induce OIS, indicating that

additional signalling pathway is required for the onset of senescence. For the future study of redox signalling in senescence, I propose to use the cysteine labelling assay to profile for the proteins that undergo reversible oxidation. As discussed in the Chapte 2, I propose to optimize the cysteine labelling assay so as to identify more PTPs which undergo redox regulation in senescent cells for further characterization.

5.1.2 Regulation of ROS/PTP1B signaling in senescence

Increasing amounts of studies have shown that PTP oxidation participates in the regulation of signal transduction in physiological events (Chen et al., 2008; Frijhoff et al., 2014; Meng et al., 2004). Our study demonstrated that PTP1B was oxidized in RAS signalling and the oxidative inhibition of PTP1B was important of RAS-induced senescence. It provided a new piece of evidence that links redox regulation of PTP with a physiological process. As mentioned in Chapter 2, the source of ROS which contributed to redox regulation of PTP1B is yet to be defined. Both NOX proteins and mitochondria might generate ROS in RAS-induced senescent cells and cause PTP1B oxidation. The future study to identify the source responsible for PTP1B oxidation will help our understanding of the regulation ROS signalling.

5.2 Ago2 is a major substrate of PTP1B in OIS

In Chapter 3, we identified PTP1B substrates in RAS-induced senescent cells. Identifying these direct targets of PTP1B in senescence will help us further understand the role of PTP1B in regulating senescence through specific signalling pathways. We used a PTP1B substrate

trapping strategy to pull down PTP1B substrates in RAS-induced senescence. We found that Ago2, a core enzyme in RNA-induced silence complex (RISC) is 8 fold more enriched by the PTP1B trapping mutant in senescent cells and was a major substrate of PTP1B. We measured that 34% of the total Ago2 in senescent cells associated with PTP1B trapping mutant in senescent cells, suggesting that PTP1B significantly affected Ago2 phosphorylation. Interestingly, we found that Ago2, but not Ago1, 3 and 4 or other components of the RISC complex (Dicer and TRBP), was specifically enriched with PTP1B (DA) in HEK293 cells.

5.2.1 Regulation of Ago2 phosphorylation by PTP1B

Proteins of the RNAi pathway are found in most subcellular compartments. Although PTP1B has been described as an ER-anchored phosphatase (Frangioni et al., 1992), its location would have the potential to expose it to most of the cytoplasmic compartment. Although there is no consensus on the exact subcellular sites of RNA silencing, a recent report investigating this aspect of RNAi biology found that mi- and si-RNA loaded Ago2, Dicer and TRBP almost exclusively co-sedimented with the markers of the rough ER membranes (Stalder et al., 2013). The proximity of active PTP1B and an ER-anchored RISC complex may be sufficient to keep Ago2 in a dephosphorylated state. Further investigation on the colocalization of PTP1B and Ago2 under different conditions can help to elucidate the detailed mechanism of the spatial and temporal regulation of PTP1B/Ago2 pathway.

Previous studies have provided evidence that Ago2 is tightly regulated by post-translational modifications. Phosphorylation at serine 387 by AKT3 mediates its localization at

GW182-rich processing bodies (P-bodies) and up-regulates translational repression of miRNA targets (Horman et al., 2013; Zeng et al., 2008a). Conversely, phosphorylation of Ago2 at Tyr 529, which has been proposed to occur during RISC disassembly, has been shown to prevent efficient binding of small RNAs (Rüdel et al., 2011). A third phosphorylation site, Tyr 393, has also been identified (Rüdel et al., 2011; Shen et al., 2013a). Using a model of hypoxic stress, Shen *et al.* reported that Ago2 was associated with the epidermal growth factor receptor (EGFR), which directly phosphorylated Ago2 on Tyr 393 (Shen et al., 2013a). In turn, this led to the dissociation of Ago2 and Dicer, inhibited the maturation of miRNAs, enhanced cell survival and invasiveness, and correlated with poor survival in breast cancer patients. Interestingly, PTP1B transcription is repressed by HIF in hypoxic stress, consistent with reduced PTP1B activity and the potential for phosphorylation of Ago2 on Tyr 393 in these conditions (Shen et al., 2013a; Suwaki et al., 2011). It will be interesting to test whether the PTP1B/Ago2 pathway also participates in EGFR signalling under hypoxia condition, or even serves as a common regulatory mechanism in redox mediated signalling.

5.2.2 Potential substrates of PTP1B in RAS-induced senescence

Using MS analysis, we identified potential substrates of PTP1B in RAS-induced senescence. Other than Ago2, the potential substrates particularly HIC5, S100A8 might be worth further investigation. They are suggested to have tumour suppressor functions and might play a role in regulating senescence (Khammanivong et al., 2013; Shibanuma et al., 1994). Further characterization of their roles in RAS-induced senescence and the regulatory

mechanisms of these proteins mediated via tyrosine phosphorylation can give us a more complete picture of how ROS regulate senescence through PTP1B and its targets.

5.3 Dephosphorylation of Ago2 Y393 by PTP1B regulates Ago2 function and leads to oncogene-induced senescence

We identified that PTP1B selectively regulated Ago2 phosphorylation at Y393 residue. Phosphorylation on Y393 disrupted Ago2 association with Dicer. This observation was consistent with the findings of Shen, et al, that Ago2 Y393 phosphorylation impairs miRNA maturation because of the disruption of the interaction between Ago2 and Dicer (Shen et al., 2013b).

Ago2 can bind single stranded siRNAs *in vitro* (Rivas et al., 2005). However, the Ago2 loading complex, comprised with Ago2/Dicer/TRBP is required for efficient microRNA loading to Ago2 (Matranga et al., 2005; Meister, 2013).Thus the dissociation between Ago2 and Dicer impairs microRNA loading. We observed that microRNA loading to phosphorylated Ago2 was attenuated in RAS-induced senescent cells and that the mutation of tyrosine 393 into a charged residue aspartic acid impaired microRNA loading as well.

We demonstrated that Ago2 phosphorylation and loss of function was important for OIS. Overexpressing WT Ago2 rescued RAS-induced senescence in IMR90 cells. In contrast overexpression of a Y393D mutant which contained a charged residue to 393 site did not prevent RAS-induced senescence. We also revealed that Ago2 acted downstream of PTP1B in

the signalling pathway regulating senescence. PTP1B could not attenuate RAS-induced senescence in Ago2 null MEF cells.

Furthermore, we showed that Ago2 loading with oncogenic microRNAs: mir-20a, mir-20b, and mir-106 was impaired in senescent cells. Unloading with these oncogenic microRNAs in senescent cells leads to a dissociation and derepression of the target of these miRs: p21, a key regulator of senescence.

5.3.1. PTP1B/Ago2 pathway is important in RAS signalling

Initial gene-targeting studies to generate PTP1B-deficient mice demonstrated that this phosphatase is a critical regulator of metabolism (Elchebly et al., 1999b; Klaman et al., 2000); however, PTP1B has also been shown to act either as a tumor suppressor or as an oncogene, depending on the specific tissue and modifier genes (Julien et al., 2011; Tonks, 2013; Tonks and Muthuswamy, 2007). Previous reports have linked PTP1B function to regulation of the RAS/ERK pathway downstream of growth factor signalling; it was shown that loss of PTP1B led to decreased RAS activation and signalling upon growth factor receptor activation (Dube et al., 2004; Julien et al., 2007). Our data also implicate PTP1B as a regulator of AGO2 downstream of oncogenic RAS signalling in senescence. In our hands, expression of an activated *RAS* allele (*H-RAS*^{V12}) triggered RAS oncogenic signalling in primary human diploid fibroblasts (Schubbert et al., 2007) and bypassed this effect of PTP1B upstream of RAS. Hence, cancer cells affected by gain-of-function mutations in the *RAS* gene may depend on PTP1B-mediated dephosphorylation of Tyr 393 in Ago2 to limit the effects of excessive RAS signalling. Interestingly, increased PTP1B expression has been reported in various cancers (Julien et al., 2011), which may contribute to

progression by suppressing Ago2 Tyr 393 phosphorylation and senescence. It is noteworthy that expression of a catalytically inactive PTP1B or an AGO2 pseudo-phospho Tyr 393 mutant was not sufficient in itself to cause senescence; hence, inhibiting PTP1B alone would not be expected to induce senescence. Nevertheless, developing an inhibitor for PTP1B could represent an interesting avenue for a senescence-inducing therapy to block oncogenic RAS-mediated tumour progression.

5.3.2 Role of RNAi pathway in OIS

Various miRNAs modulate gene expression programs central to senescence (Gorospe and Abdelmohsen, 2011). Up-regulation of miRNAs such as the miR-106b family was shown to overcome RAS-induced senescence by silencing p21 and other cell cycle regulators in human mammary epithelial cells (Borgdorff et al., 2010). Gene silencing by miRNAs can be shaped by qualitative changes in miRNA profiles, or globally by activation or inhibition of core protein factors (Lujambio and Lowe, 2012). We showed that Ago2 unloading with mir-20a, mir-20b and mir-106b facilitate the expression of p21 which is essential for OIS. However, the question remains whether phosphorylation mediated Ago2 unloading has a global impact on gene silencing or only affects specific targets. Ago2 Y393 phosphorylation was observed to preferentially inhibit the maturation of pre-miRNA with long stem loop (Shen et al., 2013b), indicating Ago2 might affect a selected group of targets. To address the specificity of PTP1B/Ago2 pathway in senescence, we can perform a RNA profiling to study the microRNAs and their targets associated with Ago2 under proliferation or senescence status.

5.4 Perspectives

Overall, the novel pathway delineated herein reveals PTP1B as a critical checkpoint in oncogenic RAS signalling. We show that PTP1B activity was a direct target of ROS signalling and its inactivation allowed phosphorylation of AGO2 at Tyr 393, which prevented AGO2 from associating with miRNAs and from performing post-transcriptional regulation of mRNAs, including for p21. Our observations contribute to a better understanding of the induction of senescence in response to oncogenic RAS signalling in primary human fibroblasts and contribute further to the growing body of evidence that the activity of miRNA mediated gene silencing is highly regulated post-translationally.

Our study has potential therapeutic implication for human diseases including cancer. PTP1B is overexpressed in several types of cancer such as breast, ovarian and prostate cancers(Feldhammer et al., 2013). PTP1B overexpression might compensate for its oxidative inactivation during transformation, preventing senescence induction in response to initiating pro-oncogenic events. Furthermore, increased Ago2 protein level is found in prostate cancer(Fu et al., 2010), myeloma(Zhou et al., 2010) and gastric cancer(Zhang et al., 2013). Further understanding on the function and regulation of ROS/PTP1B/Ago2 pathway might provide novel therapeutic methods for treating diseases.

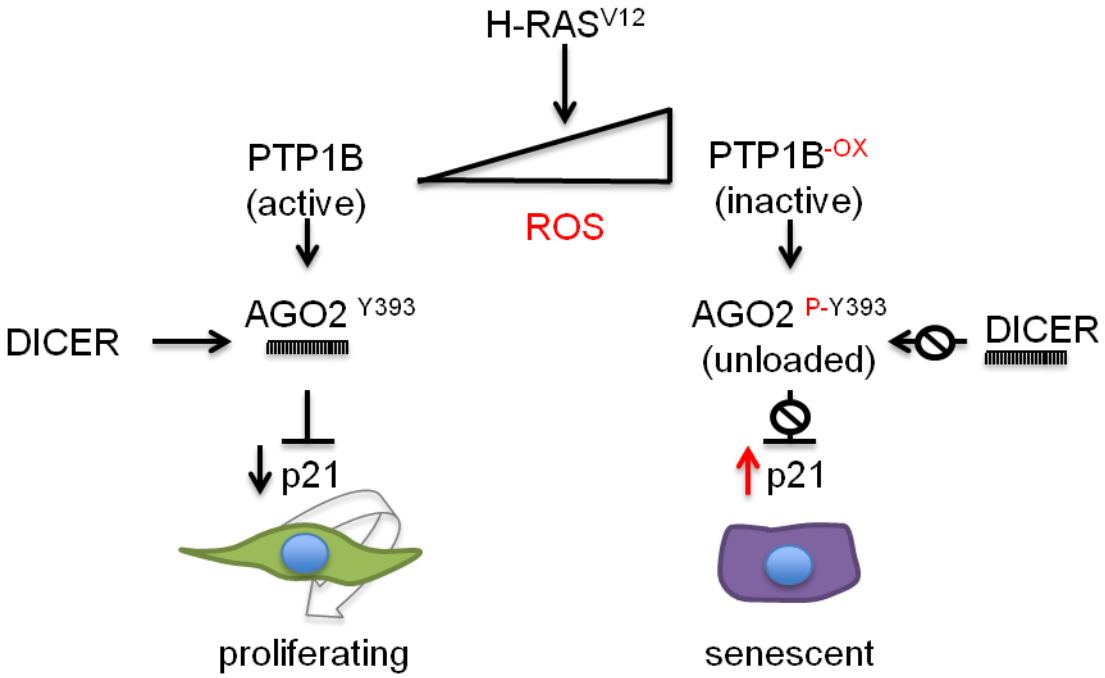

Figure 5.1 Schematic model of ROS regulation of PTP1B and Ago2 activity in RAS-mediated senescence

Reference

<OIS lowe lab.pdf>.
Abo, A., Pick, E., Hall, A., Totty, N., Teahan, C.G., and Segal, A.W. (1991). Activation of the NADPH oxidase involves the small GTP-binding protein p21rac1. Nature *353*, 668-670.
Aicher, B., Lerch, M.M., Muller, T., Schilling, J., and Ullrich, A. (1997). Cellular redistribution of protein tyrosine phosphatases LAR and PTPsigma by inducible proteolytic processing. The Journal of cell biology *138*, 681-696.
Bae, Y.S., Kang, S.W., Seo, M.S., Baines, I.C., Tekle, E., Chock, P.B., and Rhee, S.G. (1997). Epidermal growth factor (EGF)-induced generation of hydrogen peroxide. Role in EGF receptor-mediated tyrosine phosphorylation. The Journal of biological chemistry *272*, 217-221.
Bantscheff, M., Schirle, M., Sweetman, G., Rick, J., and Kuster, B. (2007). Quantitative mass spectrometry in proteomics: a critical review. Anal Bioanal Chem *389*, 1017-1031.
Barford, D., Flint, A.J., and Tonks, N.K. (1994). Crystal structure of human protein tyrosine phosphatase 1B. Science *263*, 1397-1404.
Bedard, K., and Krause, K.H. (2007). The NOX family of ROS-generating NADPH oxidases: physiology and pathophysiology. Physiol Rev *87*, 245-313.
Beitzinger, M., and Meister, G. (2011). Experimental identification of microRNA targets by immunoprecipitation of Argonaute protein complexes. Methods Mol Biol *732*, 153-167.
Benhamed, M., Herbig, U., Ye, T., Dejean, A., and Bischof, O. (2012). Senescence is an endogenous trigger for microRNA-directed transcriptional gene silencing in human cells. Nature cell biology *14*, 266-275.
Bennett, A.M., Tang, T.L., Sugimoto, S., Walsh, C.T., and Neel, B.G. (1994). Protein-tyrosine-phosphatase SHPTP2 couples platelet-derived growth factor receptor beta to Ras. Proceedings of the National Academy of Sciences of the United States of America *91*, 7335-7339.
Bentires-Alj, M., and Neel, B.G. (2007). Protein-tyrosine phosphatase 1B is required for HER2/Neu-induced breast cancer. Cancer research *67*, 2420-2424.
Bernstein, E., Caudy, A.A., Hammond, S.M., and Hannon, G.J. (2001). Role for a bidentate ribonuclease in the initiation step of RNA interference. Nature *409*, 363-366.
Bienert, G.P., Moller, A.L., Kristiansen, K.A., Schulz, A., Moller, I.M., Schjoerring, J.K., and Jahn, T.P. (2007). Specific aquaporins facilitate the diffusion of hydrogen peroxide across membranes. The Journal of biological chemistry *282*, 1183-1192.
Boivin, B., Chaudhary, F., Dickinson, B.C., Haque, A., Pero, S.C., Chang, C.J., and Tonks, N.K. (2013). Receptor protein-tyrosine phosphatase alpha regulates focal adhesion kinase phosphorylation and ErbB2 oncoprotein-mediated mammary epithelial cell motility. The Journal of biological chemistry *288*, 36926-36935.
Boivin, B., Yang, M., and Tonks, N.K. (2010a). Targeting the Reversibly Oxidized Protein Tyrosine Phosphatase Superfamily. Science Signaling *3*, pl2-pl2.
Boivin, B., Yang, M., and Tonks, N.K. (2010b). Targeting the reversibly oxidized protein tyrosine phosphatase superfamily. Sci Signal *3*, pl2.
Boivin, B., Zhang, S., Arbiser, J.L., Zhang, Z.Y., and Tonks, N.K. (2008). A modified cysteinyl-labeling assay reveals reversible oxidation of protein tyrosine phosphatases in angiomyolipoma cells. Proc Natl Acad Sci USA *105*, 9959-9964.
Bondarenko, P.V., Chelius, D., and Shaler, T.A. (2002). Identification and relative quantitation of protein mixtures by enzymatic digestion followed by capillary reversed-phase liquid chromatography-tandem mass spectrometry. Anal Chem *74*, 4741-4749.
Borgdorff, V., Lleonart, M.E., Bishop, C.L., Fessart, D., Bergin, A.H., Overhoff, M.G., and Beach, D.H. (2010). Multiple microRNAs rescue from Ras-induced senescence by inhibiting p21(Waf1/Cip1). Oncogene *29*, 2262-2271.

Bos, J.L. (1989). ras oncogenes in human cancer: a review. Cancer research *49*, 4682-4689.
Boxall, S., McCormick, J., Beverley, P., Strobel, S., De Filippi, P., Dawes, R., Klersy, C., Clementi, R., De Juli, E., Ferster, A.*, et al.* (2004). Abnormal cell surface antigen expression in individuals with variant CD45 splicing and histiocytosis. Pediatr Res *55*, 478-484.
Braig, M., Lee, S., Loddenkemper, C., Rudolph, C., Peters, A.H., Schlegelberger, B., Stein, H., Dorken, B., Jenuwein, T., and Schmitt, C.A. (2005). Oncogene-induced senescence as an initial barrier in lymphoma development. Nature *436*, 660-665.
Brand, M.D. (2010). The sites and topology of mitochondrial superoxide production. Exp Gerontol *45*, 466-472.
Brown, D.I., and Griendling, K.K. (2009a). Nox proteins in signal transduction. Free radical biology & medicine *47*, 1239-1253.
Brown, D.I., and Griendling, K.K. (2009b). Nox proteins in signal transduction. Free Radic Biol Med *47*, 1239-1253.
Bulavin, D.V., Saito, S., Hollander, M.C., Sakaguchi, K., Anderson, C.W., Appella, E., and Fornace, A.J., Jr. (1999). Phosphorylation of human p53 by p38 kinase coordinates N-terminal phosphorylation and apoptosis in response to UV radiation. The EMBO journal *18*, 6845-6854.
Campan, M., Yoshizumi, M., Seidah, N.G., Lee, M.E., Bianchi, C., and Haber, E. (1996). Increased proteolytic processing of protein tyrosine phosphatase mu in confluent vascular endothelial cells: the role of PC5, a member of the subtilisin family. Biochemistry *35*, 3797-3802.
Campisi, J. (2005). Suppressing cancer: the importance of being senescent. Science *309*, 886-887.
Chandel, N.S., McClintock, D.S., Feliciano, C.E., Wood, T.M., Melendez, J.A., Rodriguez, A.M., and Schumacker, P.T. (2000). Reactive oxygen species generated at mitochondrial complex III stabilize hypoxia-inducible factor-1alpha during hypoxia: a mechanism of O2 sensing. The Journal of biological chemistry *275*, 25130-25138.
Chang, N., Yi, J., Guo, G., Liu, X., Shang, Y., Tong, T., Cui, Q., Zhan, M., Gorospe, M., and Wang, W. (2010a). HuR uses AUF1 as a cofactor to promote p16INK4 mRNA decay. Mol Cell Biol *30*, 3875-3886.
Chang, N., Yi, J., Guo, G., Liu, X., Shang, Y., Tong, T., Cui, Q., Zhan, M., Gorospe, M., and Wang, W. (2010b). HuR Uses AUF1 as a Cofactor To Promote p16INK4 mRNA Decay. Molecular and Cellular Biology *30*, 3875-3886.
Chang, Y.C., Lin, S.Y., Liang, S.Y., Pan, K.T., Chou, C.C., Chen, C.H., Liao, C.L., Khoo, K.H., and Meng, T.C. (2008). Tyrosine phosphoproteomics and identification of substrates of protein tyrosine phosphatase dPTP61F in Drosophila S2 cells by mass spectrometry-based substrate trapping strategy. Journal of proteome research *7*, 1055-1066.
Chelius, D., and Bondarenko, P.V. (2002). Quantitative profiling of proteins in complex mixtures using liquid chromatography and mass spectrometry. Journal of proteome research *1*, 317-323.
Cheloufi, S., Dos Santos, C.O., Chong, M.M., and Hannon, G.J. (2010). A dicer-independent miRNA biogenesis pathway that requires Ago catalysis. Nature *465*, 584-589.
Chen, K., Kirber, M.T., Xiao, H., Yang, Y., and Keaney, J.F., Jr. (2008). Regulation of ROS signal transduction by NADPH oxidase 4 localization. The Journal of cell biology *181*, 1129-1139.
Chen, Q., and Ames, B.N. (1994). Senescence-like growth arrest induced by hydrogen peroxide in human diploid fibroblast F65 cells. Proceedings of the National Academy of Sciences of the United States of America *91*, 4130-4134.
Chendrimada, T.P., Gregory, R.I., Kumaraswamy, E., Norman, J., Cooch, N., Nishikura, K., and Shiekhattar, R. (2005). TRBP recruits the Dicer complex to Ago2 for microRNA processing and gene silencing. Nature *436*, 740-744.
Chu, C.Y., and Rana, T.M. (2007). Small RNAs: regulators and guardians of the genome. Journal of cellular physiology *213*, 412-419.

Cohen, P. (2001). The role of protein phosphorylation in human health and disease. . European Journal of Biochemistry *268*, 5001-5010.
Colavitti, R., and Finkel, T. (2005). Reactive oxygen species as mediators of cellular senescence. IUBMB Life *57*, 277-281.
Colavitti, R., Pani, G., Bedogni, B., Anzevino, R., Borrello, S., Waltenberger, J., and Galeotti, T. (2002). Reactive oxygen species as downstream mediators of angiogenic signaling by vascular endothelial growth factor receptor-2/KDR. The Journal of biological chemistry *277*, 3101-3108.
Collado, M., and Serrano, M. (2010). Senescence in tumours: evidence from mice and humans. Nat Rev Cancer *10*, 51-57.
Conkrite, K., Sundby, M., Mukai, S., Thomson, J.M., Mu, D., Hammond, S.M., and MacPherson, D. (2011). miR-17~92 cooperates with RB pathway mutations to promote retinoblastoma. Genes Dev *25*, 1734-1745.
Courtois-Cox, S., Jones, S.L., and Cichowski, K. (2008). Many roads lead to oncogene-induced senescence. Oncogene *27*, 2801-2809.
d'Adda di Fagagna, F., Reaper, P.M., Clay-Farrace, L., Fiegler, H., Carr, P., Von Zglinicki, T., Saretzki, G., Carter, N.P., and Jackson, S.P. (2003). A DNA damage checkpoint response in telomere-initiated senescence. Nature *426*, 194-198.
d'Adda di Fagagna, F., Teo, S.H., and Jackson, S.P. (2004). Functional links between telomeres and proteins of the DNA-damage response. Genes & development *18*, 1781-1799.
Dadke, S., Cotteret, S., Yip, S.C., Jaffer, Z.M., Haj, F., Ivanov, A., Rauscher, F., 3rd, Shuai, K., Ng, T., Neel, B.G.*, et al.* (2007). Regulation of protein tyrosine phosphatase 1B by sumoylation. Nature cell biology *9*, 80-85.
Dance, M., Montagner, A., Salles, J.P., Yart, A., and Raynal, P. (2008). The molecular functions of Shp2 in the Ras/Mitogen-activated protein kinase (ERK1/2) pathway. Cellular signalling *20*, 453-459.
DeNicola, G.M., and Tuveson, D.A. (2009a). RAS in cellular transformation and senescence. Eur J Cancer *45*, 211-216.
DeNicola, G.M., and Tuveson, D.A. (2009b). RAS in cellular transformation and senescence. Eur J Cancer *45 Suppl 1*, 211-216.
Denli, A.M., Tops, B.B., Plasterk, R.H., Ketting, R.F., and Hannon, G.J. (2004). Processing of primary microRNAs by the Microprocessor complex. Nature *432*, 231-235.
Denu, J.M., Lohse, D.L., Vijayalakshmi, J., Saper, M.A., and Dixon, J.E. (1996). Visualization of intermediate and transition-state structures in protein-tyrosine phosphatase catalysis. Proceedings of the National Academy of Sciences of the United States of America *93*, 2493-2498.
Denu, J.M., and Tanner, K.G. (1998). Specific and reversible inactivation of protein tyrosine phosphatases by hydrogen peroxide: evidence for a sulfenic acid intermediate and implications for redox regulation. Biochemistry *37*, 5633-5642.
Desai, D.M., Sap, J., Schlessinger, J., and Weiss, A. (1993). Ligand-mediated negative regulation of a chimeric transmembrane receptor tyrosine phosphatase. Cell *73*, 541-554.
Desai, D.M., Sap, J., Silvennoinen, O., Schlessinger, J., and Weiss, A. (1994). The catalytic activity of the CD45 membrane-proximal phosphatase domain is required for TCR signaling and regulation. The EMBO journal *13*, 4002-4010.
Di Stefano, P., Cabodi, S., Boeri Erba, E., Margaria, V., Bergatto, E., Giuffrida, M.G., Silengo, L., Tarone, G., Turco, E., and Defilippi, P. (2004). P130Cas-associated protein (p140Cap) as a new tyrosine-phosphorylated protein involved in cell spreading. Mol Biol Cell *15*, 787-800.
Dickinson, B.C., Peltier, J., Stone, D., Schaffer, D.V., and Chang, C.J. (2011a). Nox2 redox signaling maintains essential cell populations in the brain. Nat Chem Biol *7*, 106-112.
Dickinson, B.C., Peltier, J., Stone, D., Schaffer, D.V., and Chang, C.J. (2011b). Nox2 redox signaling maintains essential cell populations in the brain. Nat Chem Biol *7*, 106-112.

Diederichs, S., and Haber, D.A. (2007). Dual role for argonautes in microRNA processing and posttranscriptional regulation of microRNA expression. Cell *131*, 1097-1108.
Dimri, G.P., Lee, X., Basile, G., Acosta, M., Scott, G., Roskelley, C., Medrano, E.E., Linskens, M., Rubelj, I., Pereira-Smith, O.*, et al.* (1995). A biomarker that identifies senescent human cells in culture and in aging skin in vivo. Proceedings of the National Academy of Sciences of the United States of America *92*, 9363-9367.
Dinauer, M.C., Orkin, S.H., Brown, R., Jesaitis, A.J., and Parkos, C.A. (1987). The glycoprotein encoded by the X-linked chronic granulomatous disease locus is a component of the neutrophil cytochrome b complex. Nature *327*, 717-720.
Downward, J. (2003). Targeting RAS signalling pathways in cancer therapy. Nat Rev Cancer *3*, 11-22.
Dube, N., Cheng, A., and Tremblay, M.L. (2004). The role of protein tyrosine phosphatase 1B in Ras signaling. Proceedings of the National Academy of Sciences of the United States of America *101*, 1834-1839.
Elchebly, M., Payette, P., Michaliszyn, E., Cromlish, W., Collins, S., Loy, A.L., Normandin, D., Cheng, A., Himms-Hagen, J., Chan, C.C.*, et al.* (1999a). Increased insulin sensitivity and obesity resistance in mice lacking the protein tyrosine phosphatase-1B gene. Science *283*, 1544-1548.
Elchebly, M., Payette, P., Michaliszyn, E., Cromlish, W., Collins, S., Loy, A.L., Normandin, D., Cheng, A., Himms-Hagen, J., Chan, C.C.*, et al.* (1999b). Increased insulin sensitivity and obesity resistance in mice lacking the protein tyrosine phosphatase-1B gene [see comments]. Science *283*, 1544-1548.
Eswaran, J., von Kries, J.P., Marsden, B., Longman, E., Debreczeni, J.E., Ugochukwu, E., Turnbull, A., Lee, W.H., Knapp, S., and Barr, A.J. (2006). Crystal structures and inhibitor identification for PTPN5, PTPRR and PTPN7: a family of human MAPK-specific protein tyrosine phosphatases. The Biochemical journal *395*, 483-491.
Fabian, M.R., and Sonenberg, N. (2012). The mechanics of miRNA-mediated gene silencing: a look under the hood of miRISC. Nat Struct Mol Biol *19*, 586-593.
Fan, C.Y., Katsuyama, M., and Yabe-Nishimura, C. (2005). PKCdelta mediates up-regulation of NOX1, a catalytic subunit of NADPH oxidase, via transactivation of the EGF receptor: possible involvement of PKCdelta in vascular hypertrophy. The Biochemical journal *390*, 761-767.
Ferbeyre, G. (2007). Barriers to Ras transformation. Nature cell biology *9*, 483-485.
Finkel, T. (1998). Oxygen radicals and signaling. Current opinion in cell biology *10*, 248-253.
Finkel, T. (2011). Signal transduction by reactive oxygen species. The Journal of cell biology *194*, 7-15.
Fischer, E.H., and Krebs, E.G. (1955). Conversion of phosphorylase b to phosphorylase a in muscle extracts. The Journal of biological chemistry *216*, 121-132.
Flint, A.J., Tiganis, T., Barford, D., and Tonks, N.K. (1997a). Development of "substrate-trapping" mutants to identify physiological substrates of protein tyrosine phosphatases. Proceedings of the National Academy of Sciences of the United States of America *94*, 1680-1685.
Flint, A.J., Tiganis, T., Barford, D., and Tonks, N.K. (1997b). Development of "substrate trapping" mutants to identify physiological substrates of protein tyrosine phosphatases. Proc Natl Acad Sci USA *94*, 1680-1685.
Frangioni, J.V., Beahm, P.H., Shifrin, V., Jost, C.A., and Neel, B.G. (1992). The nontransmembrane tyrosine phosphatase PTP-1B localizes to the endoplasmic reticulum via its 35 amino acid C-terminal sequence. Cell *68*, 545-560.
Frangioni, J.V., Oda, A., Smith, M., Salzman, E.W., and Neel, B.G. (1993). Calpain-catalyzed cleavage and subcellular relocation of protein phosphotyrosine phosphatase 1B (PTP-1B) in human platelets. The EMBO journal *12*, 4843-4856.
Frank, F., Sonenberg, N., and Nagar, B. (2010). Structural basis for 5'-nucleotide base-specific recognition of guide RNA by human AGO2. Nature *465*, 818-822.

Freeman, D.J., Li, A.G., Wei, G., Li, H.H., Kertesz, N., Lesche, R., Whale, A.D., Martinez-Diaz, H., Rozengurt, N., Cardiff, R.D*., et al.* (2003). PTEN tumor suppressor regulates p53 protein levels and activity through phosphatase-dependent and -independent mechanisms. Cancer Cell *3*, 117-130.
Frijhoff, J., Dagnell, M., Augsten, M., Beltrami, E., Giorgio, M., and Ostman, A. (2014). The mitochondrial reactive oxygen species regulator p66Shc controls PDGF-induced signaling and migration through protein tyrosine phosphatase oxidation. Free radical biology & medicine *68*, 268-277.
Fu, X., Xue, C., Huang, Y., Xie, Y., and Li, Y. (2010). The activity and expression of microRNAs in prostate cancers. Mol Biosyst *6*, 2561-2572.
Fuchs, M., Muller, T., Lerch, M.M., and Ullrich, A. (1996). Association of human protein-tyrosine phosphatase kappa with members of the armadillo family. The Journal of biological chemistry *271*, 16712-16719.
Gaits, F., Li, R.Y., Ragab, A., Ragab-Thomas, J.M., and Chap, H. (1995). Increase in receptor-like protein tyrosine phosphatase activity and expression level on density-dependent growth arrest of endothelial cells. The Biochemical journal *311 (Pt 1)*, 97-103.
Gartel, A.L., and Radhakrishnan, S.K. (2005). Lost in transcription: p21 repression, mechanisms, and consequences. Cancer research *65*, 3980-3985.
Giamas, G., Man, Y.L., Hirner, H., Bischof, J., Kramer, K., Khan, K., Ahmed, S.S., Stebbing, J., and Knippschild, U. (2010). Kinases as targets in the treatment of solid tumors. Cellular signalling *22*, 984-1002.
Giorgio, M., Trinei, M., Migliaccio, E., and Pelicci, P.G. (2007). Hydrogen peroxide: a metabolic by-product or a common mediator of ageing signals? Nat Rev Mol Cell Biol *8*, 722-728.
Gorospe, M., and Abdelmohsen, K. (2011). MicroRegulators come of age in senescence. Trends Genet *27*, 233-241.
Graves, D.J., Fischer, E.H., and Krebs, E.G. (1960). Specificity studies on muscle phosphorylase phosphatase. The Journal of biological chemistry *235*, 805-809.
Graves, J.D., and Krebs, E.G. (1999). Protein Phosphorylation and Signal Transduction. Pharmacology & Therapeutics *82*, 111-121.
Gregory, R.I., Chendrimada, T.P., Cooch, N., and Shiekhattar, R. (2005). Human RISC couples microRNA biogenesis and posttranscriptional gene silencing. Cell *123*, 631-640.
Gregory, R.I., Yan, K.P., Amuthan, G., Chendrimada, T., Doratotaj, B., Cooch, N., and Shiekhattar, R. (2004). The Microprocessor complex mediates the genesis of microRNAs. Nature *432*, 235-240.
Gygi, S.P., Rist, B., Gerber, S.A., Turecek, F., Gelb, M.H., and Aebersold, R. (1999). Quantitative analysis of complex protein mixtures using isotope-coded affinity tags. Nat Biotechnol *17*, 994-999.
Haase, A.D., Jaskiewicz, L., Zhang, H., Laine, S., Sack, R., Gatignol, A., and Filipowicz, W. (2005). TRBP, a regulator of cellular PKR and HIV-1 virus expression, interacts with Dicer and functions in RNA silencing. EMBO Rep *6*, 961-967.
Halle, M., Liu, Y.C., Hardy, S., Theberge, J.F., Blanchetot, C., Bourdeau, A., Meng, T.C., and Tremblay, M.L. (2007). Caspase-3 regulates catalytic activity and scaffolding functions of the protein tyrosine phosphatase PEST, a novel modulator of the apoptotic response. Mol Cell Biol *27*, 1172-1190.
Han, J., Lee, Y., Yeom, K.H., Kim, Y.K., Jin, H., and Kim, V.N. (2004). The Drosha-DGCR8 complex in primary microRNA processing. Genes & development *18*, 3016-3027.
Haque, A., Andersen, J.N., Salmeen, A., Barford, D., and Tonks, N.K. (2011a). Conformation-sensing antibodies stabilize the oxidized form of PTP1B and inhibit its phosphatase activity. Cell *147*, 185-198.
Haque, A., Andersen, J.N., Salmeen, A., Barford, D., and Tonks, N.K. (2011b). Conformation-sensing antibodies stabilize the oxidized form of PTP1B and inhibit its phosphatase activity. Cell *147*, 185-198.
Haupt, Y., Maya, R., Kazaz, A., and Oren, M. (1997). Mdm2 promotes the rapid degradation of p53. Nature *387*, 296-299.
Hayflick, L. (1965). The Limited in Vitro Lifetime of Human Diploid Cell Strains. Exp Cell Res *37*, 614-636.

Heinrich, R., Neel, B.G., and Rapoport, T.A. (2002). Mathematical models of protein kinase signal transduction. Mol Cell *9*, 957-970.
Herbert, K.M., Pimienta, G., DeGregorio, S.J., Alexandrov, A., and Steitz, J.A. (2013). Phosphorylation of DGCR8 increases its intracellular stability and induces a progrowth miRNA profile. Cell Rep *5*, 1070-1081.
Hetey, S.E., Lalonde, D.P., and Turner, C.E. (2005). Tyrosine-phosphorylated Hic-5 inhibits epidermal growth factor-induced lamellipodia formation. Exp Cell Res *311*, 147-156.
Honda, R., and Yasuda, H. (1999). Association of p19(ARF) with Mdm2 inhibits ubiquitin ligase activity of Mdm2 for tumor suppressor p53. The EMBO journal *18*, 22-27.
Horman, S.R., Janas, M.M., Litterst, C., Wang, B., MacRae, I.J., Sever, M.J., Morrissey, D.V., Graves, P., Luo, B., Umesalma, S.*, et al.* (2013). Akt-mediated phosphorylation of argonaute 2 downregulates cleavage and upregulates translational repression of MicroRNA targets. Mol Cell *50*, 356-367.
Hornberg, J.J., Bruggeman, F.J., Binder, B., Geest, C.R., de Vaate, A.J., Lankelma, J., Heinrich, R., and Westerhoff, H.V. (2005). Principles behind the multifarious control of signal transduction. ERK phosphorylation and kinase/phosphatase control. The FEBS journal *272*, 244-258.
Huyer, G., Liu, S., Kelly, J., Moffat, J., Payette, P., Kennedy, B., Tsaprailis, G., Gresser, M.J., and Ramachandran, C. (1997). Mechanism of inhibition of protein-tyrosine phosphatases by vanadate and pervanadate. The Journal of biological chemistry *272*, 843-851.
Ishihama, Y., Oda, Y., Tabata, T., Sato, T., Nagasu, T., Rappsilber, J., and Mann, M. (2005). Exponentially modified protein abundance index (emPAI) for estimation of absolute protein amount in proteomics by the number of sequenced peptides per protein. Mol Cell Proteomics *4*, 1265-1272.
Ishino, M., Aoto, H., Sasaski, H., Suzuki, R., and Sasaki, T. (2000). Phosphorylation of Hic-5 at tyrosine 60 by CAKbeta and Fyn. FEBS Lett *474*, 179-183.
Ivanovska, I., Ball, A.S., Diaz, R.L., Magnus, J.F., Kibukawa, M., Schelter, J.M., Kobayashi, S.V., Lim, L., Burchard, J., Jackson, A.L.*, et al.* (2008). MicroRNAs in the miR-106b family regulate p21/CDKN1A and promote cell cycle progression. Mol Cell Biol *28*, 2167-2174.
Iwasaki, S., Kobayashi, M., Yoda, M., Sakaguchi, Y., Katsuma, S., Suzuki, T., and Tomari, Y. (2010). Hsc70/Hsp90 chaperone machinery mediates ATP-dependent RISC loading of small RNA duplexes. Mol Cell *39*, 292-299.
Jiang, G., den Hertog, J., Su, J., Noel, J., Sap, J., and Hunter, T. (1999). Dimerization inhibits the activity of receptor-like protein-tyrosine phosphatase-alpha. Nature *401*, 606-610.
Johnson, K.G., Tenney, A.P., Ghose, A., Duckworth, A.M., Higashi, M.E., Parfitt, K., Marcu, O., Heslip, T.R., Marsh, J.L., Schwarz, T.L.*, et al.* (2006). The HSPGs Syndecan and Dallylike bind the receptor phosphatase LAR and exert distinct effects on synaptic development. Neuron *49*, 517-531.
Julien, S.G., Dubé, N., Hardy, S., and Tremblay, M.L. (2011). Inside the human cancer tyrosine phosphatome. Nat Rev Cancer *11*, 35-49.
Julien, S.G., Dubé, N., Read, M., Penney, J., Paquet, M., Han, Y., Kennedy, B.P., Muller, W.J., and Tremblay, M.L. (2007). Protein tyrosine phosphatase 1B deficiency or inhibition delays ErbB2-induced mammary tumorigenesis and protects from lung metastasis. Nat Genet *39*, 338-346.
Jung, M.S., Jin, D.H., Chae, H.D., Kang, S., Kim, S.C., Bang, Y.J., Choi, T.S., Choi, K.S., and Shin, D.Y. (2004). Bcl-xL and E1B-19K proteins inhibit p53-induced irreversible growth arrest and senescence by preventing reactive oxygen species-dependent p38 activation. The Journal of biological chemistry *279*, 17765-17771.
Kamata, H., Honda, S., Maeda, S., Chang, L., Hirata, H., and Karin, M. (2005). Reactive oxygen species promote TNFalpha-induced death and sustained JNK activation by inhibiting MAP kinase phosphatases. Cell *120*, 649-661.
Kerkhoff, C., Nacken, W., Benedyk, M., Dagher, M.C., Sopalla, C., and Doussiere, J. (2005). The arachidonic acid-binding protein S100A8/A9 promotes NADPH oxidase activation by interaction with p67phox and Rac-2. FASEB J *19*, 467-469.

Khammanivong, A., Wang, C., Sorenson, B.S., Ross, K.F., and Herzberg, M.C. (2013). S100A8/A9 (calprotectin) negatively regulates G2/M cell cycle progression and growth of squamous cell carcinoma. PLoS One *8*, e69395.
Kim, B.C., Lee, H.C., Lee, J.J., Choi, C.M., Kim, D.K., Lee, J.C., Ko, Y.G., and Lee, J.S. (2012). Wig1 prevents cellular senescence by regulating p21 mRNA decay through control of RISC recruitment. The EMBO journal *31*, 4289-4303.
Kim, B.S., Jung, J.S., Jang, J.H., Kang, K.S., and Kang, S.K. (2011). Nuclear Argonaute 2 regulates adipose tissue-derived stem cell survival through direct control of miR10b and selenoprotein N1 expression. Aging Cell *10*, 277-291.
Kim, D.H., Saetrom, P., Snove, O., Jr., and Rossi, J.J. (2008). MicroRNA-directed transcriptional gene silencing in mammalian cells. Proceedings of the National Academy of Sciences of the United States of America *105*, 16230-16235.
Kim, V.N. (2004). MicroRNA precursors in motion: exportin-5 mediates their nuclear export. Trends Cell Biol *14*, 156-159.
Kim, V.N., Han, J., and Siomi, M.C. (2009). Biogenesis of small RNAs in animals. Nature Reviews Molecular Cell Biology *10*, 126-139.
Klaman, L.D., Boss, O., Peroni, O.D., Kim, J.K., Martino, J.L., Zabolotny, J.M., Moghal, N., Lubkin, M., Kim, Y.B., Sharpe, A.H.*, et al.* (2000). Increased energy expenditure, decreased adiposity, and tissue-specific insulin sensitivity in protein-tyrosine phosphatase 1B-deficient mice. Mol Cell Biol *20*, 5479-5489.
Kodama, R., Kato, M., Furuta, S., Ueno, S., Zhang, Y., Matsuno, K., Yabe-Nishimura, C., Tanaka, E., and Kamata, T. (2013). ROS-generating oxidases Nox1 and Nox4 contribute to oncogenic Ras-induced premature senescence. Genes Cells *18*, 32-41.
Koretzky, G.A., Picus, J., Thomas, M.L., and Weiss, A. (1990). Tyrosine phosphatase CD45 is essential for coupling T-cell antigen receptor to the phosphatidyl inositol pathway. Nature *346*, 66-68.
Krebs, E.G., and Fischer, E.H. (1955). Phosphorylase activity of skeletal muscle extracts. The Journal of biological chemistry *216*, 113-120.
Krebs, E.G., and Fischer, E.H. (1956). The phosphorylase b to a converting enzyme of rabbit skeletal muscle. Biochimica et biophysica acta *20*, 150-157.
Krebs, E.G., Kent, A.B., and Fischer, E.H. (1958). The muscle phosphorylase b kinase reaction. The Journal of biological chemistry *231*, 73-83.
Krieger-Brauer, H.I., and Kather, H. (1995). Antagonistic effects of different members of the fibroblast and platelet-derived growth factor families on adipose conversion and NADPH-dependent H2O2 generation in 3T3 L1-cells. The Biochemical journal *307 (Pt 2)*, 549-556.
Krishnan, N., Koveal, D., Miller, D.H., Xue, B., Akshinthala, S.D., Kragelj, J., Jensen, M.R., Gauss, C.M., Page, R., Blackledge, M.*, et al.* (2014). Targeting the disordered C terminus of PTP1B with an allosteric inhibitor. Nat Chem Biol *10*, 558-566.
Kumar, S., Zhou, B., Liang, F., Yang, H., Wang, W.Q., and Zhang, Z.Y. (2006). Global analysis of protein tyrosine phosphatase activity with ultra-sensitive fluorescent probes. Journal of proteome research *5*, 1898-1905.
Kwak, P.B., and Tomari, Y. (2012). The N domain of Argonaute drives duplex unwinding during RISC assembly. Nat Struct Mol Biol *19*, 145-151.
LaMontagne, K.R., Jr., Hannon, G., and Tonks, N.K. (1998). Protein tyrosine phosphatase PTP1B suppresses p210 bcr-abl-induced transformation of rat-1 fibroblasts and promotes differentiation of K562 cells. Proceedings of the National Academy of Sciences of the United States of America *95*, 14094-14099.
Landthaler, M., Yalcin, A., and Tuschl, T. (2004). The human DiGeorge syndrome critical region gene 8 and Its D. melanogaster homolog are required for miRNA biogenesis. Curr Biol *14*, 2162-2167.

Lee, A.C., Fenster, B.E., Ito, H., Takeda, K., Bae, N.S., Hirai, T., Yu, Z.X., Ferrans, V.J., Howard, B.H., and Finkel, T. (1999). Ras proteins induce senescence by altering the intracellular levels of reactive oxygen species. The Journal of biological chemistry *274*, 7936-7940.
Lee, R.C., Feinbaum, R.L., and Ambros, V. (1993). The C. elegans heterochronic gene lin-4 encodes small RNAs with antisense complementarity to lin-14. Cell *75*, 843-854.
Lee, S.R., Kwon, K.S., Kim, S.R., and Rhee, S.G. (1998). Reversible inactivation of protein-tyrosine phosphatase 1B in A431 cells stimulated with epidermal growth factor. The Journal of biological chemistry *273*, 15366-15372.
Lee, Y., Ahn, C., Han, J., Choi, H., Kim, J., Yim, J., Lee, J., Provost, P., Radmark, O., Kim, S.*, et al.* (2003). The nuclear RNase III Drosha initiates microRNA processing. Nature *425*, 415-419.
Lee, Y., Hur, I., Park, S.Y., Kim, Y.K., Suh, M.R., and Kim, V.N. (2006). The role of PACT in the RNA silencing pathway. The EMBO journal *25*, 522-532.
Lee, Y., Kim, M., Han, J., Yeom, K.H., Lee, S., Baek, S.H., and Kim, V.N. (2004). MicroRNA genes are transcribed by RNA polymerase II. The EMBO journal *23*, 4051-4060.
Leung, A.K., Vyas, S., Rood, J.E., Bhutkar, A., Sharp, P.A., and Chang, P. (2011). Poly(ADP-ribose) regulates stress responses and microRNA activity in the cytoplasm. Mol Cell *42*, 489-499.
Leung, A.K.L., and Sharp, P.A. (2010). MicroRNA Functions in Stress Responses. Molecular Cell *40*, 205-215.
Levene, P.A., and Alsberg, C.L. (1906). THE CLEAVAGE PRODUCTS OF VITELLIN. Journal of Biological Chemistry *2*, 127-133.
Li, R.Y., Gaits, F., Ragab, A., Ragab-Thomas, J.M., and Chap, H. (1995). Tyrosine phosphorylation of an SH2-containing protein tyrosine phosphatase is coupled to platelet thrombin receptor via a pertussis toxin-sensitive heterotrimeric G-protein. The EMBO journal *14*, 2519-2526.
Lim, K.L., Lai, D.S., Kalousek, M.B., Wang, Y., and Pallen, C.J. (1997). Kinetic analysis of two closely related receptor-like protein-tyrosine-phosphatases, PTP alpha and PTP epsilon. Eur J Biochem *245*, 693-700.
Lim, W.A., and Pawson, T. (2010). Phosphotyrosine signaling: evolving a new cellular communication system. Cell *142*, 661-667.
Lin, A.W., Barradas, M., Stone, J.C., van Aelst, L., Serrano, M., and Lowe, S.W. (1998). Premature senescence involving p53 and p16 is activated in response to constitutive MEK/MAPK mitogenic signaling. Genes Dev *12*, 3008-3019.
Lin, M., Lee, Y.H., Xu, W., Baker, M.A., and Aitken, R.J. (2006). Ontogeny of tyrosine phosphorylation-signaling pathways during spermatogenesis and epididymal maturation in the mouse. Biol Reprod *75*, 588-597.
Lin, M.T., and Beal, M.F. (2006). Mitochondrial dysfunction and oxidative stress in neurodegenerative diseases. Nature *443*, 787-795.
Lingel, A., Simon, B., Izaurralde, E., and Sattler, M. (2004). Nucleic acid 3'-end recognition by the Argonaute2 PAZ domain. Nat Struct Mol Biol *11*, 576-577.
Liu, H., Sadygov, R.G., and Yates, J.R., 3rd (2004a). A model for random sampling and estimation of relative protein abundance in shotgun proteomics. Anal Chem *76*, 4193-4201.
Liu, J., Carmell, M.A., Rivas, F.V., Marsden, C.G., Thomson, J.M., Song, J.J., Hammond, S.M., Joshua-Tor, L., and Hannon, G.J. (2004b). Argonaute2 is the catalytic engine of mammalian RNAi. Science *305*, 1437-1441.
Liu, J., Carmell, M.A., Rivas, F.V., Marsden, C.G., Thomson, J.M., Song, J.J., Hammond, S.M., Joshua-Tor, L., and Hannon, G.J. (2004c). Argonaute2 is the catalytic engine of mammalian RNAi. Science *305*, 1427-1441.

Lohse, D.L., Denu, J.M., Santoro, N., and Dixon, J.E. (1997). Roles of aspartic acid-181 and serine-222 in intermediate formation and hydrolysis of the mammalian protein-tyrosine-phosphatase PTP1. Biochemistry *36*, 4568-4575.
Lujambio, A., and Lowe, S.W. (2012). The microcosmos of cancer. Nature *482*, 347-355.
MacRae, I.J., Ma, E., Zhou, M., Robinson, C.V., and Doudna, J.A. (2008). In vitro reconstitution of the human RISC-loading complex. Proceedings of the National Academy of Sciences of the United States of America *105*, 512-517.
Maehama, T., and Dixon, J.E. (1998). The tumor suppressor, PTEN/MMAC1, dephosphorylates the lipid second messenger, phosphatidylinositol 3,4,5-trisphosphate. The Journal of biological chemistry *273*, 13375-13378.
Mahadev, K., Wu, X., Zilbering, A., Zhu, L., Lawrence, J.T., and Goldstein, B.J. (2001a). Hydrogen peroxide generated during cellular insulin stimulation is integral to activation of the distal insulin signaling cascade in 3T3-L1 adipocytes. The Journal of biological chemistry *276*, 48662-48669.
Mahadev, K., Zilbering, A., Zhu, L., and Goldstein, B.J. (2001b). Insulin-stimulated hydrogen peroxide reversibly inhibits protein-tyrosine phosphatase 1b in vivo and enhances the early insulin action cascade. The Journal of biological chemistry *276*, 21938-21942.
Majeti, R., Xu, Z., Parslow, T.G., Olson, J.L., Daikh, D.I., Killeen, N., and Weiss, A. (2000). An inactivating point mutation in the inhibitory wedge of CD45 causes lymphoproliferation and autoimmunity. Cell *103*, 1059-1070.
Maniataki, E., and Mourelatos, Z. (2005). A human, ATP-independent, RISC assembly machine fueled by pre-miRNA. Genes & development *19*, 2979-2990.
Martello, G., Rosato, A., Ferrari, F., Manfrin, A., Cordenonsi, M., Dupont, S., Enzo, E., Guzzardo, V., Rondina, M., Spruce, T.*, et al.* (2010). A MicroRNA targeting dicer for metastasis control. Cell *141*, 1195-1207.
Martinez, I., Cazalla, D., Almstead, L.L., Steitz, J.A., and DiMaio, D. (2011). miR-29 and miR-30 regulate B-Myb expression during cellular senescence. Proceedings of the National Academy of Sciences of the United States of America *108*, 522-527.
Matranga, C., Tomari, Y., Shin, C., Bartel, D.P., and Zamore, P.D. (2005). Passenger-strand cleavage facilitates assembly of siRNA into Ago2-containing RNAi enzyme complexes. Cell *123*, 607-620.
Meijer, L., Azzi, L., and Wang, J.Y. (1991). Cyclin B targets p34cdc2 for tyrosine phosphorylation. The EMBO journal *10*, 1545-1554.
Meister, G. (2013). Argonaute proteins: functional insights and emerging roles. Nature Reviews Genetics *14*, 447-459.
Meister, G., Landthaler, M., Peters, L., Chen, P.Y., Urlaub, H., Luhrmann, R., and Tuschl, T. (2005). Identification of novel argonaute-associated proteins. Curr Biol *15*, 2149-2155.
Meng, K., Rodriguez-Pena, A., Dimitrov, T., Chen, W., Yamin, M., Noda, M., and Deuel, T.F. (2000). Pleiotrophin signals increased tyrosine phosphorylation of beta beta-catenin through inactivation of the intrinsic catalytic activity of the receptor-type protein tyrosine phosphatase beta/zeta. Proceedings of the National Academy of Sciences of the United States of America *97*, 2603-2608.
Meng, T.C., Buckley, D.A., Galic, S., Tiganis, T., and Tonks, N.K. (2004). Regulation of insulin signaling through reversible oxidation of the protein-tyrosine phosphatases TC45 and PTP1B. The Journal of biological chemistry *279*, 37716-37725.
Meng, T.C., Fukada, T., and Tonks, N.K. (2002). Reversible oxidation and inactivation of protein tyrosine phosphatases in vivo. Mol Cell *9*, 387-399.
Meng, T.C., Hsu, S.F., and Tonks, N.K. (2005). Development of a modified in-gel assay to identify protein tyrosine phosphatases that are oxidized and inactivated in vivo. Methods *35*, 28-36.

Michaloglou, C., Vredeveld, L.C., Soengas, M.S., Denoyelle, C., Kuilman, T., van der Horst, C.M., Majoor, D.M., Shay, J.W., Mooi, W.J., and Peeper, D.S. (2005). BRAFE600-associated senescence-like cell cycle arrest of human naevi. Nature *436*, 720-724.
Miller, E.W., Albers, A.E., Pralle, A., Isacoff, E.Y., and Chang, C.J. (2005). Boronate-based fluorescent probes for imaging cellular hydrogen peroxide. J Am Chem Soc *127*, 16652-16659.
Miller, E.W., and Chang, C.J. (2007). Fluorescent probes for nitric oxide and hydrogen peroxide in cell signaling. Curr Opin Chem Biol *11*, 620-625.
Moiseeva, O., Bourdeau, V., Roux, A., Deschenes-Simard, X., and Ferbeyre, G. (2009). Mitochondrial dysfunction contributes to oncogene-induced senescence. Mol Cell Biol *29*, 4495-4507.
Murphy, M.P. (2009). How mitochondria produce reactive oxygen species. The Biochemical journal *417*, 1-13.
Myers, M.P., Stolarov, J.P., Eng, C., Li, J., Wang, S.I., Wigler, M.H., Parsons, R., and Tonks, N.K. (1997). P-TEN, the tumor suppressor from human chromosome 10q23, is a dual-specificity phosphatase. Proceedings of the National Academy of Sciences of the United States of America *94*, 9052-9057.
Narita, M., and Lowe, S.W. (2005). Senescence comes of age. Nat Med *11*, 920-922.
Narita, M., Nunez, S., Heard, E., Narita, M., Lin, A.W., Hearn, S.A., Spector, D.L., Hannon, G.J., and Lowe, S.W. (2003). Rb-mediated heterochromatin formation and silencing of E2F target genes during cellular senescence. Cell *113*, 703-716.
Neel, B.G., Gu, H., and Pao, L. (2003). The 'Shp'ing news: SH2 domain-containing tyrosine phosphatases in cell signaling. Trends Biochem Sci *28*, 284-293.
Neilson, K.A., Ali, N.A., Muralidharan, S., Mirzaei, M., Mariani, M., Assadourian, G., Lee, A., van Sluyter, S.C., and Haynes, P.A. (2011). Less label, more free: approaches in label-free quantitative mass spectrometry. Proteomics *11*, 535-553.
Nemoto, S., and Finkel, T. (2002). Redox regulation of forkhead proteins through a p66shc-dependent signaling pathway. Science *295*, 2450-2452.
Noland, C.L., Ma, E., and Doudna, J.A. (2011). siRNA repositioning for guide strand selection by human Dicer complexes. Mol Cell *43*, 110-121.
Nunoi, H., Rotrosen, D., Gallin, J.I., and Malech, H.L. (1988). Two forms of autosomal chronic granulomatous disease lack distinct neutrophil cytosol factors. Science *242*, 1298-1301.
Oeljeklaus, S., Meyer, H.E., and Warscheid, B. (2009). New dimensions in the study of protein complexes using quantitative mass spectrometry. FEBS Lett *583*, 1674-1683.
Olsen, J.V., Blagoev, B., Gnad, F., Macek, B., Kumar, C., Mortensen, P., and Mann, M. (2006). Global, In Vivo, and Site-Specific Phosphorylation Dynamics in Signaling Networks. Cell *127*, 635-648.
Ong, S.E., Blagoev, B., Kratchmarova, I., Kristensen, D.B., Steen, H., Pandey, A., and Mann, M. (2002). Stable isotope labeling by amino acids in cell culture, SILAC, as a simple and accurate approach to expression proteomics. Mol Cell Proteomics *1*, 376-386.
Ostman, A., Yang, Q., and Tonks, N.K. (1994). Expression of DEP-1, a receptor-like protein-tyrosine-phosphatase, is enhanced with increasing cell density. Proceedings of the National Academy of Sciences of the United States of America *91*, 9680-9684.
Paduano, F., Dattilo, V., Narciso, D., Bilotta, A., Gaudio, E., Menniti, M., Agosti, V., Palmieri, C., Perrotti, N., Fusco, A*., et al.* (2013). Protein tyrosine phosphatase PTPRJ is negatively regulated by microRNA-328. The FEBS journal *280*, 401-412.
Parker, J.S., Roe, S.M., and Barford, D. (2004). Crystal structure of a PIWI protein suggests mechanisms for siRNA recognition and slicer activity. The EMBO journal *23*, 4727-4737.
Paroo, Z., Ye, X., Chen, S., and Liu, Q. (2009). Phosphorylation of the human microRNA-generating complex mediates MAPK/Erk signaling. Cell *139*, 112-122.
Parrinello, S., Samper, E., Krtolica, A., Goldstein, J., Melov, S., and Campisi, J. (2003). Oxygen sensitivity severely limits the replicative lifespan of murine fibroblasts. Nature cell biology *5*, 741-747.

Parsons, R., and Simpson, L. (2003). PTEN and cancer. Methods Mol Biol *222*, 147-166.
Patel, V.J., Thalassinos, K., Slade, S.E., Connolly, J.B., Crombie, A., Murrell, J.C., and Scrivens, J.H. (2009). A comparison of labeling and label-free mass spectrometry-based proteomics approaches. Journal of proteome research *8*, 3752-3759.
Patterson, M.K., Jr., and Orr, G.R. (1968). Asparagine biosynthesis by the Novikoff Hepatoma isolation, purification, property, and mechanism studies of the enzyme system. The Journal of biological chemistry *243*, 376-380.
Persson, C., Sjoblom, T., Groen, A., Kappert, K., Engstrom, U., Hellman, U., Heldin, C.H., den Hertog, J., and Ostman, A. (2004). Preferential oxidation of the second phosphatase domain of receptor-like PTP-alpha revealed by an antibody against oxidized protein tyrosine phosphatases. Proceedings of the National Academy of Sciences of the United States of America *101*, 1886-1891.
Petersen, C.P., Bordeleau, M.E., Pelletier, J., and Sharp, P.A. (2006). Short RNAs repress translation after initiation in mammalian cells. Mol Cell *21*, 533-542.
Qi, H.H., Ongusaha, P.P., Myllyharju, J., Cheng, D., Pakkanen, O., Shi, Y., Lee, S.W., and Peng, J. (2008). Prolyl 4-hydroxylation regulates Argonaute 2 stability. Nature *455*, 421-424.
Rand, T.A., Petersen, S., Du, F., and Wang, X. (2005). Argonaute2 cleaves the anti-guide strand of siRNA during RISC activation. Cell *123*, 621-629.
Rhee, S.G. (2006). Cell signaling. H2O2, a necessary evil for cell signaling. Science *312*, 1882-1883.
Rhee, S.G., Chang, T.S., Bae, Y.S., Lee, S.R., and Kang, S.W. (2003). Cellular regulation by hydrogen peroxide. J Am Soc Nephrol *14*, S211-215.
Rivas, F.V., Tolia, N.H., Song, J.J., Aragon, J.P., Liu, J., Hannon, G.J., and Joshua-Tor, L. (2005). Purified Argonaute2 and an siRNA form recombinant human RISC. Nat Struct Mol Biol *12*, 340-349.
Robinson-Bennett, B.L., Deford, J., Diaz-Arrastia, C., Levine, L., Wang, H.Q., Hannigan, E.V., and Papaconstantinou, J. (2008). Implications of tyrosine phosphoproteomics in cervical carcinogenesis. J Carcinog *7*, 2.
Ross, P.L., Huang, Y.N., Marchese, J.N., Williamson, B., Parker, K., Hattan, S., Khainovski, N., Pillai, S., Dey, S., Daniels, S*., et al.* (2004). Multiplexed protein quantitation in Saccharomyces cerevisiae using amine-reactive isobaric tagging reagents. Mol Cell Proteomics *3*, 1154-1169.
Royer-Pokora, B., Kunkel, L.M., Monaco, A.P., Goff, S.C., Newburger, P.E., Baehner, R.L., Cole, F.S., Curnutte, J.T., and Orkin, S.H. (1986). Cloning the gene for an inherited human disorder--chronic granulomatous disease--on the basis of its chromosomal location. Nature *322*, 32-38.
Rudel, S., Wang, Y., Lenobel, R., Korner, R., Hsiao, H.H., Urlaub, H., Patel, D., and Meister, G. (2010). Phosphorylation of human Argonaute proteins affects small RNA binding. Nucleic Acids Research *39*, 2330-2343.
Rudel, S., Wang, Y., Lenobel, R., Korner, R., Hsiao, H.H., Urlaub, H., Patel, D., and Meister, G. (2011). Phosphorylation of human Argonaute proteins affects small RNA binding. Nucleic Acids Res *39*, 2330-2343.
Rüdel, S., Wang, Y., Lenobel, R., Körner, R., Hsiao, H.H., Urlaub, H., Patel, D., and Meister, G. (2011). Phosphorylation of human Argonaute proteins affects small RNA binding. Nucleic Acids Res *39*, 2330-2343.
Rybak, A., Fuchs, H., Hadian, K., Smirnova, L., Wulczyn, E.A., Michel, G., Nitsch, R., Krappmann, D., and Wulczyn, F.G. (2009). The let-7 target gene mouse lin-41 is a stem cell specific E3 ubiquitin ligase for the miRNA pathway protein Ago2. Nature cell biology *11*, 1411-1420.
Ryu, S., Gallis, B., Goo, Y.A., Shaffer, S.A., Radulovic, D., and Goodlett, D.R. (2008). Comparison of a label-free quantitative proteomic method based on peptide ion current area to the isotope coded affinity tag method. Cancer Inform *6*, 243-255.
Sajnani-Perez, G., Chilton, J.K., Aricescu, A.R., Haj, F., and Stoker, A.W. (2003). Isoform-specific binding of the tyrosine phosphatase PTPsigma to a ligand in developing muscle. Mol Cell Neurosci *22*, 37-48.

Salmeen, A., Andersen, J.N., Myers, M.P., Meng, T.C., Hinks, J.A., Tonks, N.K., and Barford, D. (2003). Redox regulation of protein tyrosine phosphatase 1B involves a sulphenyl-amide intermediate. Nature *423*, 769-773.
Salmeen, A., and Barford, D. (2005). Functions and mechanisms of redox regulation of cysteine-based phosphatases. Antioxidants & redox signaling *7*, 560-577.
Schenten, V., Brechard, S., Plancon, S., Melchior, C., Frippiat, J.P., and Tschirhart, E.J. (2010). iPLA2, a novel determinant in Ca2+- and phosphorylation-dependent S100A8/A9 regulated NOX2 activity. Biochimica et biophysica acta *1803*, 840-847.
Schriner, S.E., Linford, N.J., Martin, G.M., Treuting, P., Ogburn, C.E., Emond, M., Coskun, P.E., Ladiges, W., Wolf, N., Van Remmen, H.*, et al.* (2005). Extension of murine life span by overexpression of catalase targeted to mitochondria. Science *308*, 1909-1911.
Schubbert, S., Shannon, K., and Bollag, G. (2007). Hyperactive Ras in developmental disorders and cancer. Nat Rev Cancer *7*, 295-308.
Schumacker, P.T. (2006). Reactive oxygen species in cancer cells: live by the sword, die by the sword. Cancer Cell *10*, 175-176.
Schwarz, D.S., Hutvagner, G., Du, T., Xu, Z., Aronin, N., and Zamore, P.D. (2003). Asymmetry in the assembly of the RNAi enzyme complex. Cell *115*, 199-208.
Serrano, M., Lin, A.W., McCurrach, M.E., Beach, D., and Lowe, S.W. (1997). Oncogenic ras provokes premature cell senescence associated with accumulation of p53 and p16INK4a. Cell *88*, 593-602.
Severino, J., Allen, R.G., Balin, S., Balin, A., and Cristofalo, V.J. (2000). Is beta-galactosidase staining a marker of senescence in vitro and in vivo? Exp Cell Res *257*, 162-171.
Shalaby, M.R., Aggarwal, B.B., Rinderknecht, E., Svedersky, L.P., Finkle, B.S., and Palladino, M.A. (1985). Activation of human polymorphonuclear neutrophil functions by interferon-gamma and tumor necrosis factors. The Journal of Immunology *135*, 2069-2073.
Sharma, P., Chakraborty, R., Wang, L., Min, B., Tremblay, M.L., Kawahara, T., Lambeth, J.D., and Haque, S.J. (2008). Redox regulation of interleukin-4 signaling. Immunity *29*, 551-564.
Shen, J., Xia, W., Khotskaya, Y.B., Huo, L., Nakanishi, K., Lim, S.O., Du, Y., Wang, Y., Chang, W.C., Chen, C.H.*, et al.* (2013a). EGFR modulates microRNA maturation in response to hypoxia through phosphorylation of AGO2. Nature *497*, 383-387.
Shen, J., Xia, W., Khotskaya, Y.B., Huo, L., Nakanishi, K., Lim, S.O., Du, Y., Wang, Y., Chang, W.C., Chen, C.H.*, et al.* (2013b). EGFR modulates microRNA maturation in response to hypoxia through phosphorylation of AGO2. Nature *497*, 383-387.
Shibanuma, M., Mashimo, J., Kuroki, T., and Nose, K. (1994). Characterization of the TGF beta 1-inducible hic-5 gene that encodes a putative novel zinc finger protein and its possible involvement in cellular senescence. The Journal of biological chemistry *269*, 26767-26774.
Song, H., Zhang, Z., and Wang, L. (2008). Small interference RNA against PTP-1B reduces hypoxia/reoxygenation induced apoptosis of rat cardiomyocytes. Apoptosis *13*, 383-393.
Stalder, L., Heusermann, W., Sokol, L., Trojer, D., Wirz, J., Hean, J., Fritzsche, A., Aeschimann, F., Pfanzagl, V., Basselet, P.*, et al.* (2013). The rough endoplasmatic reticulum is a central nucleation site of siRNA-mediated RNA silencing. EMBO J *32*, 1115-1127.
Staveley, B.E., Ruel, L., Jin, J., Stambolic, V., Mastronardi, F.G., Heitzler, P., Woodgett, J.R., and Manoukian, A.S. (1998). Genetic analysis of protein kinase B (AKT) in Drosophila. Curr Biol *8*, 599-602.
Sun, P., Yoshizuka, N., New, L., Moser, B.A., Li, Y., Liao, R., Xie, C., Chen, J., Deng, Q., Yamout, M.*, et al.* (2007). PRAK Is Essential for ras-Induced Senescence and Tumor Suppression. Cell *128*, 295-308.
Sundaresan, M., Yu, Z.X., Ferrans, V.J., Irani, K., and Finkel, T. (1995). Requirement for generation of H2O2 for platelet-derived growth factor signal transduction. Science *270*, 296-299.

Sundaresan, M., Yu, Z.X., Ferrans, V.J., Sulciner, D.J., Gutkind, J.S., Irani, K., Goldschmidt-Clermont, P.J., and Finkel, T. (1996). Regulation of reactive-oxygen-species generation in fibroblasts by Rac1. The Biochemical journal *318 (Pt 2)*, 379-382.
Suwaki, N., Vanhecke, E., Atkins, K.M., Graf, M., Swabey, K., Huang, P., Schraml, P., Moch, H., Cassidy, A.M., Brewer, D*., et al.* (2011). A HIF-regulated VHL-PTP1B-Src signaling axis identifies a therapeutic target in renal cell carcinoma. Sci Transl Med *3*, 85ra47.
Tabet, F., Schiffrin, E.L., Callera, G.E., He, Y., Yao, G., Ostman, A., Kappert, K., Tonks, N.K., and Touyz, R.M. (2008). Redox-sensitive signaling by angiotensin II involves oxidative inactivation and blunted phosphorylation of protein tyrosine phosphatase SHP-2 in vascular smooth muscle cells from SHR. Circ Res *103*, 149-158.
Tahbaz, N., Kolb, F.A., Zhang, H., Jaronczyk, K., Filipowicz, W., and Hobman, T.C. (2004). Characterization of the interactions between mammalian PAZ PIWI domain proteins and Dicer. EMBO Rep *5*, 189-194.
Tang, X., Zhang, Y., Tucker, L., and Ramratnam, B. (2010). Phosphorylation of the RNase III enzyme Drosha at Serine300 or Serine302 is required for its nuclear localization. Nucleic Acids Res *38*, 6610-6619.
Tartaglia, M., Kalidas, K., Shaw, A., Song, X., Musat, D.L., van der Burgt, I., Brunner, H.G., Bertola, D.R., Crosby, A., Ion, A*., et al.* (2002). PTPN11 mutations in Noonan syndrome: molecular spectrum, genotype-phenotype correlation, and phenotypic heterogeneity. Am J Hum Genet *70*, 1555-1563.
Tartaglia, M., Niemeyer, C.M., Fragale, A., Song, X., Buechner, J., Jung, A., Hahlen, K., Hasle, H., Licht, J.D., and Gelb, B.D. (2003). Somatic mutations in PTPN11 in juvenile myelomonocytic leukemia, myelodysplastic syndromes and acute myeloid leukemia. Nature genetics *34*, 148-150.
Tate, S., Larsen, B., Bonner, R., and Gingras, A.C. (2013). Label-free quantitative proteomics trends for protein-protein interactions. J Proteomics *81*, 91-101.
Teahan, C., Rowe, P., Parker, P., Totty, N., and Segal, A.W. (1987). The X-linked chronic granulomatous disease gene codes for the beta-chain of cytochrome b-245. Nature *327*, 720-721.
Thomas, S.M., Hagel, M., and Turner, C.E. (1999). Characterization of a focal adhesion protein, Hic-5, that shares extensive homology with paxillin. J Cell Sci *112 (Pt 2)*, 181-190.
Tomari, Y., Matranga, C., Haley, B., Martinez, N., and Zamore, P.D. (2004). A protein sensor for siRNA asymmetry. Science *306*, 1377-1380.
Tonks, N.K. (2003). PTP1B: From the sidelines to the front lines! FEBS Letters *546*, 140-148.
Tonks, N.K. (2006a). Protein tyrosine phosphatases: from genes, to function, to disease. Nature Reviews Molecular Cell Biology *7*, 833-846.
Tonks, N.K. (2006b). Protein tyrosine phosphatases: from genes, to function, to disease. Nat Rev Mol Cell Biol *7*, 833-846.
Tonks, N.K. (2013). Protein tyrosine phosphatases--from housekeeping enzymes to master regulators of signal transduction. FEBS J *280*, 346-378.
Tonks, N.K., Diltz, C.D., and Fischer, E.H. (1988a). Characterization of the major protein-tyrosine-phosphatases of human placenta. The Journal of biological chemistry *263*, 6731-6737.
Tonks, N.K., Diltz, C.D., and Fischer, E.H. (1988b). Purification of the major protein-tyrosine-phosphatases of human placenta. The Journal of biological chemistry *263*, 6722-6730.
Tonks, N.K., and Muthuswamy, S.K. (2007). A brake becomes an accelerator: PTP1B--a new therapeutic target for breast cancer. Cancer Cell *11*, 214-216.
Turck, C.W., Falick, A.M., Kowalak, J.A., Lane, W.S., Lilley, K.S., Phinney, B.S., Weintraub, S.T., Witkowska, H.E., and Yates, N.A. (2007). The Association of Biomolecular Resource Facilities Proteomics Research Group 2006 study: relative protein quantitation. Mol Cell Proteomics *6*, 1291-1298.
Tuveson, D.A., Shaw, A.T., Willis, N.A., Silver, D.P., Jackson, E.L., Chang, S., Mercer, K.L., Grochow, R., Hock, H., Crowley, D*., et al.* (2004). Endogenous oncogenic K-ras(G12D) stimulates proliferation and widespread neoplastic and developmental defects. Cancer Cell *5*, 375-387.

Ushio-Fukai, M., Alexander, R.W., Akers, M., Yin, Q., Fujio, Y., Walsh, K., and Griendling, K.K. (1999). Reactive oxygen species mediate the activation of Akt/protein kinase B by angiotensin II in vascular smooth muscle cells. The Journal of biological chemistry *274*, 22699-22704.
Ushio-Fukai, M., Zafari, A.M., Fukui, T., Ishizaka, N., and Griendling, K.K. (1996). p22phox is a critical component of the superoxide-generating NADH/NADPH oxidase system and regulates angiotensin II-induced hypertrophy in vascular smooth muscle cells. The Journal of biological chemistry *271*, 23317-23321.
Ushiro, H., and Cohen, S. (1980). Identification of phosphotyrosine as a product of epidermal growth factor-activated protein kinase in A-431 cell membranes. The Journal of biological chemistry *255*, 8363-8365.
van der Wijk, T., Overvoorde, J., and den Hertog, J. (2004). H2O2-induced intermolecular disulfide bond formation between receptor protein-tyrosine phosphatases. The Journal of biological chemistry *279*, 44355-44361.
van Montfort, R.L., Congreve, M., Tisi, D., Carr, R., and Jhoti, H. (2003). Oxidation state of the active-site cysteine in protein tyrosine phosphatase 1B. Nature *423*, 773-777.
Volarevic, S., Niklinska, B.B., Burns, C.M., June, C.H., Weissman, A.M., and Ashwell, J.D. (1993). Regulation of TCR signaling by CD45 lacking transmembrane and extracellular domains. Science *260*, 541-544.
Volpp, B.D., Nauseef, W.M., and Clark, R.A. (1988). Two cytosolic neutrophil oxidase components absent in autosomal chronic granulomatous disease. Science *242*, 1295-1297.
Wang, B., Yanez, A., and Novina, C.D. (2008). MicroRNA-repressed mRNAs contain 40S but not 60S components. Proceedings of the National Academy of Sciences of the United States of America *105*, 5343-5348.
Wang, H.W., Noland, C., Siridechadilok, B., Taylor, D.W., Ma, E., Felderer, K., Doudna, J.A., and Nogales, E. (2009). Structural insights into RNA processing by the human RISC-loading complex. Nat Struct Mol Biol *16*, 1148-1153.
Watson, J.D. (1972). Origin of concatemeric T7 DNA. Nat New Biol *239*, 197-201.
Weber, J.D., Taylor, L.J., Roussel, M.F., Sherr, C.J., and Bar-Sagi, D. (1999). Nucleolar Arf sequesters Mdm2 and activates p53. Nature cell biology *1*, 20-26.
Westermarck, J., Ivaska, J., and Corthals, G.L. (2013). Identification of protein interactions involved in cellular signaling. Mol Cell Proteomics *12*, 1752-1763.
Weyemi, U., Lagente-Chevallier, O., Boufraqech, M., Prenois, F., Courtin, F., Caillou, B., Talbot, M., Dardalhon, M., Al Ghuzlan, A., Bidart, J.M*., et al.* (2012). ROS-generating NADPH oxidase NOX4 is a critical mediator in oncogenic H-Ras-induced DNA damage and subsequent senescence. Oncogene *31*, 1117-1129.
Wiener, J.R., Hurteau, J.A., Kerns, B.J., Whitaker, R.S., Conaway, M.R., Berchuck, A., and Bast, R.C., Jr. (1994). Overexpression of the tyrosine phosphatase PTP1B is associated with human ovarian carcinomas. Am J Obstet Gynecol *170*, 1177-1183.
Wientjes, F.B., Hsuan, J.J., Totty, N.F., and Segal, A.W. (1993). p40phox, a third cytosolic component of the activation complex of the NADPH oxidase to contain src homology 3 domains. The Biochemical journal *296 (Pt 3)*, 557-561.
Winter, J., Jung, S., Keller, S., Gregory, R.I., and Diederichs, S. (2009). Many roads to maturity: microRNA biogenesis pathways and their regulation. Nature cell biology *11*, 228-234.
Woo, H.A., Yim, S.H., Shin, D.H., Kang, D., Yu, D.Y., and Rhee, S.G. (2010). Inactivation of peroxiredoxin I by phosphorylation allows localized H(2)O(2) accumulation for cell signaling. Cell *140*, 517-528.
Wosilait, W.D., and Sutherland, E.W. (1956). The relationship of epinephrine and glucagon to liver phosphorylase. II. Enzymatic inactivation of liver phosphorylase. The Journal of biological chemistry *218*, 469-481.

Wu, L., Fan, J., and Belasco, J.G. (2006). MicroRNAs direct rapid deadenylation of mRNA. Proceedings of the National Academy of Sciences of the United States of America *103*, 4034-4039.
Wu, S., Huang, S., Ding, J., Zhao, Y., Liang, L., Liu, T., Zhan, R., and He, X. (2010). Multiple microRNAs modulate p21Cip1/Waf1 expression by directly targeting its 3' untranslated region. Oncogene *29*, 2302-2308.
Wu, W., Yang, J., Feng, X., Wang, H., Ye, S., Yang, P., Tan, W., Wei, G., and Zhou, Y. (2013). MicroRNA-32 (miR-32) regulates phosphatase and tensin homologue (PTEN) expression and promotes growth, migration, and invasion in colorectal carcinoma cells. Mol Cancer *12*, 30.
Xie, Y., Massa, S.M., Ensslen-Craig, S.E., Major, D.L., Yang, T., Tisi, M.A., Derevyanny, V.D., Runge, W.O., Mehta, B.P., Moore, L.A*., et al.* (2006). Protein-tyrosine phosphatase (PTP) wedge domain peptides: a novel approach for inhibition of PTP function and augmentation of protein-tyrosine kinase function. The Journal of biological chemistry *281*, 16482-16492.
Yang, N.C., and Hu, M.L. (2004). A fluorimetric method using fluorescein di-beta-D-galactopyranoside for quantifying the senescence-associated beta-galactosidase activity in human foreskin fibroblast Hs68 cells. Anal Biochem *325*, 337-343.
Yuan, H., Kaneko, T., and Matsuo, M. (1995). Relevance of oxidative stress to the limited replicative capacity of cultured human diploid cells: the limit of cumulative population doublings increases under low concentrations of oxygen and decreases in response to aminotriazole. Mech Ageing Dev *81*, 159-168.
Yuvaniyama, J., Denu, J.M., Dixon, J.E., and Saper, M.A. (1996). Crystal structure of the dual specificity protein phosphatase VHR. Science *272*, 1328-1331.
Zabolotny, J.M., Bence-Hanulec, K.K., Stricker-Krongrad, A., Haj, F., Wang, Y., Minokoshi, Y., Kim, Y.B., Elmquist, J.K., Tartaglia, L.A., Kahn, B.B*., et al.* (2002). PTP1B regulates leptin signal transduction in vivo. Dev Cell *2*, 489-495.
Zeng, Y., and Cullen, B.R. (2004). Structural requirements for pre-microRNA binding and nuclear export by Exportin 5. Nucleic Acids Res *32*, 4776-4785.
Zeng, Y., Sankala, H., Zhang, X., and Graves, P.R. (2008a). Phosphorylation of Argonaute 2 at serine-387 facilitates its localization to processing bodies. Biochem J *413*, 429-436.
Zeng, Y., Sankala, H., Zhang, X., and Graves, P.R. (2008b). Phosphorylation of Argonaute 2 at serine-387 facilitates its localization to processing bodies. The Biochemical journal *413*, 429-436.
Zhai, Y.F., Beittenmiller, H., Wang, B., Gould, M.N., Oakley, C., Esselman, W.J., and Welsch, C.W. (1993). Increased expression of specific protein tyrosine phosphatases in human breast epithelial cells neoplastically transformed by the *neu* oncogene. Cancer Res *53*, 2272-2278.
Zhang, J., Fan, X.S., Wang, C.X., Liu, B., Li, Q., and Zhou, X.J. (2013). Up-regulation of Ago2 expression in gastric carcinoma. Med Oncol *30*, 628.
Zhou, Y., Chen, L., Barlogie, B., Stephens, O., Wu, X., Williams, D.R., Cartron, M.A., van Rhee, F., Nair, B., Waheed, S*., et al.* (2010). High-risk myeloma is associated with global elevation of miRNAs and overexpression of EIF2C2/AGO2. Proc Natl Acad Sci U S A *107*, 7904-7909.